MASS SPECTROMETRIC STRATEGIES FOR PROFILING OF ELECTROPHILIC OXYLIPIN METABOLITES AND THEIR GLUTATHIONE CONJUGATES

By

Jiangyin Bao

A DISSERTATION

Submitted to
Michigan State University
in partial fulfillment of the requirements
for the degree of

Chemistry — Doctor of Philosophy

2013

ABSTRACT

MASS SPECTROMETRIC STRATEGIES FOR PROFILING OF ELECTROPHILIC OXYLIPIN METABOLITES AND THEIR GLUTATHIONE CONJUGATES

By

Jiangyin Bao

Plants cannot escape from herbivory and other environmental stresses including cold and drought, and have evolved sophisticated defense systems to survive. Improving food production has become one of the most urgent problems facing humankind with 7 billion population and limited land available. Plants also serve as the base of the earth's sustainable fuel supply, and synthesize a diverse suite of natural compounds that help defend them against stress, but also are potential pharmaceutics. Improving our understanding of plant defense systems is a key factor in using plants as natural resources to provide solutions to these problems.

To defend themselves, plants synthesize oxidized fatty acids, or oxylipins, to regulate gene expression in response to stress. In response to wounding and certain stresses, many plants synthesize the cyclopentenone oxylipin 12-oxo-phytodienoic acid (OPDA) as a precursor of the master regulatory hormone jasmonic acid (JA). JA is then conjugated to isoleucine in cytoplasm to produce the universal defense gene regulator JA-isoleucine. OPDA has been shown to be an independent but not fully understood metabolite that regulates plant defenses. Reactive electrophiles such as OPDA are subject to conjugation to the tripeptide glutathione. This process is catalyzed by an assortment of glutathione transferase enzymes, and is expected to deactivate the biological functions of electrophiles. However, understanding of the functions of specific GSTs (>50 in model plant *Arabidopsis* from sequenced genome), particularly in plants, is limited. The research described in this dissertation has aimed to reveal biological functions of GSTs in defense response to mechanical wounding in *Arabidopsis*. The basic strategy has combined

information about GST protein levels with profiling of metabolites in a GST knockout mutant to correlate metabolic phenotypes with genotypes, for deduction of gene functions. 8 GSTs were identified in wild type *Arabidopsis* leaves, and one of them, *At*GSTU5, was shown to be highly accumulated after mechanical wounding. Several *Arabidopsis* knockout mutants, including *At*GST*u5*, were grown for wounding experiments and phenotype assessment using non-targeted metabolite profiling. The glutathione conjugate of OPDA was quantified and shown to be accumulated after mechanical wounding in leaves of wild type and other tau-family GST knockout mutants of *Arabidopsis*, but not in the knockout mutant *At*GST*u5*. This finding suggests that *At*GSTU5 is responsible for *in vivo* glutathione conjugation of OPDA. A new LC-TOF-MS protocol was developed to explore the range of endogenous glutathione conjugates in extracts of *Arabidopsis* leaves. A family of novel glutathione conjugates is also discovered and proposed to be derived from OPDA-containing galactolipids.

In the identification and quantitation of plant oxylipins, tandem mass spectrometry (MS/MS) data are often the primary source of metabolite structural information, but ion fragmentation pathways are not well understood for negative ions. This dissertation describes a novel fragmentation mechanism in negative mode involving charge-directed hydride migration for OPDA and its lower homolog dinorOPDA. This mechanism has potential to guide structure elucidation of unknown oxylipins. For other cyclopentenone prostaglandins with greater degrees of unsaturation, however, fragmentation behavior differed. Relative amounts of specific product ions distinguished prostaglandins with identical side chains but opposite cyclopentenone ring orientations.

ACKNOWLEDGMENTS

I would like to gratefully and sincerely thank my advisor, Dr. A Daniel Jones for his guidance, understanding, and especially, his friendship in these years throughout my PhD study. I came to the U.S as a fresh foreign student knowing nothing about how to do research and what my career will look like. He helped me to build my dream from scratch and taught me everything from cleaning ion source for the mass spectrometer to think independently as a scientist. I had tough times when I was struggling in my research and suffering from not being able to balance myself between research and teaching duties. But he helped me to think about my project with the basic chemistry principles, critically review literature and learn from them, and smartly distribute my time and energy on different tasks. I was a little bit shy and not as confident as I want, but he encouraged me to communicate with people and realize what my advantage is. He always asks me what I want to be famous for and his eyesight in the field helped me build my career goal. Every time that I thought I need help, he was always the one that I will go to and he was always there to guide me. Without his help I won't be able to make the achievements in my research and won't be a confident young scientist with expertise in analytical chemistry that I think I am now. Over these six years I have learned a lot from him. I think he is now proud of me and I am so happy that I am very fortunate to have him as my PhD advisor.

I also would like to thank my committee members, Dr. Spence, Dr. Blanchard and Dr. Walker for their help in my research. They made invaluable comments in my second year oral exam and they helped me in writing my thesis dissertation. They were always nice to me and treated me like close friends. It was my pleasure to work with all of them. I taught Dr. Spence's course and I enjoyed working for him as a teaching assistant.

I would like to thank Lijun Chen, Scott Smith and Ramin Vismeh from the Mass Spec Facility who helped me in operating the Qtrap and Q-tof instruments and interpreting results. I would like to thank Douglas Whitten for helping me on the analysis of proteomics sample on FTICR and Ion trap instruments.

I would like to thank my wife Zhimin for her love and support during all these years. We have been working or studying at different cities for ten years as far as 1000 miles apart. I am so grateful to have her in my life and the mother of my little girl. I would also like to thank my parents and parents-in-law for their love and understanding during these years when I pursued my dream far from home. I really appreciate their in helping us take care of our daughter, too. I enjoyed return to a warm house with smile on everyone's face in Michigan winter evenings. That really helped when I was in my bad days.

I want to thank my colleagues in Dr. Jones group, especially Chao Li and Xiaoli Gao. Chao Li was my roommate at Cherry lane apartments for a year and half. He often discussed with me about our research, everyday life, career opportunities and more. He are I are still very good friends now. Xiaoli taught me how to work with Arabidopsis and her work was where my research started. Much of my research was described in the "future work" chapter in her thesis dissertation.

I am grateful to many other people. This work is not possible without them and every one that I mentioned above.

TABLE OF CONTENTS

LIST OF TABLES

LIST OF FIGURES

KEY TO ABBREVIATIONS

ACN	acetonitrile
*At*GST	glutathione transferase in *Arabidopsis thaliana*
CID	collision-induced dissociation
DGDG	digalactosyl diacylglyceride
ESI	electrospray ionization
FA	formic acid
GST	Glutathione *S*-transferase
GSH	glutathione
GS-X	glutathione conjugates
JA	Jasmonic acid
JA-Ile	Jasmonic acid-isoleucine conjugate
LeA	linolenic acid
MeJA	methyl jasmonate
MS/MS	multi-stage mass spectrometry
KO	knockout
MGDGs	monogalactosyl diacylglycerides
MeOH	methanol
m/z	mass to charge ratio
OPC:4	3-oxo-2-[(Z)pent-2'-enyl]-cyclopentane-1-butanoic acid
OPC:8	3-oxo-2-[(Z)pent-2'-enyl]-cyclopentane-1-octanoic acid
OPDA	(9S, 10Z, 13S, 15Z)-12-oxo-phytodienoic acid
dnOPDA	(7R, 8Z, 11S, 13Z)-10-oxo-8, 13-dinor-phytodienoic acid

PGs	prostaglandins
TIC	total ion chromatogram
TOF	time-of-flight
XIC	extracted ion chromatogram

Chapter 1. Introduction

1.A. Plant secondary metabolism and overview of plant defense system

1.A.1 An important role for the biochemistry of plant specialized metabolism.

As carbon-fixing organisms, plants and photosynthetic algae and microbes serve as primary producers of organic matter from atmospheric carbon dioxide, and also provide the base of the food chain for all living things. Because plants are sessile organisms whose locations are fixed, their survival depends on their effectiveness in sensing and responding to environmental dangers and changes. Most of these changes are chemical, and plants have evolved a complex array of chemical defenses to protect against herbivores, diseases, and other competitors (Pichersky and Lewinsohn, 2011, Qi *et al.*, 2004). Many also secrete metabolites into the rhizosphere, which is the upper layer of soil, to encourage growth of beneficial microbes. Many plant specialized metabolites exhibit important biological activities that allow them to inspire development of medicines for treatments of diseases in humans and animals. These specialized metabolic pathways represent attractive targets for metabolic engineering, both for improving crop resistance to pests and as genetic resources for producing bio-based chemicals using fermentation. However, despite years of research in plant biochemistry, the biochemical pathways responsible for generating most of these chemical defenses across the plant kingdom remain largely unexplored (Schilmiller *et al.*, 2012).

1.A.2 Importance of specialized metabolites in agricultural production

Modern agriculture suffers substantial crop losses from damage by pests (Oerke, 2006), and efforts to improve agricultural productivity are often limited by pest damage. Crop plants respond to herbivory by producing an assortment of specialized metabolites and defensive proteins.

Figure 1.1 presents an example of how plants protect themselves from herbivory. Only direct defense mechanisms are summarized here, although plants are also capable of utilizing indirect defense strategies such as synthesis and release of predator-attracting molecules. To reduce the insect's desire to eat the plant, biosynthesis of bitter-tasting metabolites or digestion-interrupting protease inhibitors may be induced by herbivory (Koiwa *et al.*, 1997). Also useful for defense are strategies including cell wall strengthening (Divol *et al.*, 2007), apoptosis as a consequence of the hypersensitive response (Goodman, 1994) and degradation of necessary nutritients after ingestion by the insect (Chen *et al.*, 2007). Plants can synthesize toxic metabolites as a protective weapon as well, as is the case of biosynthesis of glucosinolates that are rapidly converted to reactive isothiocyanates (Louda, 1991).

Many transgenic crops with potent self-protection have already been introduced to the global market. Tobacco, corn and rice have been genetically modified to express the gene coding insecticidal proteins from the bacterium *Bacillus thuringiensis* (*Bt*). Based on understanding of plant response to xenobiotics, genetically-modified glyphosate-resistant crops have been developed to help farmers solve the problems of undesired weeds.

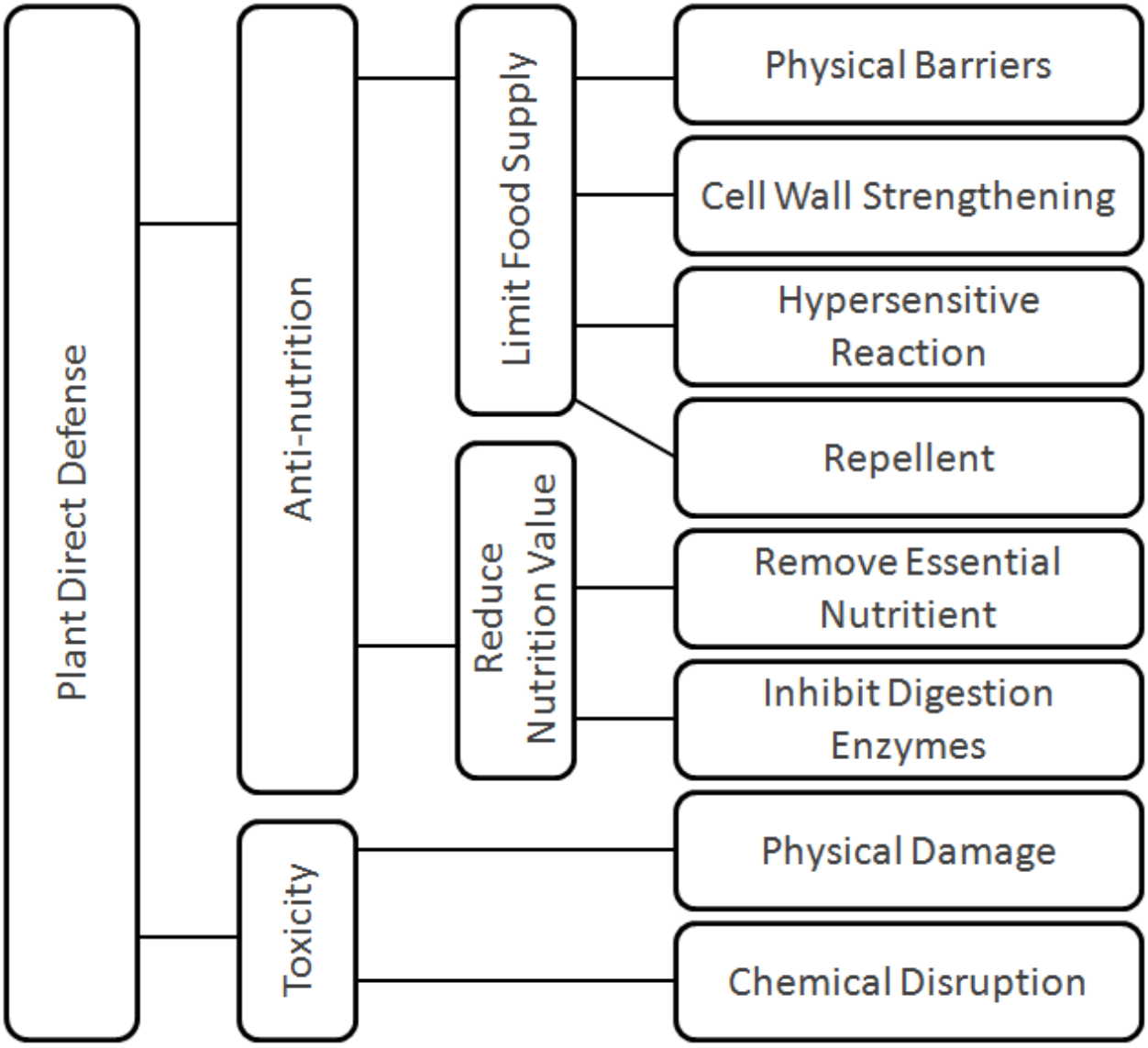

Figure 1.1 Various plant defensive responses against herbivory. Adapted from (Chen, 2008).

1.A.3 Similarities in plant and animal defense strategies

Both plants and animals synthesize bioactive fatty acid metabolites as a response to stresses. Animals produce signaling molecules including prostaglandins as part of their immune responses to wounding and infection (Straus and Glass, 2001). Prostaglandins are derived from the 20-carbon polyunsaturated fatty acid (PUFA) arachidonic acid, which is released from membrane phospholipids upon cell damage by phospholipase A_2. Prostaglandins are well-characterized

mediators of inflammation, regulating pain, fever and a wide assortment of biological functions in virtually all human cells (Narumiya *et al.*, 1999, Tsuboi *et al.*, 2002).

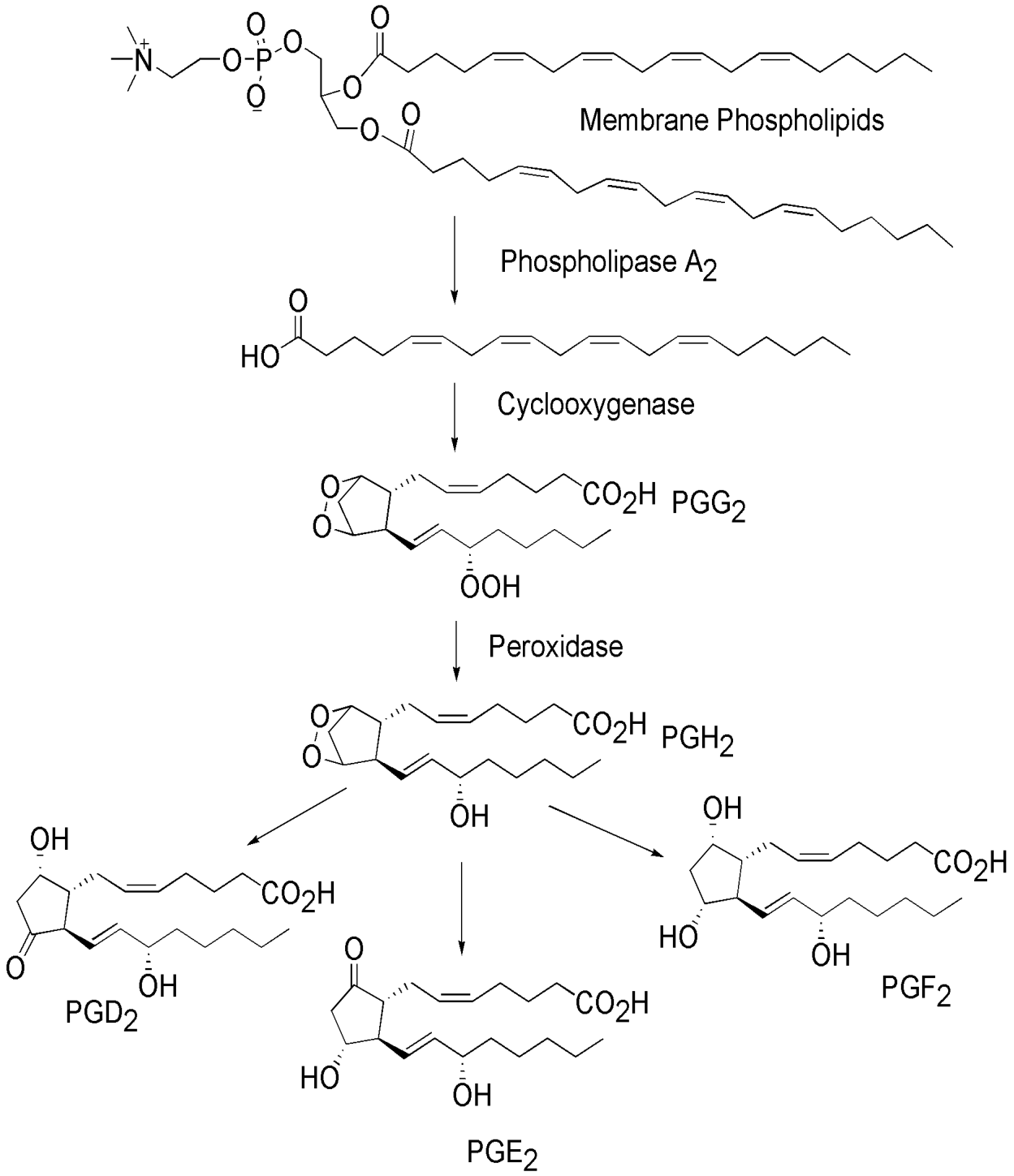

Figure1.2. Biosynthesis of selected prostaglandins. Only the initial enzymatic reactions are shown here. PGH_2 Synthase is a class of enzymes with both cyclooxygenase and peroxidase activities. Reactions producing PGD_2, PGE_2 and $PGF_{2\alpha}$ are catalyzed by PGD_2 synthase, PGE_2 synthase and $PGF_{2\alpha}$ synthase, respectively. See text for abbreviations. Adapted from (Straus and Glass, 2001).

Here is a brief summary of prostaglandin nomenclature using PGJ_2, a common prostaglandin as a good example. PG is short for prostaglandin. J is the name for the class of the prostaglandin compound. Subscript 2 represents the name of the specific compound. Compounds in the same class (such as PGJ_2 and 15-deoxy-$\Delta^{12,14}$-PGJ_2) have same number and types of functional groups, usually carbonyl and hydroxy groups.

The conversion from arachidonic acid to prostaglandin G_2 (PGG_2) and subsequent prostaglandin H_2 (PGH_2) is catalyzed by PGH synthases that exhibit both cyclooxygenase and peroxidase activities, as shown in Figure 1.2. There are two forms of PGH: PGH synthase 1 or COX1, a constitutive form and PGH synthase 2 or COX2, a stress-induced form. COX2 can be induced by proinflammatory cytokines and is the target of non-steroidal anti-inflammatory drugs including aspirin and indomethacin (Herschman *et al.*, 1999). PGE_2, PGD_2, and $PGF_{2\alpha}$ synthases catalyze the synthesis of corresponding prostaglandins from PGH_2.

Further downstream in the prostaglandin cascade are the cyclopentenone prostaglandins PGA_1, PGA_2 and PGJ_2, which are formed via non-enzymatic dehydration from PGE_1, PGE_2 and PGD_2, respectively, as shown in Figure 1.3. Double bond relocation occurs on PGA_2 and subsequent PGC_2 to form PGB_2. Similar reactions lead to Δ^{12}-PGJ_2 and 15-deoxy-$\Delta^{12,14}$-PGJ_2. These cyclopentenone metabolites are electrophiles that exert a range of biological functions (Straus and Glass, 2001). More detailed discussion of *in vivo* functions, metabolism and other aspects of prostaglandins has been extensively reviewed and will not be discussed in this dissertation (Funk, 2001, Harris *et al.*, 2002, Miller, 2006, Tsuboi, *et al.*, 2002).

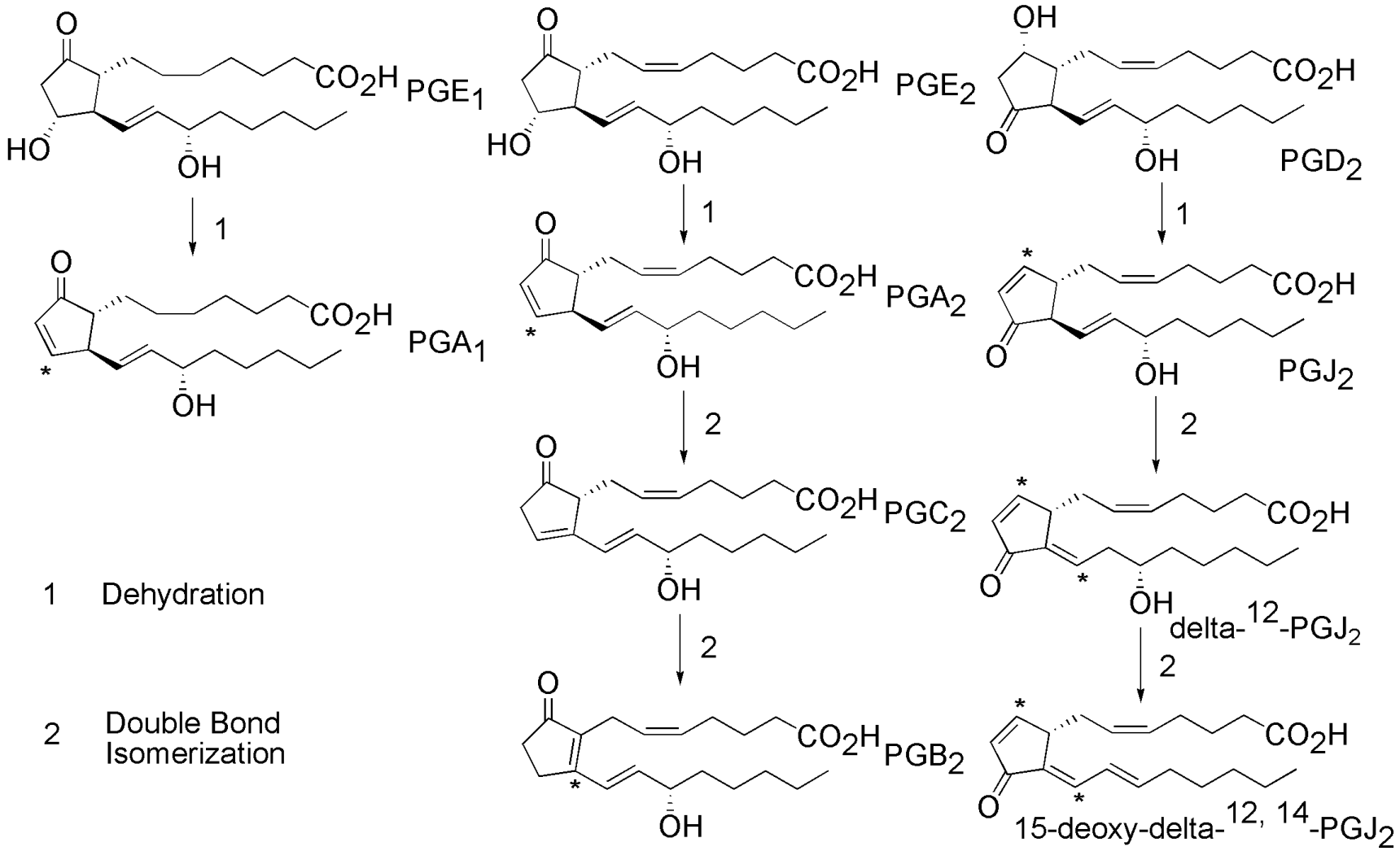

Figure 1.3. Non-enzymatic formation of cyclopentenone prostaglandins from PGE_1, PGE_2 and PGD_2 through dehydration (reactions labeled with number 1) and double bond isomerization (reactions labeled with number 2). Asterisks indicate chemically electrophilic reactive carbon atoms. Adapted from (Straus and Glass, 2001).

In similar fashion, plants biosynthesize oxylipins in response to stress, but most plants do not synthesize arachidonic acid. Plant cell membranes are largely comprised of derivatives of glycerol esters of 16- and 18-carbon fatty acids in the *sn-1* and *sn-2* positions. The *sn*-3 position is either linked via an inorganic ester linkage to phosphoric acid, or to a single or oligo galactose group. The former can be metabolically converted to phosphatidic acids (PAs), molecules known in Ca^{2+} signaling and responses to stress (Bargmann and Munnik, 2006). The latter lipids, called galactolipids, are the most abundant membrane lipids in chloroplasts. Plants utilize polyunsaturated galactolipids as precursors of the 18-carbon fatty acid linolenic acid, which in turn is converted to oxidized fatty acids that regulate gene expression in response to stress (Wasternack, 2007). The detailed biosynthesis of plant oxylipins, which is similar to the biosynthesis of prostaglandins in animals and humans, will be discussed later in this chapter.

1.B. Plant oxylipins and their functional roles

1.B.1 Jasmonic acid and its derivatives

Jasmonates are oxylipin metabolites that play pivotal signaling roles in regulating plant defenses, growth, development and reproduction (Wasternack and Hause, 2013). Jasmonic acid, its methyl ester, and other derivatives are collectively known as jasmonates. They regulate gene expression levels in an integrated network with other plant hormones including salicylic acid, auxin, ethylene and abscisic acid (Wasternack, 2007). Their detailed interaction has been recently reviewed, and exceeds the scope of this thesis, so will not be discussed further (Wasternack and Hause, 2013).

The biosynthesis of jasmonates starts in chloroplasts, which are organelles where photosynthesis occurs. As the first step, 18:3 fatty acid, or α-linolenic acid (α-LeA) is thought to be released from the *sn*-1 position of chloroplast galactolipids by phospholipase 1 (PLA_1). PLA_2, another

large family of phospholipase, are not involved in releasing α-LeA, although the particular PLA_1 catalyzing this release is still an ongoing debate. Expression levels of PLA_1 in tobacco under different stresses indicated that the lipase responsible in α-LeA release may vary following different kinds of stress (Bonaventure *et al.*, 2011). Oxidation, or oxygenation of α-LeA, catalyzed by lipoxygenases (LOX), is the next step of oxylipin biosynthesis. Oxygen molecules could be incorporated in the 9- position by 9-LOX, but the 13-LOX pathway is the one leading to jasmonates. The enzyme LOX2 was proposed to be the major enzyme in jasmonate biosynthesis (Bell *et al.*, 1995), yet recent work revealed that each 13-LOX play its own individual role in this process, and LOX6 is actually the main enzyme in wound-induced JA synthesis (Caldelari *et al.*, 2011). Allene oxide synthases (AOS) and allene oxide cyclases are enzymes that catalyze subsequent steps, and they are tightly bound to substrate and lipid membranes in chloroplasts (Farmaki *et al.*, 2007, Neumann *et al.*, 2012). These enzymes help form allene oxides and connect the 9- and 13- carbon atoms to yield the metabolic product 12-oxo-phytodienoic acid (OPDA), an electrophilic cyclopentenone oxylipin. Labeling experiments indicated that the tight binding of these enzymes to membrane lipids is consistent with OPDA being predominantly synthesized not from free α-LeA, but from esterified α-LeA esters in galactolipids, and the initial products are the corresponding OPDA-containing galactolipids. Monogalactosyl diacylglycerides (MGDG) and digalactosyl diacylglycerides (DGDG) have been identified with OPDA esterified in the *sn*-1 and *sn*-2 positions and have been shown to be accumulated in response to wounding (Buseman, 2006, Hisamatsu *et al.*, 2003, Hisamatsu *et al.*, 2005, Kourtchenko *et al.*, 2007, Stelmach, 2001).

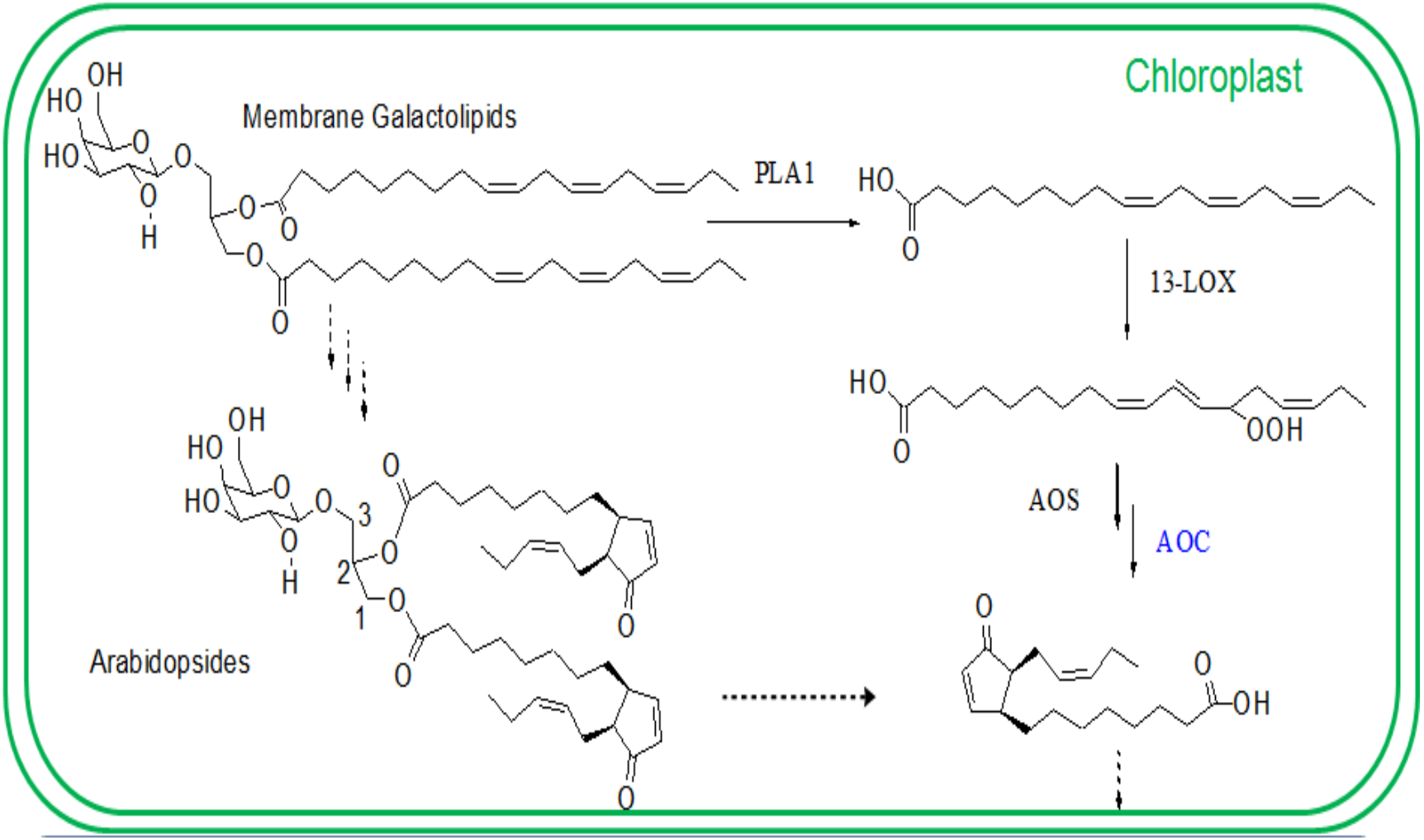

Figure 1.4. Biosynthesis of jasmonates in plant cells. Green, blue and brown boxes indicate cellular locations for biosynthesis reactions. Crystallized enzymes are highlighted in blue fonts. Solid arrows represent known reaction or transportation while dashed arrows represent putative reaction and/or transportation. See text for abbreviations. Adapted from (Wasternack and Hause, 2013) . For interpretation of the references to color in this and all other figures, the reader is referred to the electronic version of this dissertation.

Figure 1.4 (cont'd)

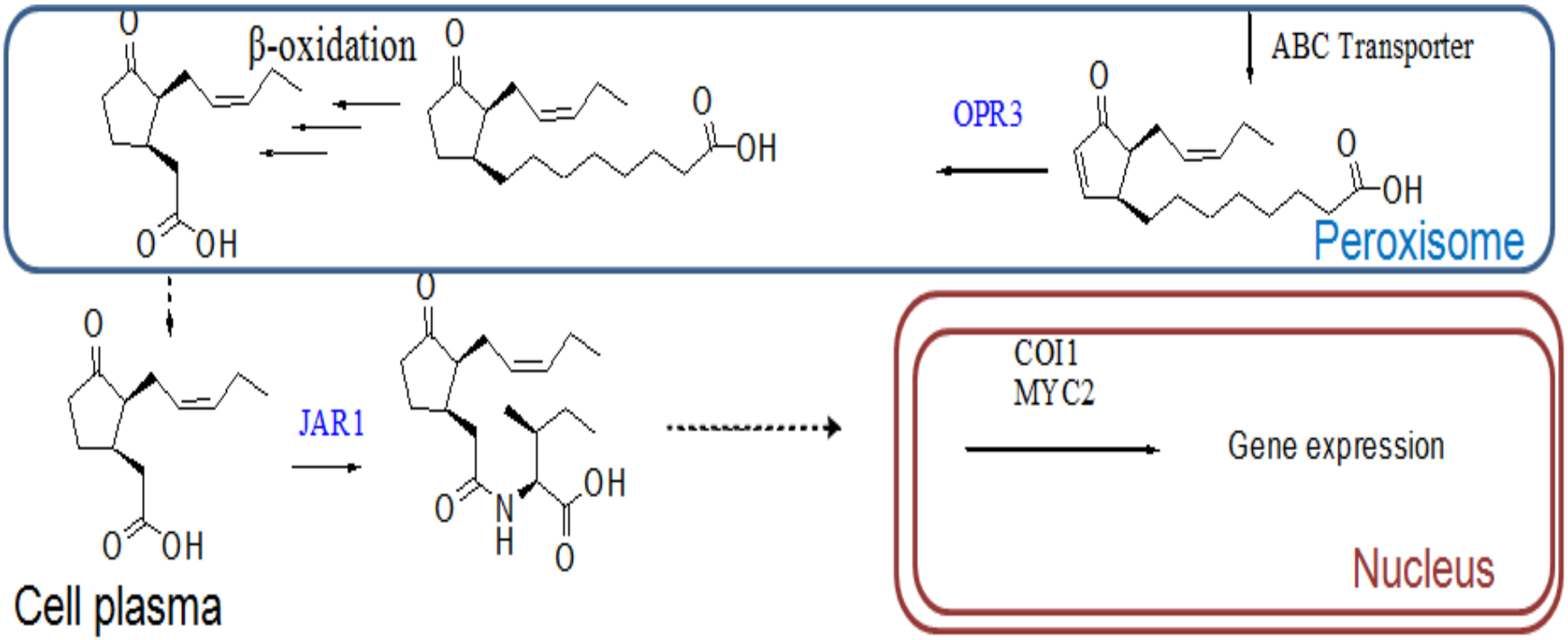

Following its release from chloroplast membranes, OPDA is then transported into peroxisomes, which are organelles common to eukaryotic cells that perform assorted functions including β-oxidative catabolism of fatty acids, where the double bond in the cyclopentenone is reduced. OPR3 is the only one of 6 OPR genes that participates in JA synthesis, and the *Arabidopsis* knockout mutant *opr3* was shown to be JA deficient. These mutants were exploited to distinguish JA and OPDA signaling(Stintzi *et al.*, 2001). However, JA accumulation was still observed in some cases, proposed to occur through RNA splicing resulting into full length functional OPR3 (Chehab *et al.*, 2011), suggesting *opr3* may not be a perfect tool in studying OPDA signaling. After reduction of the conjugated double bond, OPC:8 is subjected to 3 rounds of β-oxidation leading to jasmonic acid, which is then released into the cytoplasm where it is conjugated to isoleucine by JAR1, and this JA-isoleucine conjugate (JA-Ile) is the active form of JA(Staswick and Tiryaki, 2004). The JA-Ile binding co-receptor complex was recently characterized and crystallized, as "the missing link" that explains the pivotal mechanism in JA signaling in terms of how JA accumulation triggers defense gene expression. (Fonseca *et al.*, 2009, Sheard *et al.*, 2010).

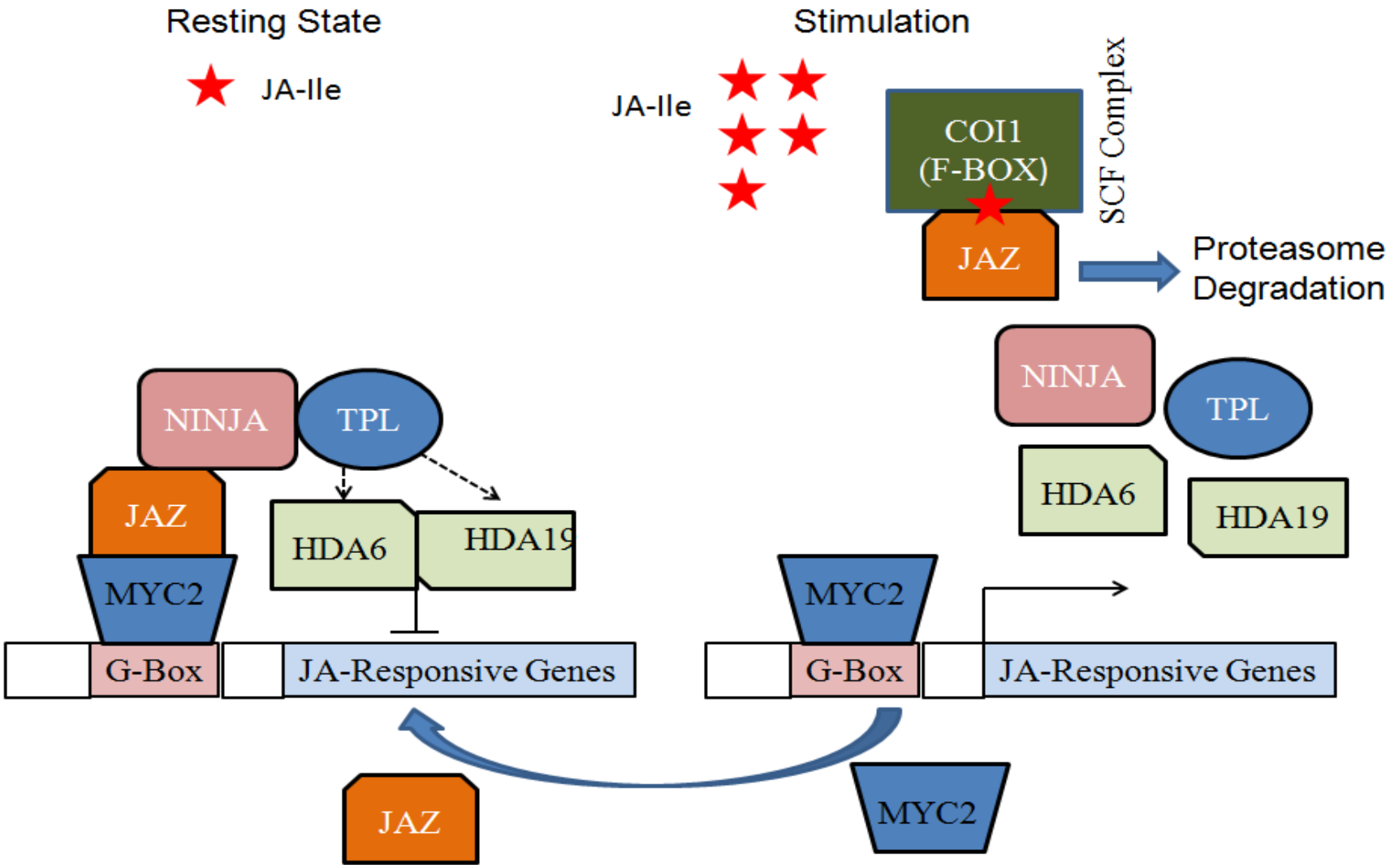

Figure 1.5. Transcriptional regulation of JA-Ile signaling. Stars represent JA-Ile. Boxes in different shapes represent various transcription factors (proteins). Black arrows represent positive interactions (induction) while ⊥ represent negative interactions (inhibition). Known interactions are shown in solid symbols and putative interactions in dashed symbols. See text for abbreviations. Adapted from(Wasternack and Hause, 2013).

Jasmonate biosynthesis is mainly regulated by available substrates, a positive feedback loop, as well as other signaling mechanisms (Wasternack and Hause, 2013). One major point of regulation comes from the competition of substrates between enzymes AOS and hydroperoxide lyase (HPL). HPL enzymes, as shown in Figure 1.8, give rise to a family of both volatile and non-volatile aldehydes and oxo fatty acids, which are herbivory-induced direct defense compounds (Andreou *et al.*, 2009, Matsui *et al.*, 2006). One HPL genes in rice, through substrate competition, down-regulated jasmonate synthesis, indicating a potential mechanism for plants to modulate HPL and AOS (Jasmonates)mediated defense mechanisms. (Tong *et al.*, 2012).

The positive feedback loop in regulating jasmonate biosynthesis comes from the action of the co-repressor complex MYC2-JAZ. MYC2 is a gene expression promoter of JA-responsive genes, which include the genes involved in JA biosynthesis such as LOX, AOS, AOC and OPR. Jasmonate ZIM domain proteins (JAZs), which bind to MYC2 and prevent the latter from functioning, are considered negative regulators for the same group of genes. JAZ is rendered to proteolytic degradation as a result of JA-Ile accumulation, in stimulation state, as illustrated in Figure 1.5 (Chung *et al.*, 2008) .

Additional regulation of jasmonate biosynthesis can be found in the network of stress-induced signaling, such as from Ca^{2+}, which is itself an important second messenger in plant response to stimuli (Kudla *et al.*, 2010). Ca^{2+} mediates control of LOX activities (Bonaventure *et al.*, 2007). Another example lies in the salicylic acid (SA)-induced down-regulation of both the basal and induced biosynthesis of JA. This repression effect can be abolished by a Ca^{2+} binding transcriptional factor (TF) through reducing SA accumulation levels (Du *et al.*, 2009, Qiu *et al.*, 2012).

JA sensing and signaling depend on ubiquitin and proteasome systems. In a Skp1/Cullin/F-box (SCF) complex, the F-box protein recognizes the protein tagged with ubiquitin and subsequently degraded in proteasome. COI1, which forms a complex with JA-Ile and JAZ, the JA signaling repressor, play the F-box role for JAZ degradation and activation of JA signaling (Xie *et al.*, 1998). This is illustrated in Figure 1.5.

In a breakthrough of finding missing links, JAZ proteins were discovered as important regulators of JA signaling through interactions with multiple TFs and JAZ themselves. Up-regulated by wounding or JA treatment themselves, their degradation allows release of TFs that activated JA signaling (Chini *et al.*, 2007, Thines *et al.*, 2007, Yan *et al.*, 2007). Their downstream component, general co-repressors such as TOPLESS (TPL) proteins and their interaction with the "Novel Interactor of JAZ" (NINJA) proteins were later discovered (Pauwels *et al.*, 2010). HDA 6 and HDA 19 are other examples of JAZ downstream co-repressors that interact with JAZ (Chini *et al.*, 2009, Pauwels and Goossens, 2011). There are 12 JAZ proteins in *Arabidopsis* that can form JAZ-JAZ homo- or hetero-dimers, the functions of which are still largely unknown (Chung *et al.*, 2010, Chung and Howe, 2009). The expression of JAZ gene is also JA responsive, suggesting a fine-tuning in JA signaling (Chung, *et al.*, 2008).

Apart from its direct role in gene expression levels, JA and its derivatives are also believed to act as messenger signals for systemic defense response. Systemic signals molecules transfer information from locally wounded tissues to other healthy tissues within the same plant. The best studied systemic response was in tomato, where an 18-aa peptide systemin was produced in splicing the prosystemin in response to wounding. This systemin activates the expression of JA biosynthesis enzymes including AOC, and therefore triggers the accumulation of JA. JA-dependent prosystemin expression and the common location of AOC and prosystemin expression

in vascular bundles indicate their role in systemic signaling (Narvaez-Vasquez and Ryan, 2004, Stenzel *et al.*, 2003). In systemic leaf, JA signaling, instead of both signaling and biosynthesis, has been shown to be essential for systemic defense response, which further supports the hypothesis that JA (or its isoleucine conjugate) is the systemic signal (Schilmiller and Howe, 2005). Labeling experiments also showed that ^{14}C-JA is relocated from leaves to roots, and spatially distributed according to phloem-based transportation (Zhang and Baldwin, 1997).

In addition to vascular signals, airborne signals act as much faster systemic signals in response to herbivory and wounding. Volatile compounds mediated defense response in nearby plants is also well known (Heil and Silva Bueno, 2007). MeJA, as a much more volatile form of JA, has potent gene regulator activity (Farmer and Ryan, 1990) and is therefore thought as a volatile systemic signal, as shown in Figure 1.7. The overall defense response is thought to be the sum of airborne signal triggered defense and the vascular signal, while the former is faster and less intense and the latter is slower but more potent (Heil and Ton, 2008).

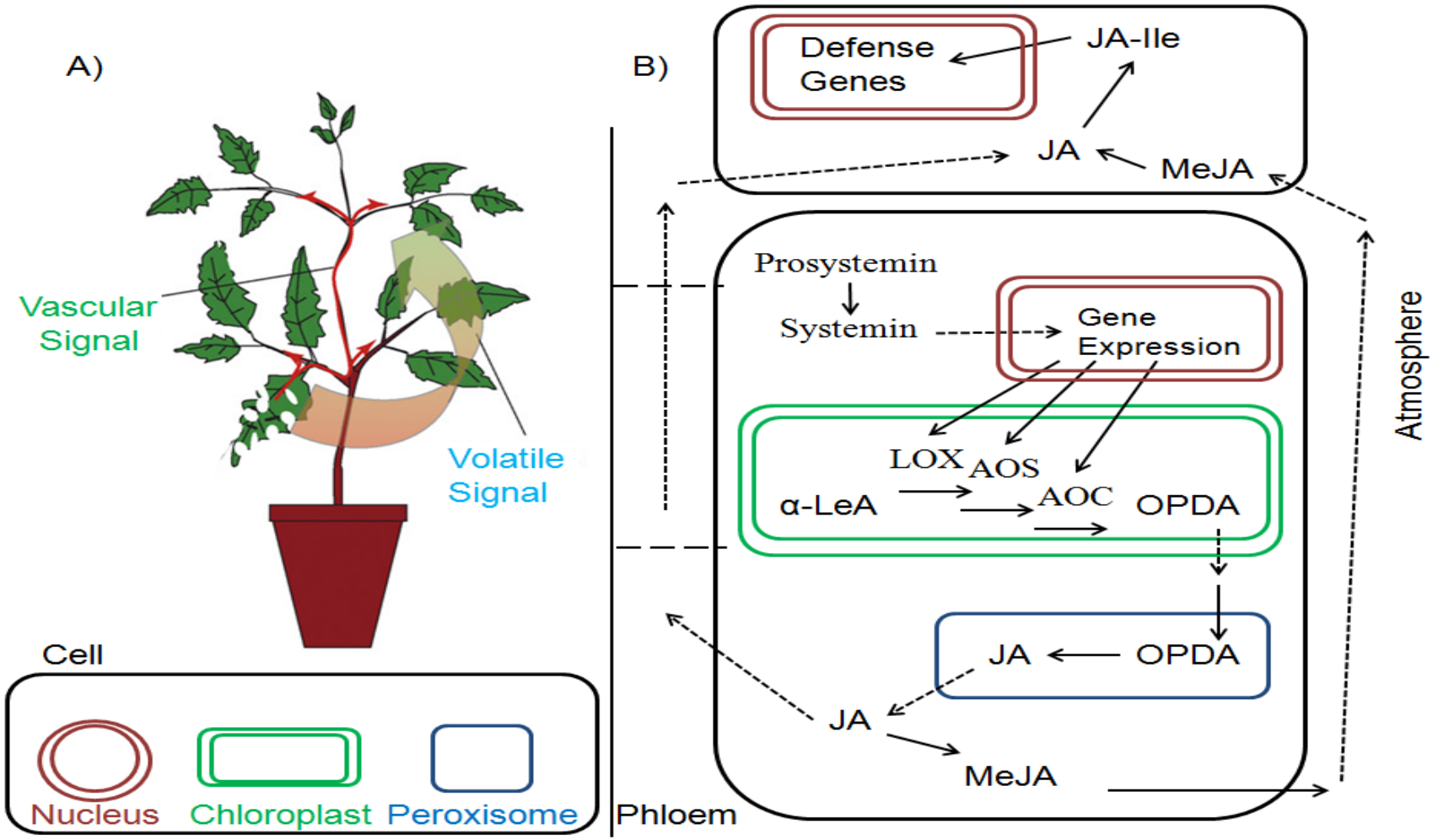

Figure 1.6. Airborne and vascular signaling in systemic response to localized herbivory stress. (A)Vascular signals are proposed to be conducted through phloem while airborne signals through volatile compounds. (B) Green, brown and blue boxes indicate cellular locations for biochemical reactions. Known reactions and transportation are shown in solid arrows while putative reactions are in dashed arrows. Adapted from (Heil and Ton, 2008).

1.B.2 OPDA biological activities as a signaling molecule

12-oxo-phytodienoic acid (OPDA), a precursor of JA, has also been shown to be an independent gene expression regulator in plant signaling. Multiple defense genes, with a small overlap with JA-responsive genes, were shown to be activated by accumulation of OPDA in mutant *opr3*, which is JA deficient (Taki *et al.*, 2005). OPDA was also shown to not be a good ligand for the COI1-JAZ complex, which further supported OPDA's independent role (Sheard, *et al.*, 2010). Although the details of its functions have not been established as extensively as for JA, it is believed that its activity derives from its electrophilic α,β-unsaturated ketone moiety (Farmer and Davoine, 2007). Additional evidence has been found for OPDA-specific signaling in plant response to stress (Wasternack *et al.*, 2013). Tendril coiling, the growth of thread-like plant shoots, stems or leaves, often seen in climbing plants such as *Cuscuta*, is mainly promoted by OPDA and much less by JA (Blechert *et al.*, 1999, Mueller *et al.*, 2008). Accumulation of OPDA in the seed coat is preferred for tomato embryo development (Goetz *et al.*, 2012).

Although the regulation of OPDA accumulation is not well understood, OPDA-containing galactolipids are thought to be storage pools of OPDA (Gobel and Feussner, 2009, Mosblech *et al.*, 2009). OPDA is transported into peroxisomes by a ATP-binding cassette (ABC) transporter (Theodoulou *et al.*, 2005). Glutathione conjugation of this electrophilic metabolite is thought to regulate this OPDA pool (Ohkama-Ohtsu *et al.*, 2010).

1.B.3 Activities and biosynthesis of other oxylipins

Jasmonates represent only a small fraction of all oxidized fatty acids or oxylipins with diverse chemical structures (Mosblech, *et al.*, 2009), and new oxylipins continue to be discovered. These compounds include fatty acid hydroperoxides, hydroxy-, oxo-, or keto fatty acids, divinyl ethers and volatile aldehydes.

Starting with 16:2, 18:2 or 18:3 fatty acids, LOX catalyzed oxidation yields hydroperoxy hexadecadienoic acid (HPHD), hydroperoxy octadecadienoic acid (HPOD) or hydroperoxy octadecatrienoic acid (HPOT), as shown in Figure 1.7. Upon further oxidation by LOX, keto-fatty acids including oxo-hexadecadienoic acid (KHD) or oxo-octadecadienoic acid (KOD) are formed.

Oxylipins may also be formed non-enzymatically following oxidative stress through reactions of PUFA with reactive oxygen species (ROS). Different positional isomers and stereoisomers are usually indications of non-enzymatic formation oxylipins formed via free radical chain reactions, leading to a variety of peroxy fatty acids and subsequent epoxy, keto fatty acids and alkenals, as shown in Figure 1.7.

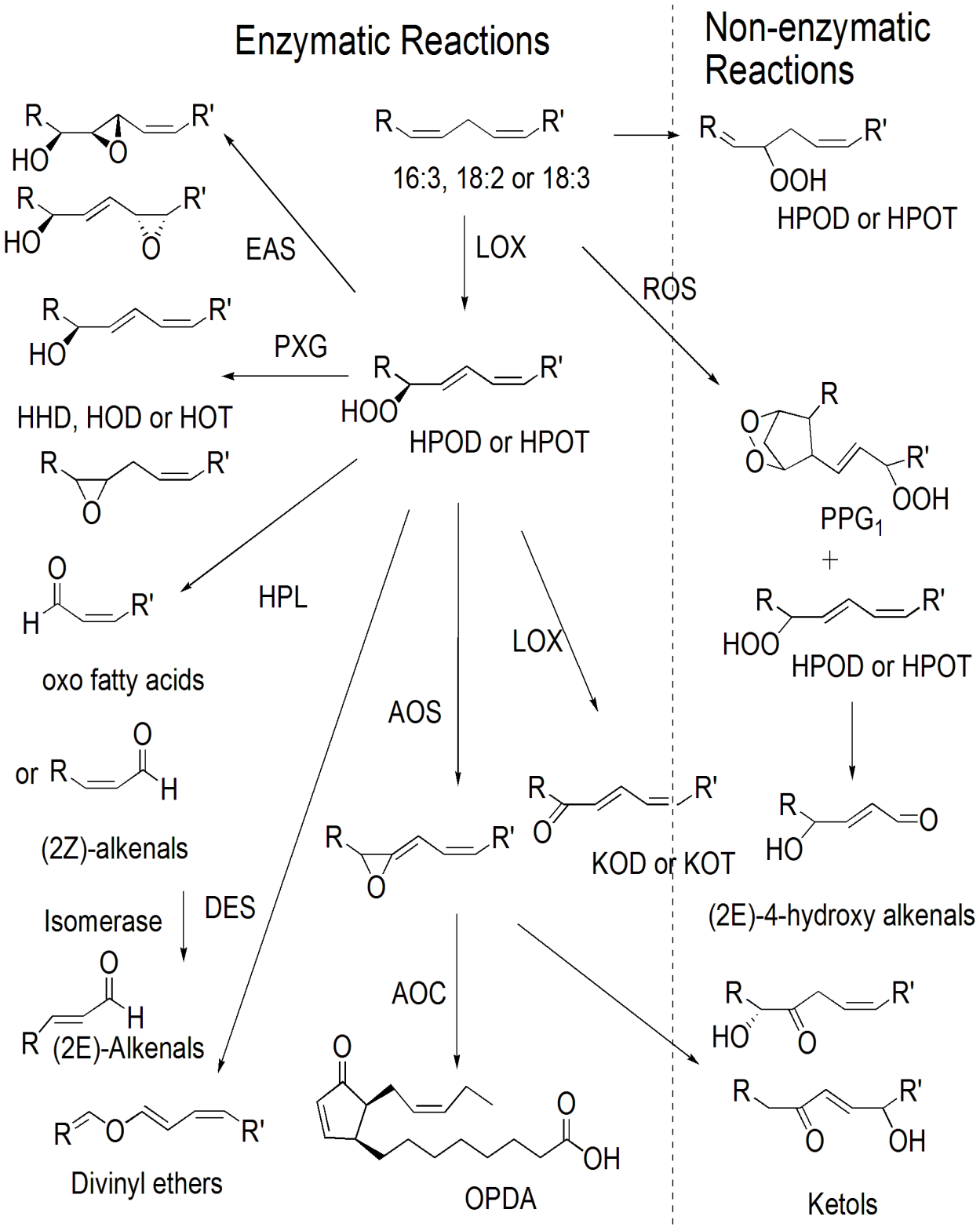

Figure 1.7. Biosynthesis of JA and other oxylipins in plants. For enzymatic reactions, enzymes are labeled alongside the arrows in upper case fonts. See text for abbreviations. Adapted from (Mosblech, *et al.*, 2009).

1.C. Glutathione *S*-transferases family and functions

1.C.1 Glutathione as antioxidant and detoxification reagent

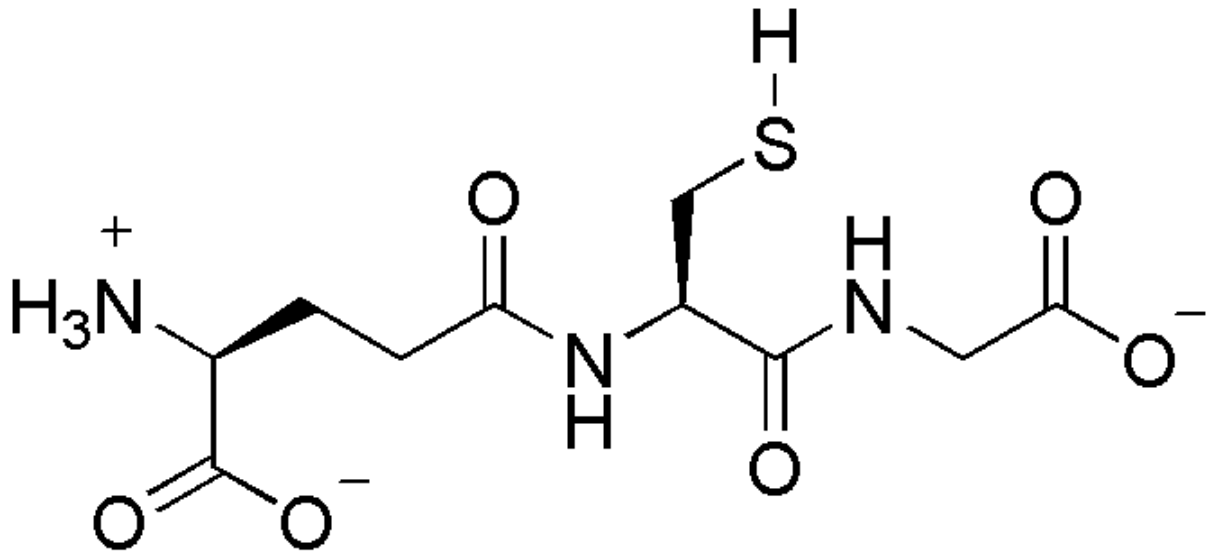

Figure 1.8. Molecular structure of glutathione shown as a zwitterion (ion with both positive and negative charge(s)) as the most common existing form in aqueous solution.

Glutathione (GSH), an abundant cysteine-containing tripeptide in virtually all cells, plays an essential role in detoxification and many other biological processes. As shown in Figure 1.8, glutathione has 3 amino acid residues and most importantly, a nucleophilic sulfhydryl group. Glutathione, as a reducing reagent and a nucleophile, readily reacts with exogenous and endogenous oxidative and electrophilic compounds (Dixon *et al.*, 1998b, Noctor and Foyer, 1998). These compounds are mostly excreted in urine in animals (Suzuki and Sugiyama, 1998) and into vacuoles in plants (Bleuel *et al.*, 2011, Tommasini *et al.*, 1998, Wolf *et al.*, 1996). Glutathione can be oxidized into its disulfide form, namely GS-SG, which contains a disulfide bond that is similar to the disulfide bonds found in most peptides and proteins. This reaction is often catalyzed by glutathione peroxidases, using hydrogen peroxide, or peroxide of fatty acids or other lipids that result from cellular oxidative stress (Dixon, *et al.*, 1998b). Glutathione can be also involved in C-S bond forming addition or substitution reactions, which are also usually

referred to as conjugation reactions. This dissertation will focus on several aspects of these reactions because they represent a sink for reactive electrophiles that are involved in many aspects of cell functions.

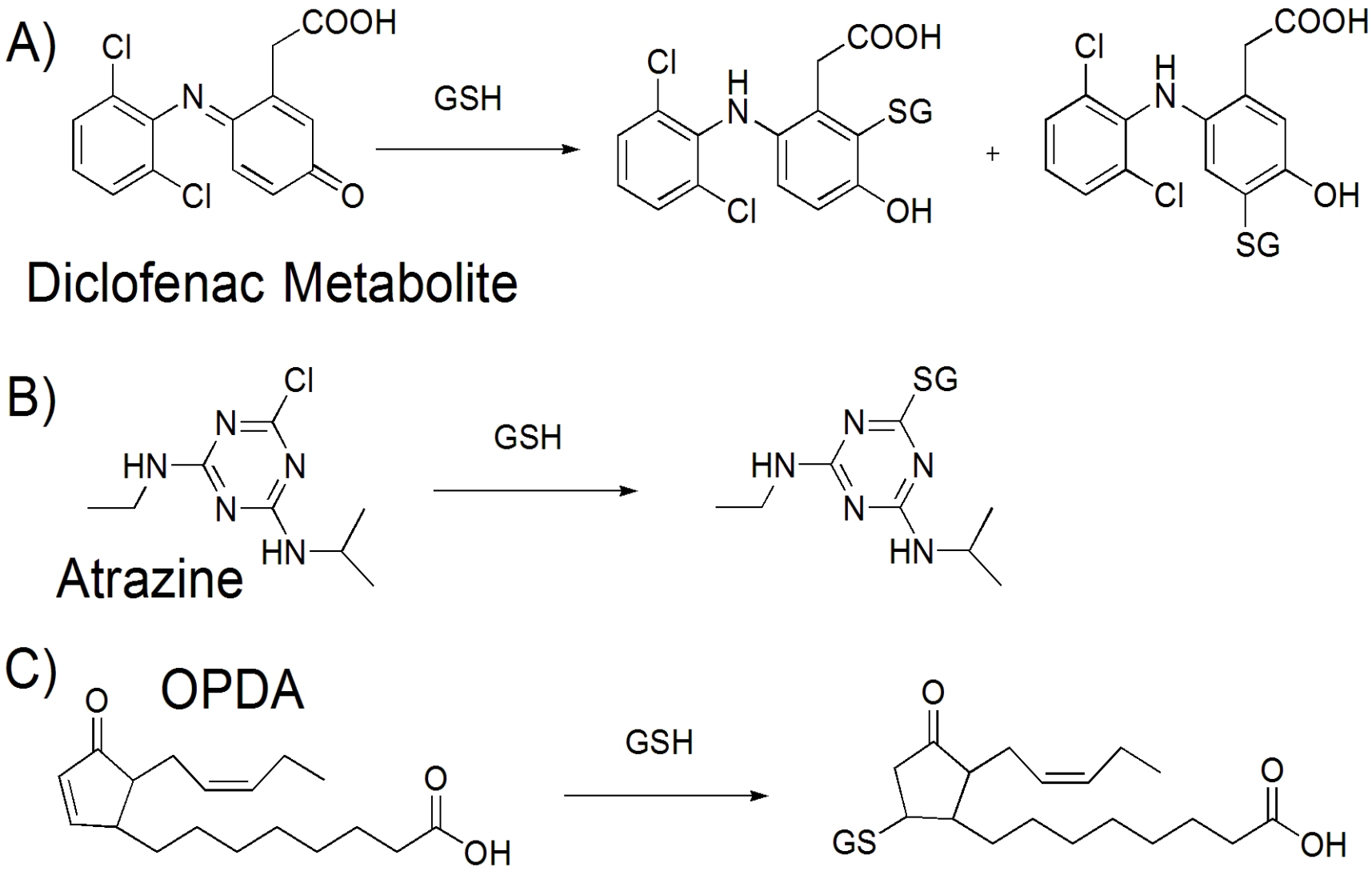

Figure 1.9 Glutathione involved conjugation reactions. A) conjugation of a quinone-like compound, a human metabolite of drug diclofenac. B) conjugation of atrazine, a widely applied herbicide, in both exposed animal and plant cells. C) conjugation of OPDA, an endogenous electrophilic oxylipin. Adapted from (Dixon *et al.*, 2010).

Several examples of GSH conjugation reactions are presented in Figure 1.9, and these are catalyzed by an assortment of glutathione *S*-transferase enzymes, though most are spontaneous even in the absence of enzymes at neutral pH. In fact, most GSTs activity assays have to be performed at pH 6, rather than in physiological pH as in many assays of other enzymes, because at higher pH the spontaneous non-enzymatic reactions would have been too fast to render the enzyme activity assay not accurate. In A) shown is a typical glutathione conjugation in human body to a metabolite of drug diclofenac after *in vivo* oxidation. This is a Michael addition to quinone resulting into products with aromatic benzene ring structures (Waldon *et al.*, 2010). In B) shown is a glutathione conjugation reaction with atrazine, a widely used herbicide. This is a typical detoxification reaction in plants (Dixon, *et al.*, 2010). In C), the substrate is 12-oxo-phytodienoic acid (OPDA), a plant hormone with α, β-unsaturated ketone structural feature in the cyclopentenone moiety. After the product, GS-OPDA was found in the plant extract, this reaction, as one of the few known glutathione conjugation to endogenous oxylipins in plants, has been proposed to be the reaction to regulate OPDA activity (Davoine, 2006).

1.C.2 Glutathione transferases family in animals and plants

Glutathione transferases make up a superfamily of enzymes that play important roles in detoxification and other non-stress processes in cells in both prokaryotes and eukaryotes. GSTs (previously termed glutathione *S*-transferases), recognized as due to their similar gene sequences, catalyze the conjugation of glutathione to diverse substrates, although some possess no catalytic activity but do catalyze other GSH-related functions as peroxidases, isomerases, and display ligand binding capabilities (Frova, 2006).

The modern capabilities of fast DNA sequencing and bioinformatics have opened new windows into protein structures and functions. The exploration of GSTs is a good example in this research

trend. Unlike in the past, when GSTs were discovered by purification and assay of enzymes, now the availability of GST gene sequences in many organisms accelerated recognition of the existence of many previous unknown GSTs, although their detailed functions have yet to be explored.

Taxa	Common		Specific	
Mammals	Zeta(Z)	2	Alpha(A)	4-6
	Theta(Θ)	2	Mu(M)	5-6
	Omega(O)	1	Pi(Π)	1-2
	Sigma (Σ)	1		
Plants	Zeta (Z)	2	Phi (Φ)	?-16
	Theta(Θ)	1-3	Tau (T)	?-39
			Lambda(Λ)	1-2
			DHAR	1-3
Bacteria	Theta(Θ)	?	Beta(B)	6-15
	?			

Table 1.1. Existence and distribution of GST genes. Genes are classified into families which are named using Greek letters. Families of GSTs that are common to animals, plants and bacteria are shown on the left side while the families specific to each kingdom are shown on the right. Questions marks represent unknown number of genes. Adapted from (Frova, 2006) .

Listed in table is the distribution of cytosolic GST genes in the biology kingdom, where GST families are named in Greek letters. Most GSTs are cytosolic, with the exception of microsomal GSTs and plasmid-encoded GSTs. The GST superfamily consists of 15-20 GSTs in human and other mammals (Hayes *et al.*, 2005) and as many as around 50 in *Arabidopsis thaliana* and other

plants (Frova, 2003, Soranzo *et al.*, 2004). Phi and tau are two plant-specific families of GST that have been proposed to have catalytic activity in glutathione conjugation (phi family for flavonoid transportation as well) , but their detailed functions and substrate specificities are still largely unknown (Dixon, *et al.*, 2010).

The GST families can be further explored with gene sequence similarity. In *Arabidopsis*, the comparison of GST gene sequences yielded a phylogenetic tree (Wagner *et al.*, 2002) built based on a multiple sequence alignment of the full length protein amino acid sequences (Wagner, *et al.*, 2002). Distances between GST genes represent their relative dissimilarity. Most members belong to the phi and tau family, while others in zeta and theta are also shown. Roughly the tau family can be divided into 3 subfamilies: *At*GSTU1-10, 11-18 and 19-28. Phi family can also be viewed as the sum of two subfamilies: *At*GSTf1-8 and 9-14.

1.C.3. Plant Glutathione *S*-transferase structures and functions

Most cytosolic GSTs are dimers in solution, either homodimers or heterodimers. Each unit in GST dimers is encoded by individual GST genes and with a molecular weight of around 25 kDa. Heterodimers are only possible within each family due to structure compatibility.

Dimeric GSTs are usually spherical in shape in solution. Shown in Figure 1.10 are space-filling models of GST structure. From genomic DNA sequences, most GSTs are thought to have two binding domains, one near each N-terminus for glutathione, where the gene sequences are fairly conserved in the superfamily; and the other one near the C-terminal, which could be quite different even between close neighbors within the same family, indicating diverse substrate preferences(Edwards *et al.*, 2000). The 3-D structure is surprisingly conserved throughout the superfamily, suggesting the necessity of this 2 domain structure in catalyzing conjugation reactions.

In the glutathione binding domain, highly conserved Tyr7 (mammalian Alpha/Mu/Pi families) or Ser17 (common Theta and Zeta, and the plant specific Phi and Tau) are essential for glutathione transferase activity. This has been proved by site-oriented mutagenesis in tyrosine of porcine Pi (Dirr *et al.*, 1994) and the serine of human Theta (Tan *et al.*, 1996), insect Delta (Caccuri *et al.*, 1997) and plant Zeta (Thom *et al.*, 2001) enzymes.

Figure 1.10 3-D crystal structure of the *Arabidopsis* phi family glutathione *S*-transferase (GST) dimer *At*GSTF2. α-helices are shown in pink and β-folds are shown in yellow. This dimer structured GST was crystallized with *S*-hexyl glutathione together. Each unit has one N-terminal domain for glutathione, which is close to the dimer interface, and one C-terminal domain for the substrate, which interacts with the *S*-hexyl (gray colored) chain. This image was generated from http://www.pdb.org/pdb/explore/explore.do?structureId=1GNW.

Data from mRNA microarrays have been helpful in suggesting enzyme expression levels and providing suggestions and testing hypothesizes in gene functions. GST expression data are now integrated into a user-friendly website for fast and straightforward access (https://www.genevestigator.ethz.ch/at/). Many plant GSTs are expressed individually and specifically in tissue distribution and timing in response to stress. *At*GSTF8 and *At*GSTU19 were shown to be expressed mainly in root, especially in lateral root cap. *At*GSTU5, sharing a similar transcript expression pattern in root at weaker abundances, was expressed in adult leaf. *At*GSTU17 was primarily expressed in adult leaf. *At*GSTU13, 16 and 18 were also expressed in leaf tissues, although they each are expressed in other tissues.

Most GSTs are thought to have transferase activities toward either exogenous or endogenous compounds, but the substrates in the plant kingdom have remained largely unidentified. Phi family GSTs in maize were first shown to catalyze conjugation to xenobiotics (Mozer *et al.*, 1983). Similar activities were also found later for tau family GSTs (Dixon *et al.*, 1998a). Expression and *in vitro* incubation, and observation of *in vivo* herbicide resistance supported this hypothesis (Dixon *et al.*, 2009, McGonigle *et al.*, 2000, Milligan *et al.*, 2001, Skipsey *et al.*, 2005).

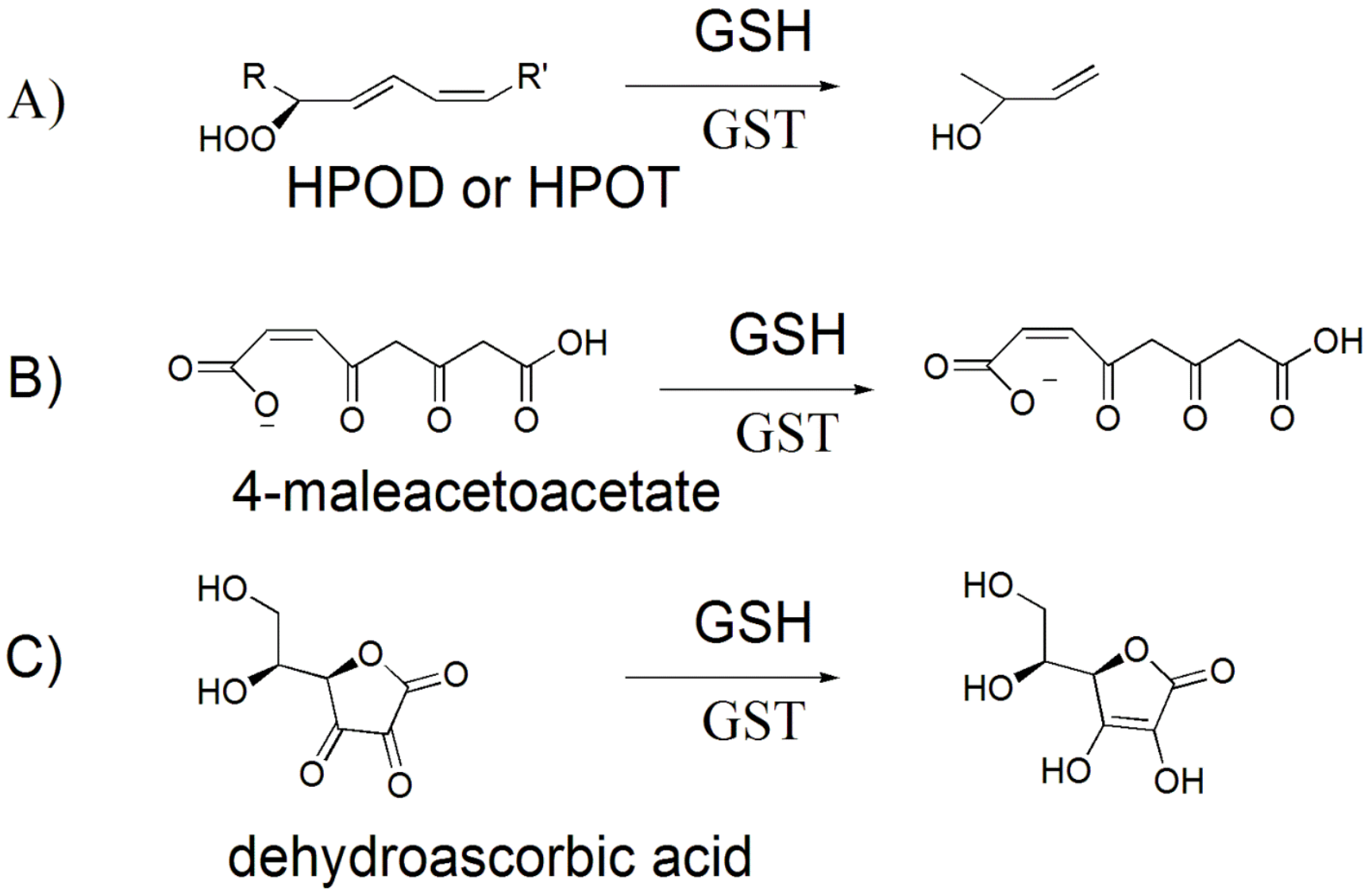

Figure 1.11 GSH and GST in non-conjugating reactions. A) Reduction of fatty acid peroxides. B) Isomerization of 4-maleylacetoacetate. C) Reduction of dehydroascorbic acid. Adapted from (Dixon, *et al.*, 2010) .

Many GSTs also participate in other GSH-involving, but non-conjugating reactions. The most well known such reaction is peroxidase activity, in which GSH serves as reducing agent to reduce fatty acid peroxides, as catalyzed by many tau, phi and theta family GSTs (Figure 1.11A; (Dixon, et al., 2009). GSH will be accordingly oxidized to GSSG, which can be recycled through glutathione reductase. The GSSG to GSH ratio, which serves as a measure of the cell reduction/oxidation (redox) potential, must be tightly regulated as a vital part of cell function. Another example lies in the families of GSTs where cysteine substitutes the catalytic serine residue. In dehydroascorbate reductase (DHAR) family, for example, GSTs catalyze the reduction of dehydroascorbate to ascorbic acid using GSH as reductant (Dixon *et al.*, 2002); Figure 1.11 C). Lambda family GSTs have an analogous cysteine amino acid residue, although their oxidative substrates have not yet been discovered. A disulfide bond will be made between GSH and GST in this reaction, but this is displaced by GSH, generating GSSG. GSH may also participate in a reaction as a catalyst, together with zeta family GSTs, to isomerize 4-maleylacetoacetate, as an essential step in tyrosine catabolism (Fernandez-Canon and Penalva, 1998)Figure 1.11 B). Similar activities have been found in animals and plants and fungi (Dixon and Edwards, 2006).

1.D. Gene function study strategies

1.D.1 Knock out mutation and other techniques in gene function research

Forward genetics, i.e., the strategy of looking for the unknown genotype responsible for a known phenotype, was widely applied in research of gene functions. Reverse genetics, the opposite approach, or trying to characterize the corresponding phenotype for a known genotype, has become the leading strategy in genetics research in the last two decades(Alonso and Ecker, 2006). The technical advances of genome-wide sequencing and controllable mutagenesis have made it

not only practically possible, but also convenient to perform reverse genetics, which involves creating the cell line or organisms of a certain genotype first and then trying to define its consequent phenotype. Unlike mRNA microarray results or small molecule quantification, both of which only yield indirect proof to support hypothesis about gene functions, reverse genetics provides direct and unambiguous causal relationships to establish gene functions(Krysan *et al.*, 1999) unless gene redundancy prevents knockout mutants from exhibiting phenotypes.

In *Arabidopsis*, knockout mutants are mostly obtained by insertional mutagenesis. The underlying principles are simple: once a certain length (5 to 25 kb) of foreign DNA is inserted into the middle of a particular gene, the original coding sequence is disrupted and the corresponding transcripts and translated proteins are no longer functional any more. The insertion is usually performed with infection of bacteria such as *Agrobacterium tumefaciens* or *Agrobacterium rhizogenes*. These wildtype bacteria will transform their plasmid DNAs into the plant host cell nucleus where these plasmid DNAs are integrated into plant DNA and expressed to induce a plant tumor and provide food for bacteria to survive and reproduce. In genetic use, the tumor inducing DNA fragments are removed and substituted with the gene(s) that researchers want to introduce (or null sequences for knockout genes) and a marker(Valvekens *et al.*, 1988). This method has been optimized from transforming root tissues, to seeds, and to whole plants for higher successful rates and throughput(Bechtold *et al.*, 1993, Feldmann and Marks, 1987).

The mechanism of T-DNA insertion can be best illustrated as in Figure 1.12. Once an insertion occurs in the coding region of a gene, depending on the exact location of the insertion, total or partial loss of function of this gene can occur. Insertion in the promoter region will alter the transcript level of the gene. Other phenomenon such as multiple insertions in the same gene or

chromosome rearrangement in the gene region can also result in the total loss of gene function, but in different mechanisms.

Because the exact position of insertion on the plant chromosomes cannot be directly controlled, a large number of transformed plants need to be screened to isolate the knockout mutant of a particular gene of interest. Efforts have been made to generate knockout mutants for as many genes as possible. The ultimate goal is to achieve comprehensive genome single point mutagenesis.

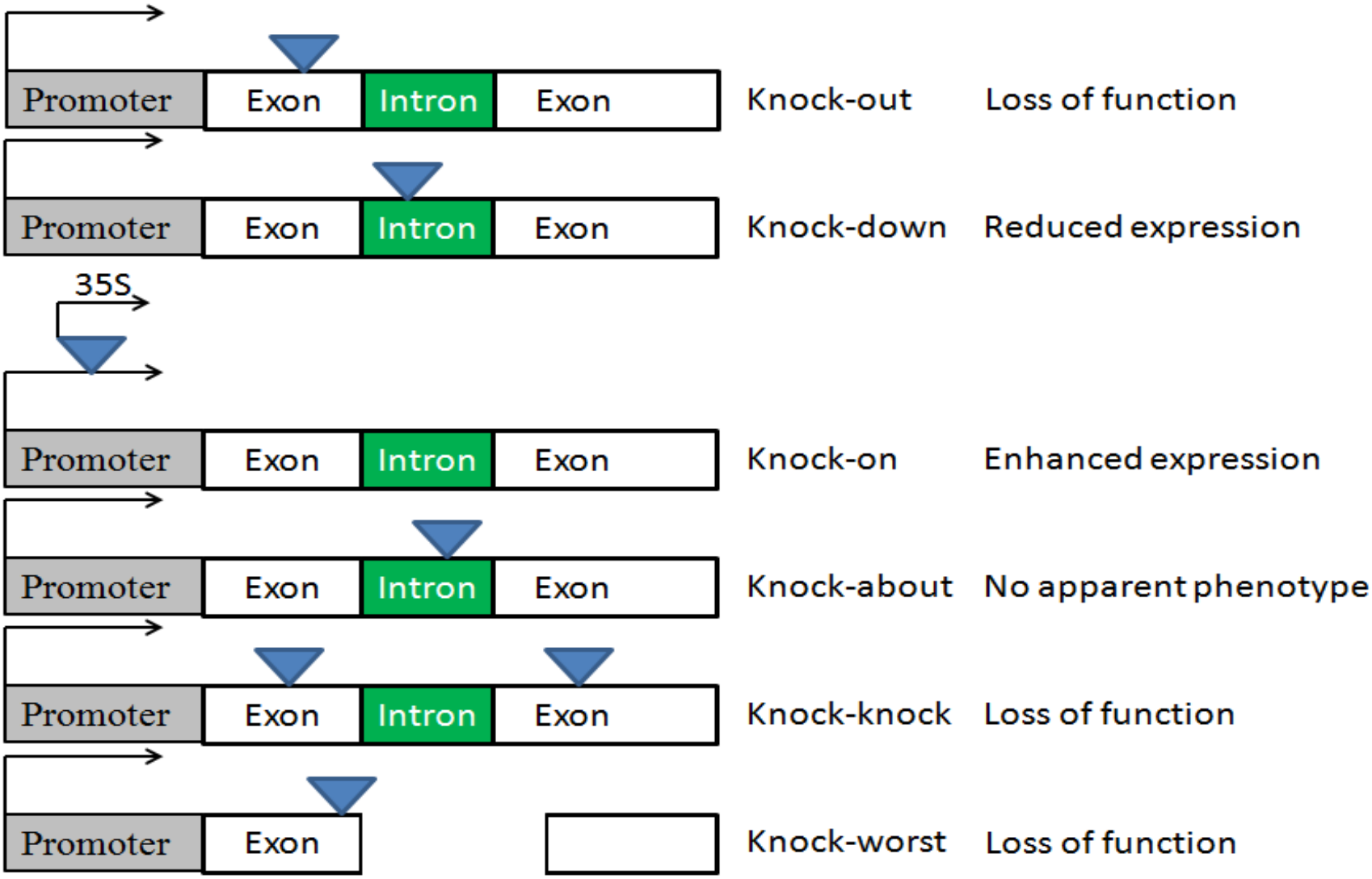

Figure 1.12. Different results from T-DNA insertions into Arabidopsis chromosomes at various locations. Shown at the left side are the layout of the gene (including intron and exon) and its promoter with T-DNA inserted at various locations. Shown at the right side are the nomenclature of the event and consequent gene expression alterations. Adapted from(Krysan, *et al.*, 1999) .

1.D.2 Proteomics and metabolomics as tools for gene function discovery

Reverse genetic approaches to gene function discovery require powerful tools for comprehensive definition of phenotypes in knockout mutants. When genes have functions relevant to metabolism, a non-targeted approach for metabolite profiling is appropriate. Metabolomics, named similar to genomics and proteomics, is a fast emerging research field that aims to provide such information. The metabolome is defined as the complete suite of all small molecules present in a biological context, and represents the metabolic phenotype of the organism resulting from influences of both genotype and environment(Saito and Matsuda, 2010). Assessment of metabolomes relies on recent advances in analytical methods, most notably high throughput liquid chromatography (LC) and mass spectrometry (MS) in the past two decades.

Metabolomics research plays a pivotal role in understanding gene functions, particularly for enzymes. Identification of the sequence of a new gene often cannot unambiguously characterize its functions, although similarity to known sequences to some extent provides some indication of potential functions(Sumner *et al.*, 2003). Expression level data from microarray experiments and proteomic studies reveals the timing, tissue distribution, and relative quantity of the expression of genes and complement our understanding of gene functions. Protein interaction research helps in discovering signaling pathway and understanding the network of gene function regulations. However, only until small molecule research characterizes and quantifies the substrates and products, this process can be completed as a confident and comprehensive description of the functions of this gene(Fridman and Pichersky, 2005). This is because the information needed for comprehensive description of the catalytic activity of an enzyme, such as preferred *in vivo* substrate, up- and downstream influences in small molecules metabolism, cannot be provided by other research strategies. Nevertheless, metabolomics data alone are not enough to reveal the

complexity of cell functions. Due to factors such as gene function redundancy and enzyme substrate preferences overlapping, many lines of evidence are usually needed for a positive enzyme activity characterization(Humphreys *et al.*, 1999).

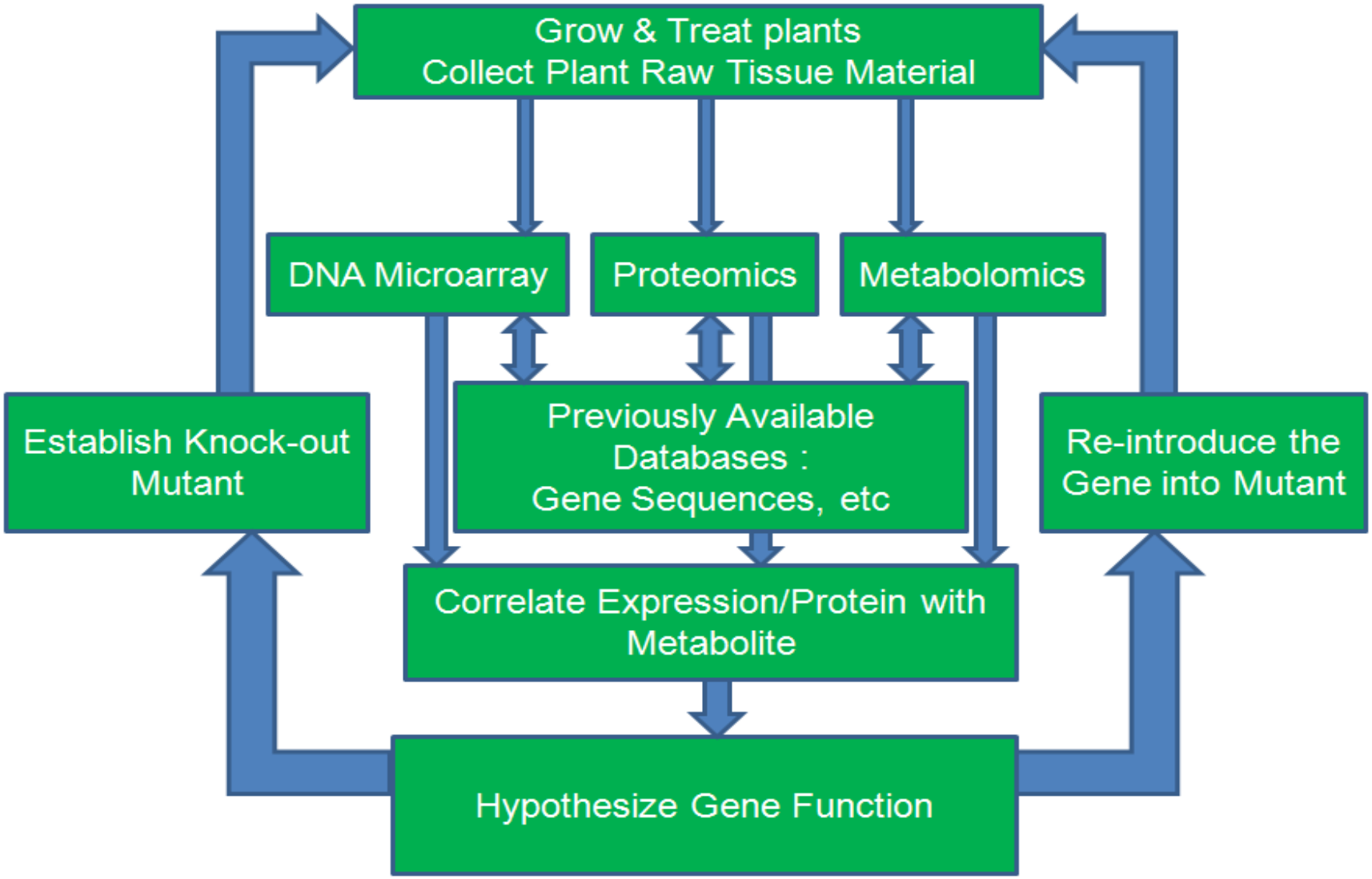

Figure 1.13 Typical workflow for reverse genetics to determine gene functions. Hypothesizes about gene functions are made by combining mRNA/protein/metabolite level data and tested again knockout mutagenesis/complementing experiments. Adapted from (Fridman and Pichersky, 2005) .

Shown in Figure 1.13 is a scheme about the current start-of-the-art work flow of the gene functions workflow in plant biology. Combinations of proteomics and metabolomics data are helpful for developing hypothesizes about biochemical functions, and data from knockout and complemented mutants provide further testing of the hypothesis.

1.E. Research objectives

The overall goal of the research described in this dissertation has been to establish GST gene functions in plant defense signaling. The starting point will be identifying candidate GST genes that are highly expressed in *Arabidopsis thaliana* leaves in response to mechanical wounding. Assessment of GST functions was then assessed by wounding GST knockout mutant plants and profiling the small molecule metabolites to find *in vivo* substrates and products that differ between wild type and knockout plants. For comprehensive profiling of the metabolites and their glutathione conjugates, novel analytical strategies based on LC-MS have been evaluated.

Chapter 2 Proteomic identification of glutathione *S*-transferases from Arabidopsis leaf extract

2.A Introduction of bottom up proteomics

2.A.1 Peptide fragmentation and data-dependent MS/MS for protein identification

Proteomics aims at large scale and global analysis of proteins to understand cell and gene function at molecular level. The term "proteomics" is derived from "protein" and "genomics", indicating the foundation of this new research field (Wilkins *et al.*, 1996). Traditional protein identifications mainly relied on isolation and sequencing of individual proteins, often using Edman degradation for N-terminal sequencing. In recent years, advances in DNA sequencing made comprehensive genomic DNA sequence information available (Lander *et al.*, 2001, Venter *et al.*, 2001), enabling analysis of the more complex proteome, *i.e.*, all protein forms expressed in the biological sample of interest. This concept includes all splice isoforms, post-translational modifications (PTMs), and, unlike genomes, differs across tissues and individual cells are different from cell to cell, and changes in response to endogenous and exogenous stimuli (Han *et al.*, 2008). This challenging task requires an analytical method that can confidently identify and reliably quantify thousands of proteins in the same biological sample, in spite of their distinct abundances and diverse chemical properties. Mass spectrometry (MS) has been recognized as the method of choice for proteome characterization because of its unmatched advantages in unambiguous identification, sensitivity and throughput.

Bottom-up proteomics is the most commonly applied research strategy in this field. Proteomics research is often classified into 3 categories (top-down, middle-down or bottom up) depending on whether the targets directly measured are intact proteins, large peptides or small peptides (Zhang *et al.*, 2013). The bottom-up strategy utilizes proteases, especially trypsin, to digest

proteins into smaller peptides for ease of fractionation, ionization and fragmentation. All these conveniences made bottom-up proteomics more successful in the past decade in handling complex protein mixtures, or shotgun proteomics, named for its similarity to shotgun genomics(Yates, 1998). In a typical bottom-up proteomics research experiment, total protein extracts from biological sample are subjected to enzymatic digestion to yield a more complex mixture of peptides, which is then fractioned through reverse phase liquid chromatography and ionized using electrospray ionization for mass spectrometric analysis. The mass spectrometer then repeatedly performs survey scans of the ions exiting the LC column, and in real-time, uses this information to trigger acquisition of MS/MS spectra of the most abundant peptide ions for structure elucidation. The recorded spectra are then submitted to protein sequences calculated from genomic DNA sequence databases to search for matches with theoretical spectra for known proteins generated from *in silico digestion*. Identifications of peptides are then pooled and grouped for identification of proteins.

2.A.2 Spectral count semi-quantitation

Label-free strategies, being those that do not require chemical derivatization of peptides, are still widely applied in quantification of proteins, although numerous isotopic labeling method has been introduced for accurate and even absolute quantitation (Bantscheff *et al.*, 2007). One label-free method known as spectral counting is commonly used to compare protein abundances between two or more samples. In spectra counting, the numbers of MS/MS spectra generated that match a specific protein have shown good correlations with the relative abundances of the protein detected (Gilchrist *et al.*, 2006, Liu *et al.*, 2004, Washburn *et al.*, 2001). Therefore relative quantitation can be achieved by comparing such number of spectra between experiments. The main advantages of this spectral counting method come from fewer sample preparation steps,

lower costs with absence of isotopic standards, more straightforward normalizing and statistical analysis, extended dynamic range, and the ease of comparing many experiments (Bantscheff, *et al.*, 2007, Zhang, *et al.*, 2013).

In this chapter, the application of proteomic analyses to identify, and quantify with spectral counting, individual glutathione *S*-transferase proteins in leaves of wounded and unwounded *Arabidopsis thaliana* leaves is presented.

2.B Materials and methods

2.B.1 Chemicals

SDS-PAGE sample loading buffer (4x), running buffer (10x) and 12% Ready Gel were purchased from BioRad. Promega Sequencing Grade trypsin was purchased from Promega and stored in -80℃ freezer until use. Protease inhibitor cocktail, glutathione-agarose affinity resin, Comassie brilliant blue R-250, dithiothreitol (DTT), polyvinylpyrrolidone (PVP)**,** *S*-hexyl glutathione**,** glycerol**,** ammonium bicarbonate, tris(hydroxymethyl)aminomethane (Tris), trifluoroacetic acid (TFA), ethylenedinitrilotetraacetic acid (EDTA), iodoacetamide, potassium chloride (KCl), acetonitrile (ACN), formic acid (FA), acetic acid (HAC) and methanol (MeOH) were purchased from SigmaAldrich.

2.B.2 Growth of *Arabidopsis* plants

Soil-grown ecotype Columbia-0 (Col-0) *Arabidopsis thaliana* plants were grown from seed provided by the Arabidopsis Biological Resource Center at Ohio State University, maintained in a growth chamber (at the Michigan State University Growth Chamber Facility) at 22°C under 16 h light (100 µE m^{-2} s^{-1}) and 8 h dark per day. 200 biological replicates for each group of unwounded and wounded were grown. For mechanical wounding treatments, fully expanded rosette leaves on 5-week-old plants were wounded three times by crushing the leaf across the

midrib with a hemostat. This wounding protocol, which resulted in damage to approximately 40% of the leaf area, was administered to approximately six rosette leaves per plant(Chiwocha *et al.*, 2003). Leaf tissues were harvested from control and wounded plants at 12 hours after wounding, frozen in liquid nitrogen immediately and stored in -80°C until use.

Homogenization Buffer (A)	0.1M Tris-HCl	5mM DTT	Inhibitor Mix	2mM EDTA	50g/kg PVP	
Post-Centrifuge-Buffer (B)	10mM K_3PO_4	1mM DTT	Inhibitor Mix	1mM EDTA		
Column Washing Buffer (C)	10mM K_3PO_4					
Column Equilibrate Buffer (D)	10mM K_3PO_4	1mM DTT	Inhibitor Mix	1mM EDTA		
Impurity Washing Buffer (E)	10mM K_3PO_4	1mM DTT	Inhibitor Mix			
GSTs Elution Buffer (F)	10mM K_3PO_4	1mM DTT	Inhibitor Mix	1mM EDTA	0.2M KCl	5mM S-HG

Table 2.1 List of buffers used in extraction and affinity chromatography

2.B.3 Extraction of total protein and Bradford protein assay

All buffers used in extraction and affinity chromatography are listed in Table 2.1. Polyvinylpyrrolidone (PVP) was added to extractions to bind plant polyphenols, DTT to protect proteins from oxidation, inhibitor cocktail to minimize proteolytic degradation, EDTA to form chelates with heavy metal ions, and *S*-hexyl-glutathione and potassium chloride based high ion strength buffer to elute GSTs from the affinity column.

Plant leaf tissues were combined and ground in portions to fine powder in liquid nitrogen with pestle and mortar and mixed with buffer A at a 1:6 (g:mL) tissue to buffer ratio. Mixtures were allowed to thaw at room temperature and combined for each group to extract satisfactory total amount of protein in each sample. Combined samples were then centrifuged at 10,000*g*, 0°C for 20 min using a refrigerated Eppendorf 5804R centrifuge, evaporated using Thermo SPD131DDA Speed-Vac to near complete dryness, reconstituted in 1000 µL of buffer B, and stored at -80°C until use.

2.B.4 Affinity chromatography

Following a well-established method for purification of glutathione *S*-transferases via affinity chromatography(Simons and Vanderjagt, 1977), 1mL of glutathione immobilized on agarose was loaded into a plastic column (i.d=10 mm, bed height =50 mm), washed with 10 mL buffer C, and equilibrated with 2 mL buffer D, all at a flow rate of 3 mL/min. A 1-mL aliquot of combined crude protein extract from plant leaves was loaded, washed with 10 mL of buffer E, and eluted with 4 mL of buffer F, all at flow rate of 0.25 mL/min. Eluate was evaporated using Thermo SPD131DDA Speed-Vac to near complete dryness and recovered with buffer F to 100 µL and stored at -80°C until use.

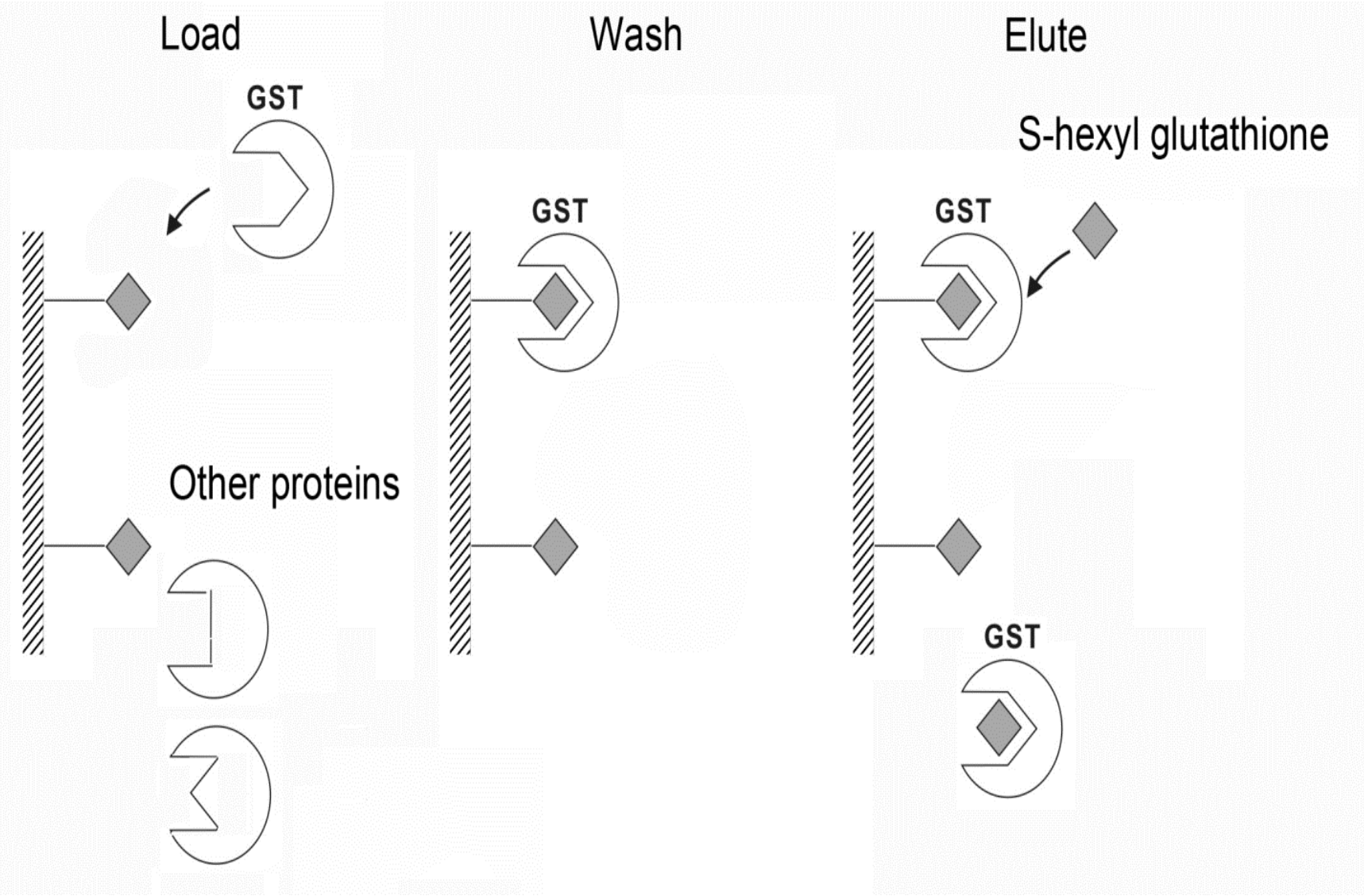

Figure 2.1 Scheme for principles of affinity chromatography of GSTs. GSTs are selectively retained on the column and then eluted with *S*-hexyl glutathione, a glutathione analogue. Adapted from (Li. J, 2013).

2.B.5 SDS-PAGE and in-gel digestion

Gel electrophoresis was performed according to a common protocol (Laemmli, 1970) to use an electric field to separate soluble proteins in a highly denaturing solution. A mixture was prepared from 100 µL protein extract, 50 µL 4x sample loading buffer, 40 µL 50% glycerol and 10 µL 2 M DTT in water, and this was boiled for 5 minutes to prepare proteins for electrophoresis. After the gel cassette was assembled and positioned in the electrophoresis tank and running buffer was added to appropriate level, 20 µL of prepared protein extract or kaleidoscope protein standard was loaded to each well for electrophoresis under 200 V for about 4 hours. Gels were then removed and soaked in staining solution for about 2 hours. Staining solution consisted of Comassie Blue Stain R-250 2.5g, methanol 1.0 L, acetic acid 0.2 L and deionized H_2O 0.8L. Stained gels were then destained with solution 1 (50% MeOH, 7% HAC) twice, 30 minutes each at 50°C, and solution 2 (50% MeOH, 7% HAC) for 2 more hours at room temperature. Bands were excised for digestion and further analysis.

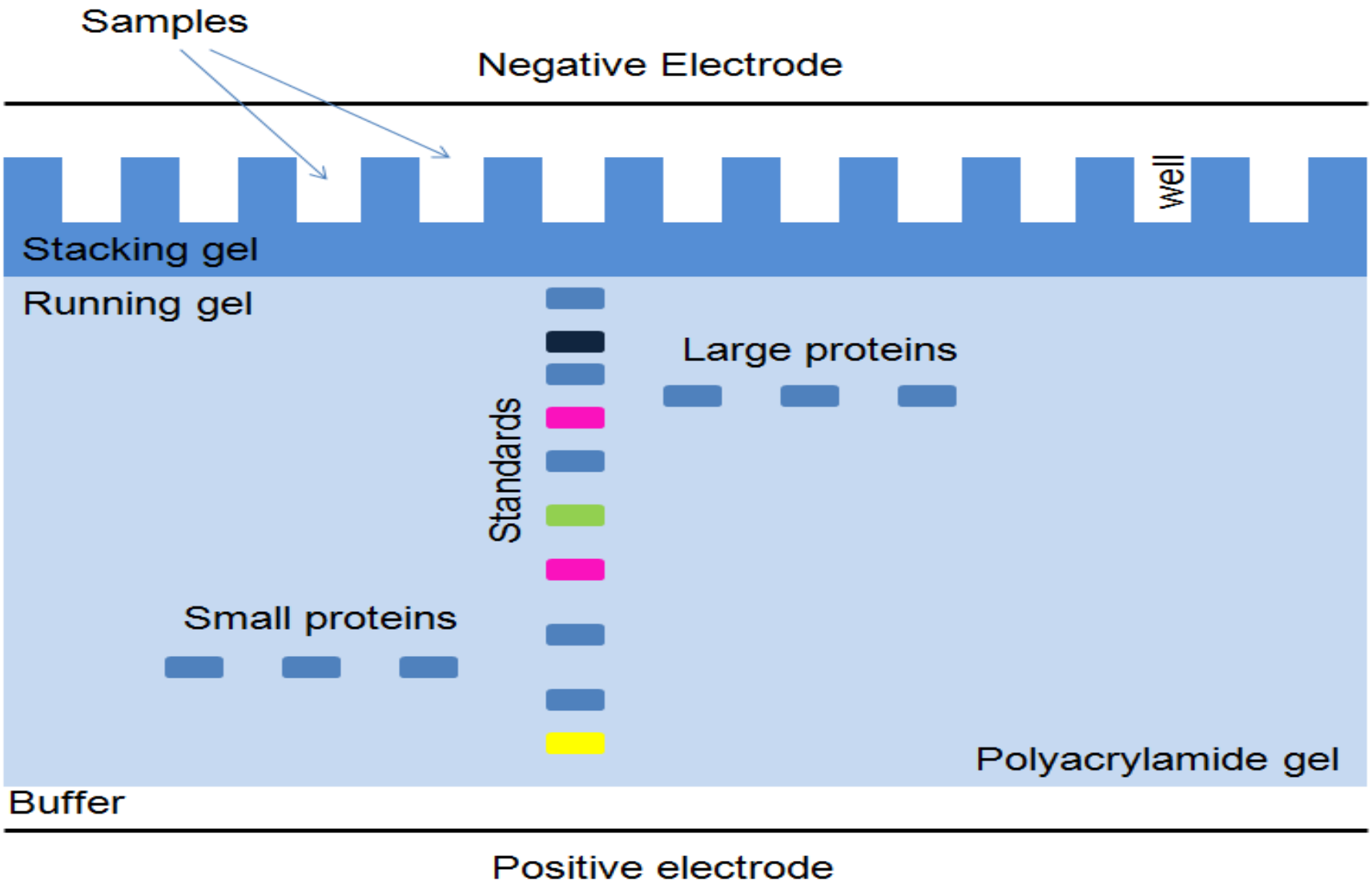

Figure 2.2 An illustration of SDS-PAGE. Proteins are separated when they migrate through gel driven by an electric field. Small proteins travel faster and large proteins travel slower.

This digestion procedure is done following a well established method(Shevchenko *et al.*, 1996). Gel pieces were dried under vacuum using a Thermo SPD131DDA Speed-Vac to near complete dryness, and each piece of gel was soaked in 50-100 µL of 20 mM DTT (dithiothreitol) in 100 mM ammonium bicarbonate, and incubated for 1 h at 60°C. After supernatant solution was removed, 50 µL of 55 mM IAM (iodoacetamide) in 100 mM ammonium bicarbonate was added to the gel for incubation of another 1 h at room temperature to alkylate cysteine side chains. Supernatant solution was again removed. Gels were then repeatedly immersed 3 times each alternating between 100 mM ammonium bicarbonate and ACN, with supernatant removed each time before adding the other solvent. Gels were then completely dried under vacuum using the Thermo SPD131DDA Speed-Vac before adding 50 µL 20 µg/mL trypsin solution to each piece of gel and incubating for 1 hour on ice. Enough 50 mM ammonium bicarbonate was added to cover the gel slices, which were then incubated at room temperature overnight. 50 µL x2 5% acetonitrile/0.1% TFA and 50 µL 50% acetonitrile/0.1% TFA were used to wash the gel slices with 15 min shaking at room temperature for each wash. All washes from each group were combined and evaporated Thermo SPD131DDA Speed-Vac to near complete dryness, recovered to 100 µL and stored at -80°C until use.

2.B.6 LC-MS/MS analysis

The peptide samples were separated with a 35 min water-acetonitrile gradient on a 3 µm particle sized capillary C-18 HPLC column, and sprayed into ThermoFisher LTQ ion trap interfaced to a Fourier Transform-Ion Cyclotron Resonance (FTICR) mass analyzer (for wounded and unwounded, respectively) using a Michrom ADVANCE nanospray source. Survey scans were taken in the Fourier Transform (FT) mass spectrometer (25,000 resolution determined at *m/z* 400), and the top 10 ions in each survey scan were then subjected to automatic low-energy

collision-induced dissociation in the linear ion trap. Peaks were determined using centroiding. Peaks from the survey or Zoom-Scan mass spectra were subjected to charge-state screening before MS/MS scan was performed on them. All peaks with +2 or +3 charges were considered peptide peaks and subjected to collision-induced dissociation. Collision energy (CE) was set to 35 V uniformly.

2.C Results and discussion

2.C.1 Signature peptides and identification confidences of 8 GSTs

Shown in Figure 2.3 are chromatograms of peptides resulted from digestion of enriched GSTs from unwounded *Arabidopsis* plant extract. Figure 2.3 A) presents a total ion chromatogram showing that the 35-min gradient was used to fractionate peptides and spread them out into a roughly 15 min long retention time window from retention time 10 to 25 min. As shown in Figure 2.3 B) a 0.02 *m/z* units mass window was chosen to display an extracted ion chromatogram for *m/z* 923.49, which consists of one major peak and a few small peaks.

The LC conditions were tuned to obtain as many different MS/MS scans as possible from the LC-MS run. The numerous coeluting peaks in Figure 2.3 A) are typical in bottom-up proteomics. A much longer gradient might further separate peptide peaks but reduce the ion signals owing to broader chromatographic elution, and risks failure to detect some peptide peaks. A shorter gradient improves signal-to-noise (S/N) ratios but allows more peptides to coelute in a relatively short time period, and risks missing more peptides owing to the data-dependent acquisition criteria because the total number of MS/MS scans that can be executed in a certain time period is limited by the instrument scan rate.

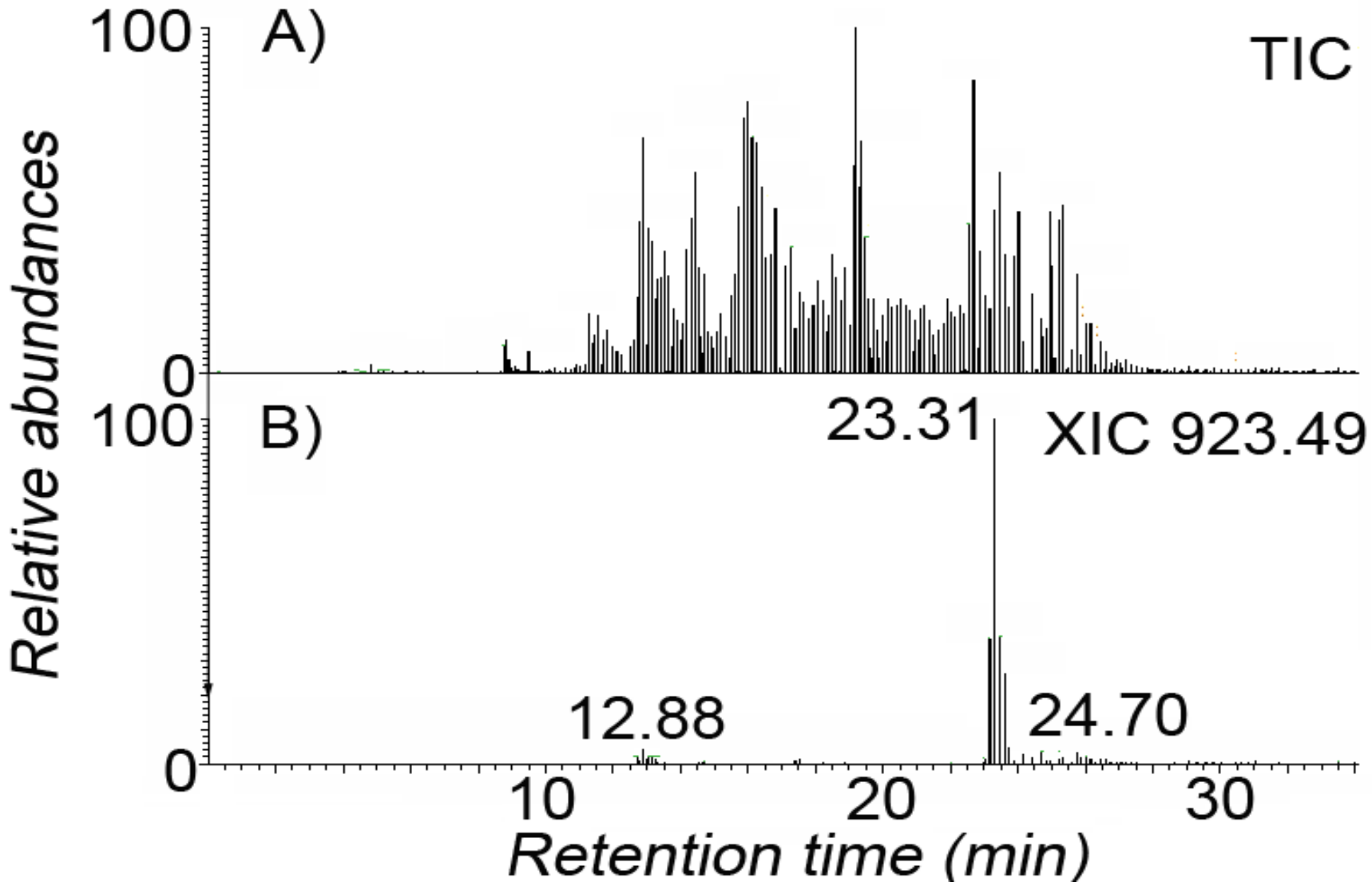

Figure 2.3 Overview of proteomic analysis: LC-MS detection of tryptic peptides from unwounded Arabidopsis leaf extract. A) Total ion chromatogram (TIC) and B) extracted ion chromatogram (XIC) of 923.49.

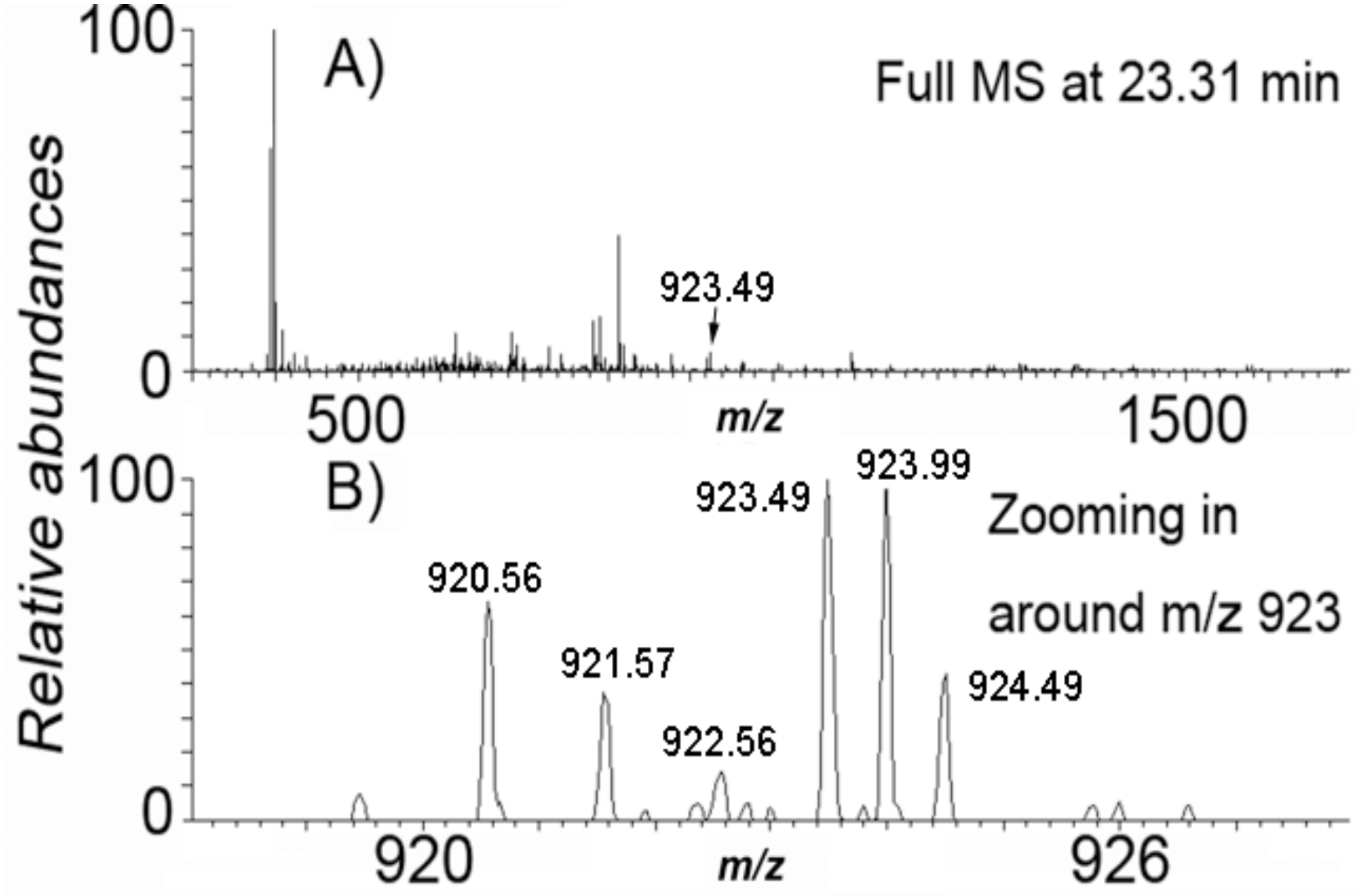

Figure 2.4. Peptides are detected and chosen for MS/MS. A) Full MS scan showing peaks including *m/z* 923.49. B) *m/z* 923.49 is determined to be with two positive charges (on FTICR instrument).

Shown in Figure 2.4 is an example of how charge state determination in used to select MS peaks for MS/MS. If the ion was recognized as +2 or +3 based on the separation of the individual isotopologs, it satisfied criteria to be chosen for MS/MS product ion scans.

Charge state determination is based on the isotopic distribution of mass peaks of the same elementary composition ions due to natural abundance of ^{13}C atoms. Compared to a molecule with all ^{12}C atoms, a molecule with 1 ^{12}C substituted by ^{13}C will be 1 Dalton heavier and result in another *m/z* peak. However, if the ion has two positive charges, the difference in mass to charge ratio (*m/z*) will be only about 1/2. Peptides generated from tryptic digestion will have an average molecular mass of 1-2 kDa. Owing to the free amino group in N-terminal and the basic function group in lysine or arginine, where trypsin cleaves protein, most tryptic peptides have two positive charges when ionized in ESI, so the *m/z* ratio for such a doubly-charged peptide is therefore around 2000/2=1000. To resolve two mass peaks half a Dalton apart, a mass resolution of 1000/0.5=2000 is required. FTICR instruments routinely give mass resolution of 25,000 at medium scan rate set for DDA, so the survey mass spectra can be used directly for charge state determination. While quadrupole ion trap instruments are able to deliver a mass resolution of 2000, the scan rate must be adjusted to a slow setting to achieve such resolution, and generating such spectra across a wide mass range results in loss of chemical information because the scan rate is slow compared to the elution window for an individual peptide. In these analyses, a slower zoom scan was performed across a much narrower mass window (usually 10 *m/z*) around the most abundant ions after a fast full MS scan, and the higher mass resolution within this windows allowed determination of charge states without compromising the number of MS/MS spectra obtained.

One example of charge state determination is presented in Figure 2.4. In Figure 2.4 A) *m/z* 923.49 is one of the top 10 abundant mass peaks recorded from FTICR instrument, and in Figure 2.4 B) the charge state of the ion at *m/z* 923.49 is determined to be 2+ directly from zooming in the full MS scan, because the *m/z* difference between 923.49 and the next isotopolog peak at *m/z* 923.99 is 0.50. In contrast, another coeluting mass peak of 920.56, was determined to have a charge of 1+ (because the difference between 921.57 and 920.56 is around 1), and was therefore not chosen for MS/MS.

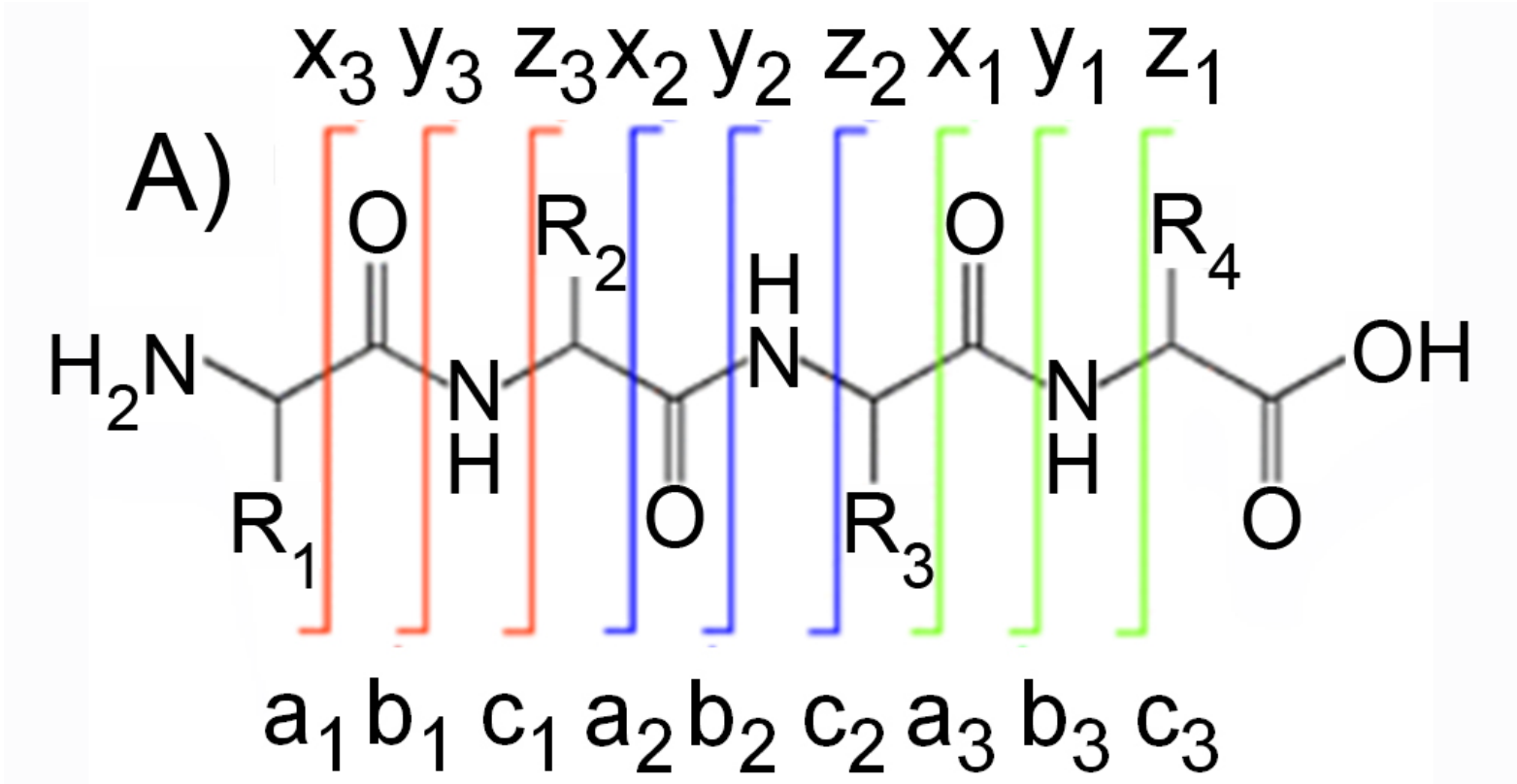

Figure 2.5 Typical MS/MS spectra of peptides and sequence determination. A) MS/MS product ion spectrum of *m/z* 923.49, and B) peak assignments after searching against protein database showing mostly *b* and *y* type product ions.

Figure 2.5 (cont'd)

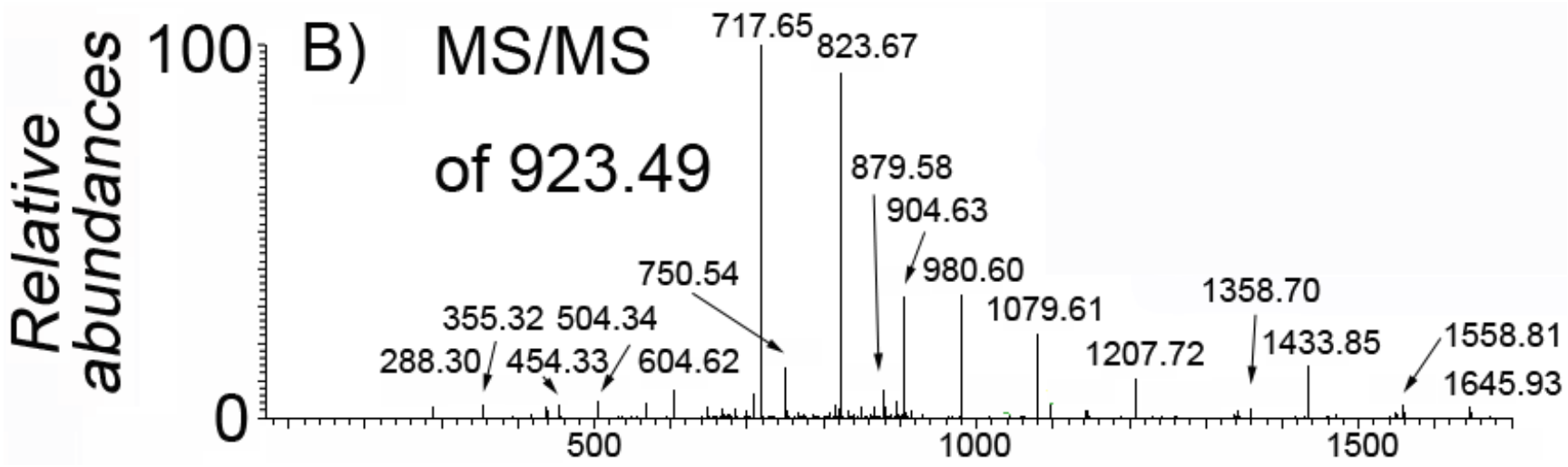

Figure 2.5 (cont'd)

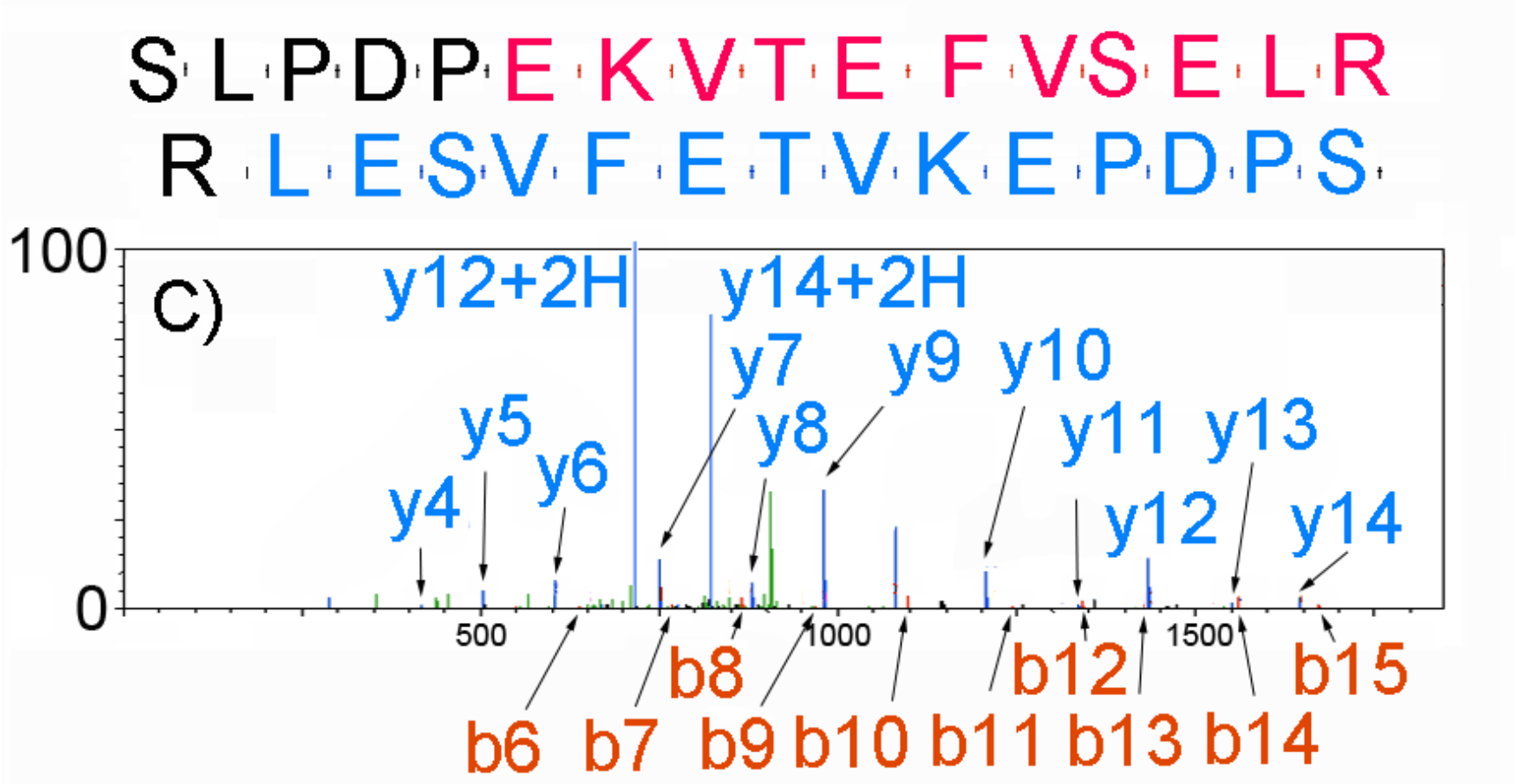

Peptide sequences can often be confidently identified through MS/MS. Shown in Figure 2.5A is the MS/MS product ion spectrum of an example peptide. By submitting this spectra to search in MASCOT database for all known proteins in *Arabidopsis*, the sequence of this peptide SLPDPEKVTEFVSELR can be determined, as illustrated in Figure 2.5B). The searching algorithm is robust because it takes into account all possible MS peaks that are different from predicted *b*/*y* product ions (those derived from cleaving at the peptide bond) due to charge state, water or ammonium loss, oxidation, carbamidomethylation (from alkylation of cysteine before digestion), disulfide bond formation (incomplete reduction) and, of course, mass resolution of the instrument, and searches against a database of predicted fragment masses generated from available sequence databases. Most product ion resulted from CID of peptides are produced through cleavages of the peptide backbone. According to the common nomenclature, those product ions retaining the N-terminal part of the peptide molecule are named as *a, b and c* series product ions, while those with C-terminal part are named as *x, y and z* series product ions(Figure 2.5 A) insert)(Biemann, 1992). Most detected MS/MS fragments were *b*/*y* series of ions as expected.

The total number of peptides that can be identified in a single LC-MS/MS analysis is limited by the speed of mass analysis. All peptides are eluted from the LC column in the retention time window of 11-26 minutes. Ideally, with dynamic exclusion algorithm (after an ion is picked for MS/MS, a mass will be excluded for 10 seconds), in the time window of this 15 minutes, about 900 MS/MS spectra can be obtained. However, charge state distributions in mass peaks of peptides (multiple MS/MS spectra will be interpreted as from the same peptide), and multiple peptides obtained from digestion of a single protein are examples of factors that will reduce the total amount of information obtained from each LC-MS/MS analysis.

Based on the identification of peptides, the corresponding GSTs can be identified as well. As summarized in Figure 2.6, 20 detected peptides out of a total of 26 identified are unique peptides, i.e., peptides that cannot be produced from digestion of any other *Arabidopsis* proteins.. Other peptides, if they are consistent with other proteins identified, will be used as supplemental proof for identification of these proteins in calculating probabilities of identification.

With all unique peptides combined, we can determine how many amino acid residues of each protein identified are actually detected. This is best illustrated in Figure 2.7, where amino acid residues detected are highlighted in yellow. A comprehensive coverage is solid proof for confident identification, although close to 100% coverage is almost never achieved. Possible causes include different ionization efficiency of peptides, especially under suppression from other abundant coeluting peptides, post translational modifications, chemical modifications occurred during sample preparation and partial digestion that are not specified in searching algorithm, failure to trap peptides on the column, and the natural limit of data dependent analysis (only 10 most abundant peaks from each survey scan are subjected to MS/MS).

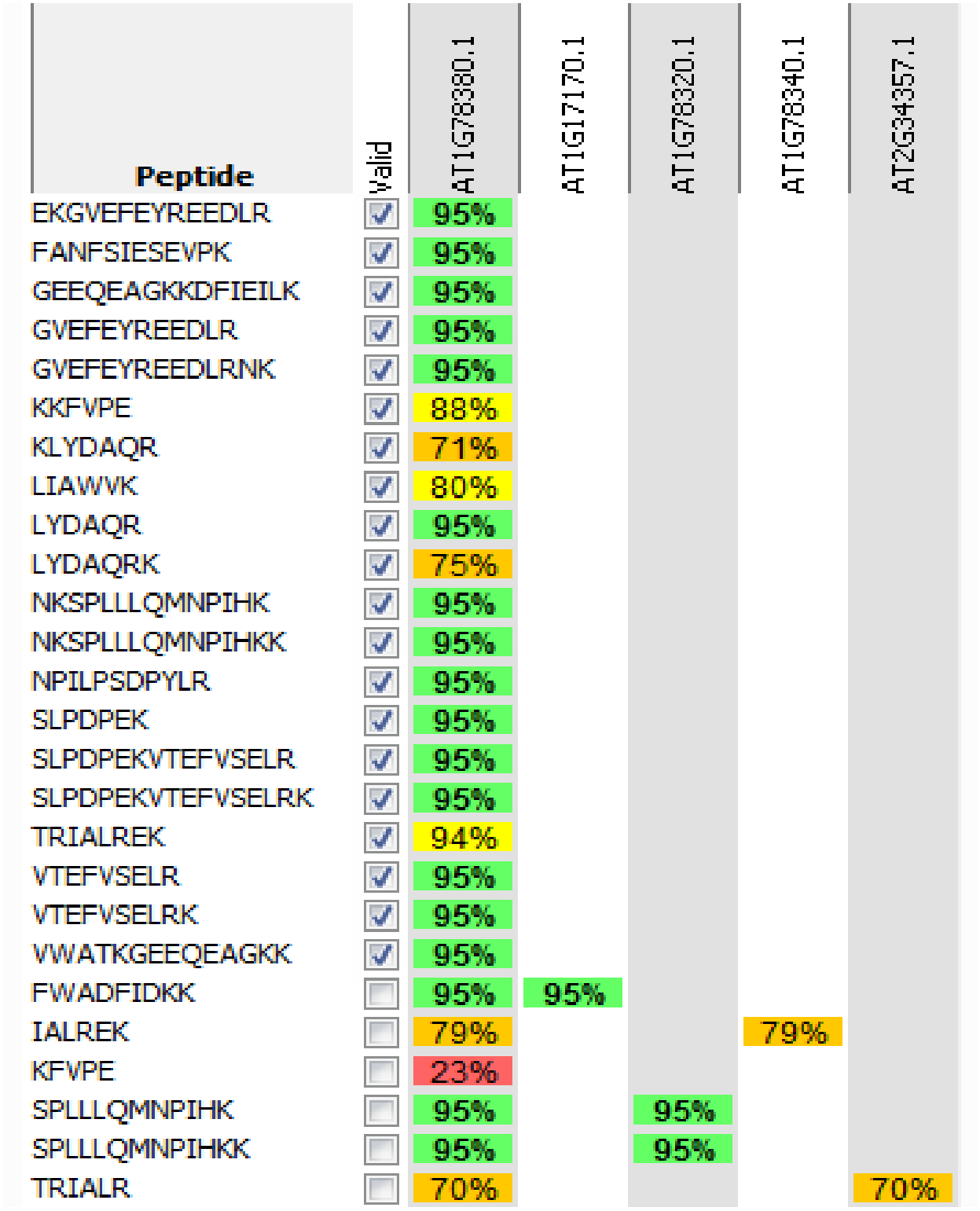

Peptide	Valid	AT1G78380.1	AT1G17170.1	AT1G78320.1	AT1G78340.1	AT2G34357.1
EKGVEFEYREEDLR	☑	95%				
FANFSIESEVPK	☑	95%				
GEEQEAGKKDFIEILK	☑	95%				
GVEFEYREEDLR	☑	95%				
GVEFEYREEDLRNK	☑	95%				
KKFVPE	☑	88%				
KLYDAQR	☑	71%				
LIAWVK	☑	80%				
LYDAQR	☑	95%				
LYDAQRK	☑	75%				
NKSPLLLQMNPIHK	☑	95%				
NKSPLLLQMNPIHKK	☑	95%				
NPILPSDPYLR	☑	95%				
SLPDPEK	☑	95%				
SLPDPEKVTEFVSELR	☑	95%				
SLPDPEKVTEFVSELRK	☑	95%				
TRIALREK	☑	94%				
VTEFVSELR	☑	95%				
VTEFVSELRK	☑	95%				
VWATKGEEQEAGKK	☑	95%				
FWADFIDKK	☐	95%	95%			
IALREK	☐	79%			79%	
KFVPE	☐	23%				
SPLLLQMNPIHK	☐	95%		95%		
SPLLLQMNPIHKK	☐	95%		95%		
TRIALR	☐	70%				70%

Figure 2.6 Summary of identified peptides for identification of *At*GSTU19. Shown are the 14 unique peptides, labeled as valid, (20 detected peptides due to incomplete digestion), other 6 non-unique peptides and their corresponding identification confidence (%).

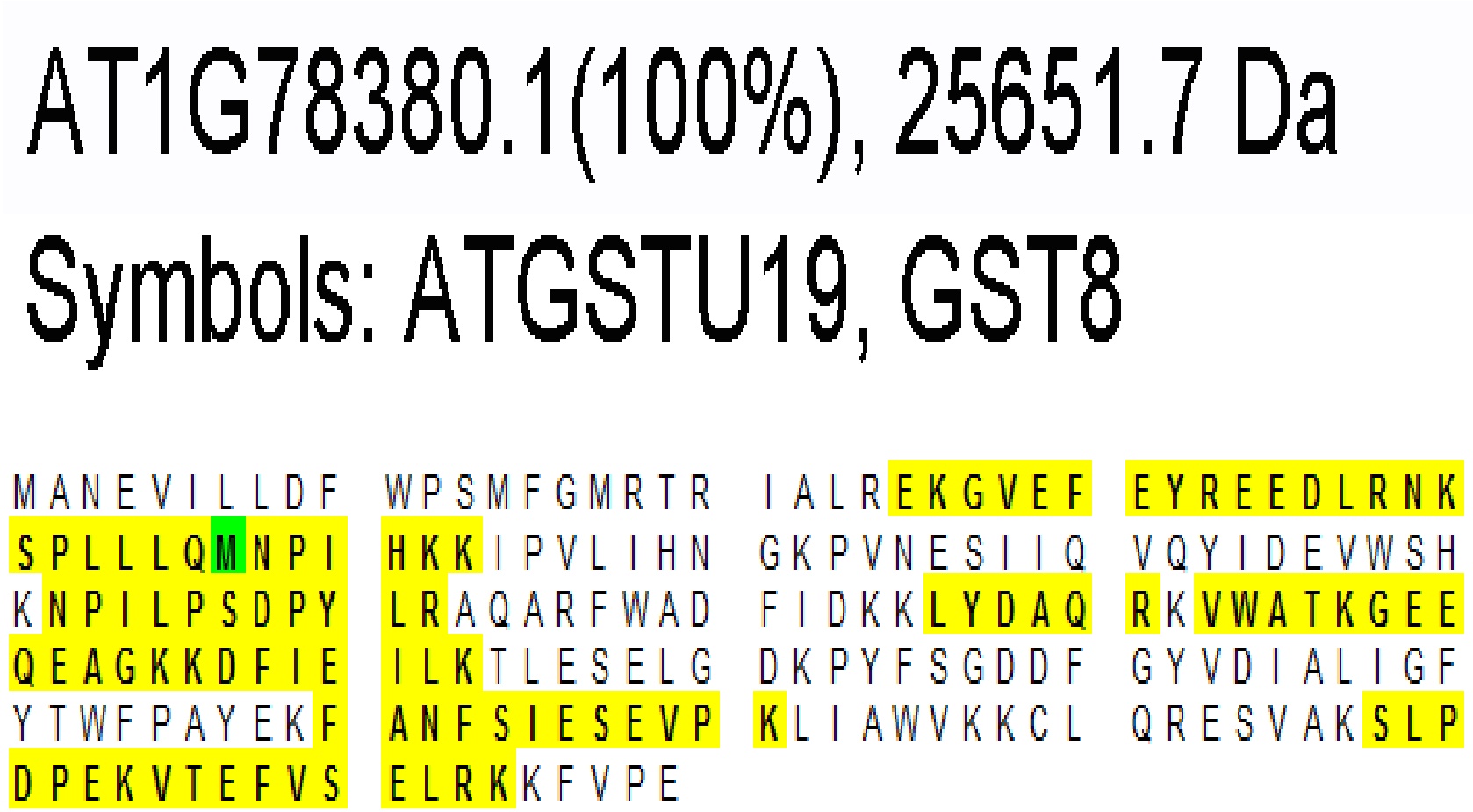

Figure 2.7 Sequence coverage (44%) of identification of *At*GSTU19. Amino acid residues in detected peptides are shown in yellow color. Oxidized methionine is shown in green color.

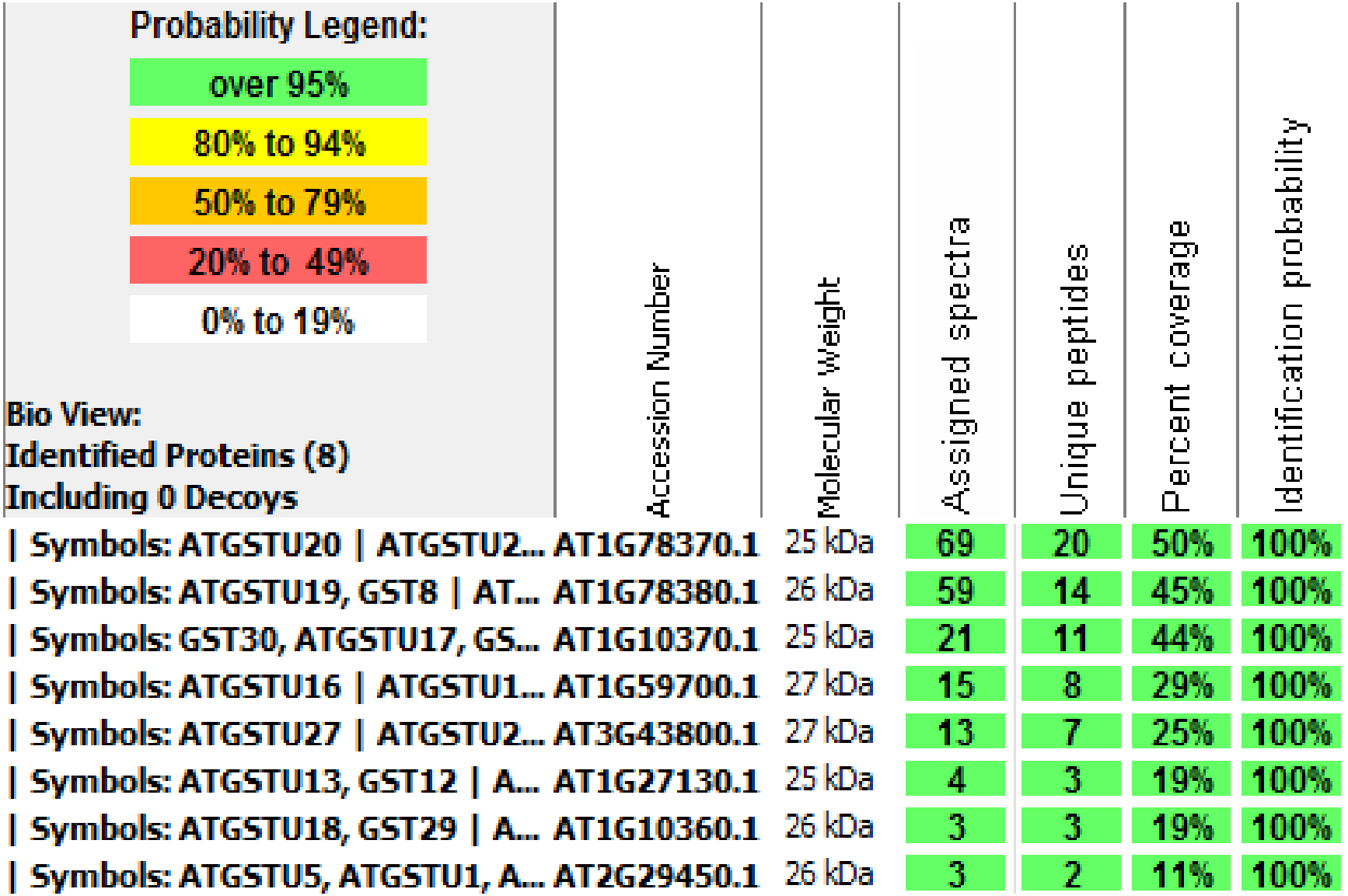

Figure 2.8 Summary of GSTs identification. Listed are *At*GSTs identified, protein molecular weights, number of assigned spectra and unique peptides, sequence coverage and identification probabilities.

In this way 8 GSTs enriched from *Arabidopsis* leaves were identified, as listed in Figure 2.8B, each with at least two characteristic peptides (the peptides that cannot be produced from digestion of any other proteins), and 6 of them were identified in the extract from wounded leaves, but not *At*GSTU13 and 18. The probabilities of all GSTs identification are 100%. And sequence coverages are within 10% to 50%, a reasonable range for confident protein identification.

2.C.2 Comparison between unwounded and wounded leaf extracts

The identification of GSTs from both control and wounded plants gave similar results, although *At*GSTU13 and 18 were assigned lower probability numbers from the wounded plant sample and therefore not considered confidently identified. However, a comparison of GSTs abundances between the two groups will be useful in revealing which GST(s) are actively highly expressed in response to mechanical wounding.

Overall scan frequency was about 5000 scans/ 35 min or 2-3 scans per second. MS/MS scan times and zoom scan (to determine charge state to filter out unwanted peaks) times were set to 1 sec. But full FTICR survey scans usually take 3 seconds to achieve the desired mass resolution. Each survey scan was followed by up to 10 MS/MS scans and also up to 10 zoom scans (for the LTQ experiments only). So the intervals between full MS scans are often 5 to 10 seconds. Typical peptide peaks with this chromatographic configuration are about 20 to 30 seconds wide, so the survey scans are not fast enough to provide 10 data points across a LC peak, which is considered the common limit for accurate peaks area integration for quantification. Also due to the unavailability of authenticated analytical standards for these GSTs or corresponding peptides with known concentration, absolute quantitation of GSTs are not feasible. Instead, the approach of spectral counting was used for relative quantitation. In this method, the total number of

MS/MS spectra recorded for each protein is counted and normalized to total number of MS/MS spectra in each LC-MS/MS analysis to calculate relative abundances. The results can be then used for relative comparison between experiment groups and control groups. In this work, from spectrum counts we can compare the expression levels of *At*GSTs between wounded and unwounded *Arabidopsis* leaf extracts.

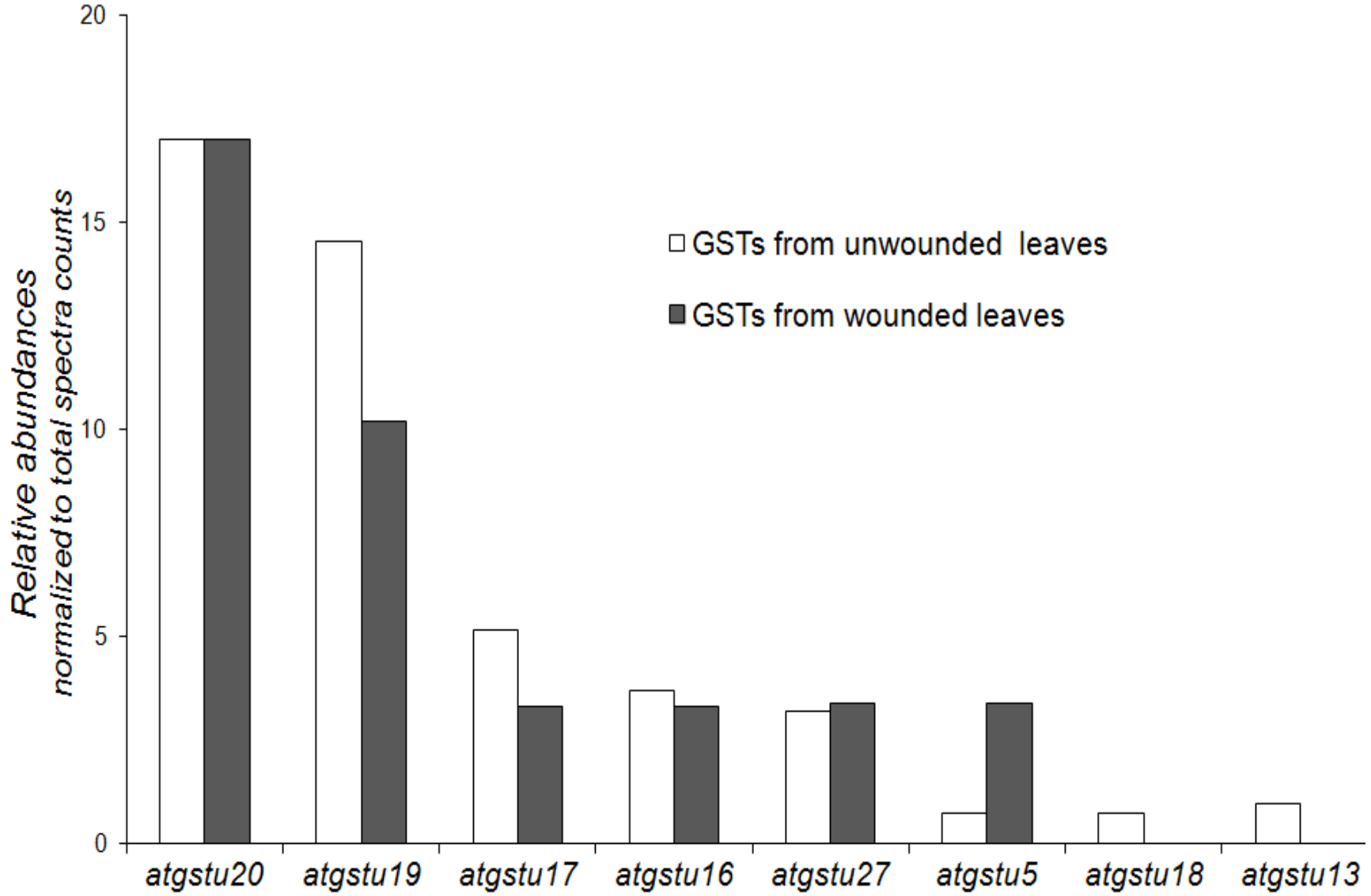

Figure 2.9 GSTs relative abundances in Arabidopsis leaf extract. Samples were collected 12 hours after mechanical wounding. Relative abundances were normalized to total spectra counts detected in data dependent analysis.

In Figure 2.9, unshaded bars represent relative abundances of GSTs in unwounded leaves while shaded bars are from wounded leaf extracts. *At*GSTU13 and 18 were not identified in the wounded sample. Therefore quantitative comparisons between treatments cannot be drawn. But for the other GSTs, their abundances appear to be consistent before and after wounding. It is obvious that the concentration of *At*GSTU5 was the only GST to show increased abundance after wounding, which suggests that *At*GSTU5 is part of the *Arabidopsis* response to wounding stress. The results of GST identifications agreed with reported microarray data for mRNA expression levels. The expression of *At*GSTU17, 19 and 20 was consistent with microarray data shown in Genevestigator (https://www.genevestigator.ethz.ch/at/)(Dixon, *et al.*, 2010). *At*GSTU5 was shown to be expressed in adult *Arabidopsis* leaf and exhibited conjugation activity with substrate 1-chloro-2,4-dinitrobenzene (CDNB) and benzyl isothiocyanate ( )(Dixon, *et al.*, 2009, Zimmermann *et al.*, 2004), and its expression can be induced by methyl jasmonic acid (MeJA)(Wagner, *et al.*, 2002), which is consistent with wound induced expression of *At*GSTU5 found in this work because MeJA has been well known to be accumulated after wounding (Wasternack, *et al.*, 2013). Its cytosolic localization was further supported by the accumulation of other *At*GSTUs in cytosol (Wagner, *et al.*, 2002). All these are consistent with *At*GSTU5 playing an induced and important role in defense response, probably by catalyzing cytosolic glutathione conjugation to endogeneous electrophiles. Considering that OPDA is an essential biosynthesis precursor for jasmonates as pivotal phytohormones, and is also a potent gene expression inducer (Stintzi, *et al.*, 2001, Taki, *et al.*, 2005) and a cyclopentenone electrophile, the hypothesis is proposed *At*GSTU5 is an enzyme that catalyzes *in vivo* glutathione conjugation of OPDA. This hypothesis is further supported by the discovery of glutathione conjugates *in vivo* in

tobacco (Davoine *et al.*, 2005), and their accumulation in response to wounding found in previous work in the Jones laboratory (Gao, 2009).

The *in vivo* abundance of these GSTs made them good candidates for investigation of metabolic profiles in knockout mutants. To assess the biological function of the GSTs identified in this chapter, mutants were selected for wounding experiments in which individual GSTs are knocked out. When possible, homozygous seeds were selected to avoid the need for plant breeding and selection of homozygous progeny. Homozygous mutant seeds have the mutation in both DNA copies from parents. As a result, our selections are listed below: SALK_025503C (alias *atgsyu17 (1)* in this paper) and SALK_139615C (alias *atgstu17 (2)* in this paper) were used for *atgstu17s*. SALK_107148 was used for *atgstu5*. SALK_077958C was used for *atgstu19*. SALK_091292C was used for *atgstu20*. Results from the analyses of oxylipin metabolites from these mutant plants are presented in Chapter 3.

2.D Conclusions

The identification of 8 GSTs in this chapter laid the foundation for the research described in subsequent chapters of this dissertation, as it helped in selecting the GST candidates to further investigate with metabolite profiling. The application of affinity-isolation with proteomic strategies, followed by metabolomics to define mutant phenotypes allows for probing of gene functions as described in this dissertation. *At*GSTU5 expression was found to be induced by mechanical wounding, suggesting its role in defense response. Based on current understanding of plant defense signaling, we hypothesize that *At*GSTU5 is the enzyme catalyzing *in vivo* glutathione conjugation of OPDA, and will test this in the following chapters.

Chapter 3 LC-TOF MS Profiling of glutathione conjugates of endogenous oxylipins in Arabidopsis leaf extract

3.A. Introduction

3.A.1 Glutathione conjugates

Drug metabolism studies have become essential parts of preclinical research of drug candidates. A significant number of candidate drugs have been withdrawn from the pharmaceutical market due to safety concerns owing to their conversion to reactive and toxic metabolites (Stepan *et al.*, 2011, Walgren *et al.*, 2005). Glutathione, an abundant cysteine-containing tripeptide in virtually all cells, detoxifies a wide variety of exogenous compounds in humans and other animals, and facilitates their removal into urine through conjugation, one of the most important routes of phase II metabolism (Suzuki and Sugiyama, 1998). Early stages of drug discovery research routinely involve screening for formation of glutathione conjugates of lead compounds to predict metabolism and toxicity (Evans *et al.*, 2004, Samuel *et al.*, 2003). Glutathione transferases (GSTs), a superfamily of enzymes that exist in most living organisms, catalyze the glutathione conjugation reactions to diverse substrates (Hayes, *et al.*, 2005, Sheehan *et al.*, 2001). Mammalian GSTs have been extensively studied in drug therapeutics research as it pertains to asthma and cancer(Matsushita *et al.*, 1998, Ruscoe *et al.*, 2001).

Similarly, in plants, glutathione reacts to detoxify xenobiotics including herbicides(Sandermann, 1992), especially when induced by safeners in crops(Edwards *et al.*, 2005). (Herbicide safeners are chemicals used in combination with herbicides to reduce their damage to crop plants. Induction of glutathione accumulation is one of the major action mechanisms.) Moreover, glutathione conjugates of endogenous compounds including oxidized fatty acids have been found in plant leaves after stimuli(Davoine, 2006, Davoine, *et al.*, 2005). Some of these glutathione

conjugates have been shown to have their own biological activities(Davoine, 2006). Plant glutathione *S*-transferase enzymes (GSTs) are expected to catalyze these conjugation reactions. Expression of many plant GSTs have been induced by biotic and abiotic stresses, indicating that GSTs are involved in plant defenses (Dixon, *et al.*, 2010). Although well known in detoxification of xenobiotics(Cummins *et al.*, 2011), plant GSTs have also been found to have isomerase and peroxidase activities(Dixon, 2000) (Bartling *et al.*, 1993, Cummins *et al.*, 1999), and many other biological activities(Gonneau *et al.*, 1998). Although progress has been made toward characterizing roles of tau and phi plant-specific classes of GSTs that are similar to animal GSTs (Edwards and Dixon, 2005) that metabolize endogenous oxidized fatty acid derivatives(Dixon and Edwards, 2009, Kilili, 2004) ,the detailed roles for individual GST isoenzymes still largely remain unexplored in plants(Dixon and Edwards, 2009).

3.A.2 Cyclopentenone oxylipins in plant defense are glutathione substrates

Oxidized fatty acids, collectively known as oxylipins, are ubiquitous signaling molecules (Howe and Schilmiller, 2002). Much research on plant oxylipins has focused on jasmonic acid (JA), its methyl ester, methyl jasmonate (MeJA), and other derivatives, collectively named "jasmonates" (Wasternack, 2007). Jasmonates mediate resistance responses to insect attack (Browse and Howe, 2008), to pathogens(Glazebrook, 2005), and other abiotic stresses (stresses not originated from other organisms, such as cold temperature, drought, and explosion to environmental chemicals)(Balbi and Devoto, 2008). The roles of these compounds in reproductive development are also well characterized(Wasternack, *et al.*, 2013). The conjugate of JA with isoleucine (JA-Ile) has been found to be the active form of JA (Fonseca, *et al.*, 2009, Koo *et al.*, 2009b, Staswick and Tiryaki, 2004). The discovery of negative regulators of JA-induced gene

expression, Jasmonate ZIM domain (JAZ) proteins, provided another important breakthrough in jasmonate research (Chini, *et al.*, 2007, Thines, *et al.*, 2007).

Nevertheless, 12-oxo-phytodienoic acid (OPDA), the biosynthetic precursor of JA, has also been characterized as another independent gene expression regulator, and it plays important roles in plant signaling (Stintzi, *et al.*, 2001, Taki, *et al.*, 2005). In addition to its free form, OPDA and its 16-carbon homolog 10-oxo-8,13-dinor-phytodienoic acid (dnOPDA) are incorporated into galactolipids that accumulate in tissues of the model plant *Arabidopsis thaliana* in response to mechanical wounding (Kourtchenko, *et al.*, 2007). To date, many OPDA and/or dnOPDA-containing galactolipids have been unambiguously characterized, including monogalactosyl diacylglycerides (MGDGs) and digalactosyl diacylglycerides (DGDGs) (Andersson *et al.*, 2006, Buseman, 2006, Hisamatsu, *et al.*, 2003, Hisamatsu, *et al.*, 2005, Nakajyo *et al.*, 2006, Stelmach, 2001). The biosynthetic oxidation of OPDA and dnOPDA has been shown to be performed on these esterified forms instead of free acid forms (Böttcher and Weiler, 2007, Nilsson *et al.*, 2012). These oxidized galactolipids has been shown to confer antibacterial, antifungal, and herbivory resistant activities (Andersson, et al., 2006, Glauser *et al.*, 2009, Kourtchenko, et al., 2007).

Evidence for *in vivo* glutathione conjugation of endogenous oxylipins has been scarce (Dixon, *et al.*, 2010). Examples include free oxidized fatty acids (Davoine, *et al.*, 2005), most notably OPDA (Davoine, 2006). The metabolic fate of GS-OPDA has been determined to be the same as other xenobiotic glutathione conjugates: the conjugate is transported into and degraded in vacuoles (Bleuel, *et al.*, 2011, Ohkama-Ohtsu, *et al.*, 2010, Tommasini, *et al.*, 1998, Wolf, *et al.*, 1996). However, the existence of glutathione conjugates of other fatty acid derivatives *in vivo* in plants, such as those of oxidized galactolipids, which are also Michael addition substrates with α, β-unsaturated carbonyl moieties, has not been reported before. A comprehensive exploratory

screening and profiling method would be helpful in finding these novel glutathione conjugates and setting the stage to probe their *in vivo* biological functions.

3.A.3 LC-MS method to explore glutathione conjugates

In terms of searching for glutathione conjugates, liquid chromatography-tandem mass spectrometric methods are the methods of choice, among which the neutral loss of 129.0426 *m/z* units (dehydrated glutamate) from the protonated GSH conjugates in positive-ion collision-induced dissociation (CID) has been widely studied and used as the gold standard for screening for glutathione conjugates (Castro-Perez *et al.*, 2005, Jin *et al.*, 1996, Loughlin *et al.*, 2001, Murphy *et al.*, 1992, Oberth and Jones, 1997, Waldon, *et al.*, 2010). Precursor MS/MS scans for *m/z* 272.0883 (deprotonated glutathione residue after loss of H_2S) in negative-ion mode CID was also proposed for unbiased exploration of glutathione conjugates (Dieckhaus *et al.*, 2005). Precursor scans for *m/z* 254 (dehydration product of *m/z* 272), *m/z* 306.0768 (deprotonated glutathione) have also been used for this purpose (Mahajan and Evans, 2008, Rathahao *et al.*, 2004, Xie *et al.*, 2013). However, due to variability in the moieties to which glutathione is conjugated, many of these methods, the 129 Da constant neutral loss scan in particular, have failed to provide reliable comprehensive screening of glutathione conjugates that avoid false negative results (Dieckhaus, *et al.*, 2005).

In this work, a novel method of screening glutathione conjugates based upon non-targeted data acquisition with negative-ion multiplexed CID is presented. This approach involves generating extracted ion chromatograms for *m/z* 306.0708 at elevated collision energies for discovery of glutathione conjugates, with follow-up MS/MS analyses in positive-ion mode for structure elucidation. A new family of glutathione conjugates of endogenous oxylipins, specifically OPDA-containing MGDG, is discovered and profiled in wild type *Arabidopsis thaliana* leaf

extracts. Five homozygous GST knockout mutants with individual GSTU (tau class GST) genes knocked out were grown and used for glutathione conjugate profiling.

3.B Materials and methods

3.B.1 Materials

Arabidopsis thaliana wildtype Col-0 seeds and homozygous knockout mutant seeds were purchased from The Arabidopsis Biological Research Center at Ohio State University. The germplasms used are listed below: SALK_025503C (alias *atgstu17 (1)* in this thesis) and SALK_139615C (alias *atgstu 17 (2)* in this dissertation) were used for *atgstu17s*. SALK_107148 was used for *atgstu5*. SALK_077958C was used for *atgstu19*. SALK_091292C was used for *atgstu20*. Plants were grown from seeds cultivated in separate pots and used in wounding experiments. Chemicals including methanol, acetonitrile, ammonium formate and propyl 4-hydroxybenzoate were purchased from Sigma Aldrich.

3.B.2 Growth of *Arabidopsis thaliana* plants

Soil-grown plants were maintained in a growth chamber at 22°C under 16 h light (100 μE m^{-2} s^{-1}) and 8 h dark per day. For mechanical wounding treatments, fully expanded rosette leaves on 5-week-old plants were wounded three times by crushing the leaf across the midrib with a hemostat. This wounding protocol, which resulted in damage to approximately 40% of the leaf area, was administered to approximately six rosette leaves per plant (Chiwocha, *et al.*, 2003). Leaf tissues were harvested from control and wounded plants at 0, 0.25, 0.5, 1, 2, and 4 hours after wounding, were frozen in liquid nitrogen immediately, and stored at -80°C until use. Eight biological replicates were performed. Location and wounding order of the plants were randomized to minimize possible systemic errors.

3.B.3 Extraction of the glutathione conjugates and other oxylipin metabolites

For each sample, 0.3 g portions of leaf tissue were ground in liquid nitrogen to fine powder and immediately mixed with 2 mL 80% methanol containing 10 µM propyl 4-hydroxybenzoate (PHB) as internal standard ("extraction solvent A") for extraction. Mixtures were allowed to thaw at room temperature and were centrifuged at 10,000*g* for 20 min at 0°C using an Eppendorf 5804R centrifuge, evaporated under vacuum using a Thermo SPD131DDA Speed-Vac to near complete dryness and recovered with "extraction solvent A" to 200 µL and immediately transferred to LC-MS auto sampler vials for analysis.

3.B.4 LC-MS analysis of glutathione conjugates and other oxylipin metabolites

For exploratory profiling of glutathione conjugates, a 110 minute gradient from 5% B to 95% B at 0.3 mL/min, 40°C was used with a Supelco Ascentis Express C18 HPLC column (100 x 2.1 mm, 2.7 µm pore size). Mobile phase A was 0.15% FA for ESI+ and 10 mM ammonium formate for negative mode electrospray (ESI-). Mobile phase B was acetonitrile. For quantitation, a shorter 45 minute gradient from 5% B to 95% B gradient of 0.15 FA and methanol at 0.3 mL/min, 40°C was used with a Supelco Ascentis Express C18 HPLC column (50 x 2.1 mm, 2.7 µm particles).

Mass spectrometric analyses were performed on a Waters LCT Premier TOF mass spectrometer using electrospray ionization. Capillary voltages were set to +3000V and -2500V for positive-ion and negative-ion analyses, respectively. For both polarities, the same source temperature and gas conditions were used. Source temperature was set to 100 °C and desolvation temperature was set to 250°C. Cone gas and desolvation gas were set to 40 and 350 L/min, respectively. Five quasi-simultaneous data acquisition functions were used for detection of pseudo molecular ions and

fragments using 5 to 45 V of Aperture 1 voltages with increments of 10 V for generation of collision-induced dissociation spectra in the transit lens of the mass spectrometer.

3.B.5 LC-MS/MS analysis of glutathione conjugates

Due to low metabolite abundances, leaf extracts from 8 biological replicates were combined and evaporated under vacuum using a Thermo SPD131DDA Speed-Vac and recovered in extraction solvent to about one-tenth of the original volume. The same 110 min LC method described above was used. Positive and negative mode MS/MS analyses were performed on a Waters Xevo G2-S Qtof mass spectrometer. Capillary voltage was set to 2.14 kV for positive mode and 2.50 kV for negative mode. Sampling cone and source offset voltages were set to 5 and 80 V, respectively. Source and desolvation temperature were set to 90 and 280 $^{\circ}$C, respectively. Cone and desolvation gas were set to 0 and 800 L-h^{-1}, respectively. Scan times were set to 0.5 seconds for both survey and MS/MS scans. Data dependent analysis rules were set to pick peaks within 0.3 *m/z* units of calculated accurate masses for MS/MS using a mass inclusion list. Lock mass calibration was included as another MS function using leucine encephalin $[M+H]^+$ and $[M-H]^-$ ions accordingly.

3.B.6 Peak Integration and Quantification

Peaks in extracted ion chromatograms (XICs) were automatically aligned between samples with retention times relative to internal standard, integrated and normalized to the total mass spectrometry signal in each LC gradient using Waters Markerlynx software.

3.C Results and discussion

3.C.1 Exploration of putative glutathione conjugates

To search for potential glutathione conjugates, especially those from cyclopentenone oxylipins or OPDA-like molecules, it was anticipated that retro-Michael addition would be one of the major fragmentation pathways in negative CID yielding *m/z* 306.0708 ions, just as reported with glutathione conjugates of acrolein and its derivatives (Oberth and Jones, 1997). Analysis using HPLC-TOF with multiplexed CID was chosen because it provided simultaneous accurate mass detection of both pseudo molecular ions and fragments of all compounds eluted using the LC gradient. Oxylipins were extracted from wildtype *Arabidopsis* leaves 1 hour after wounding.

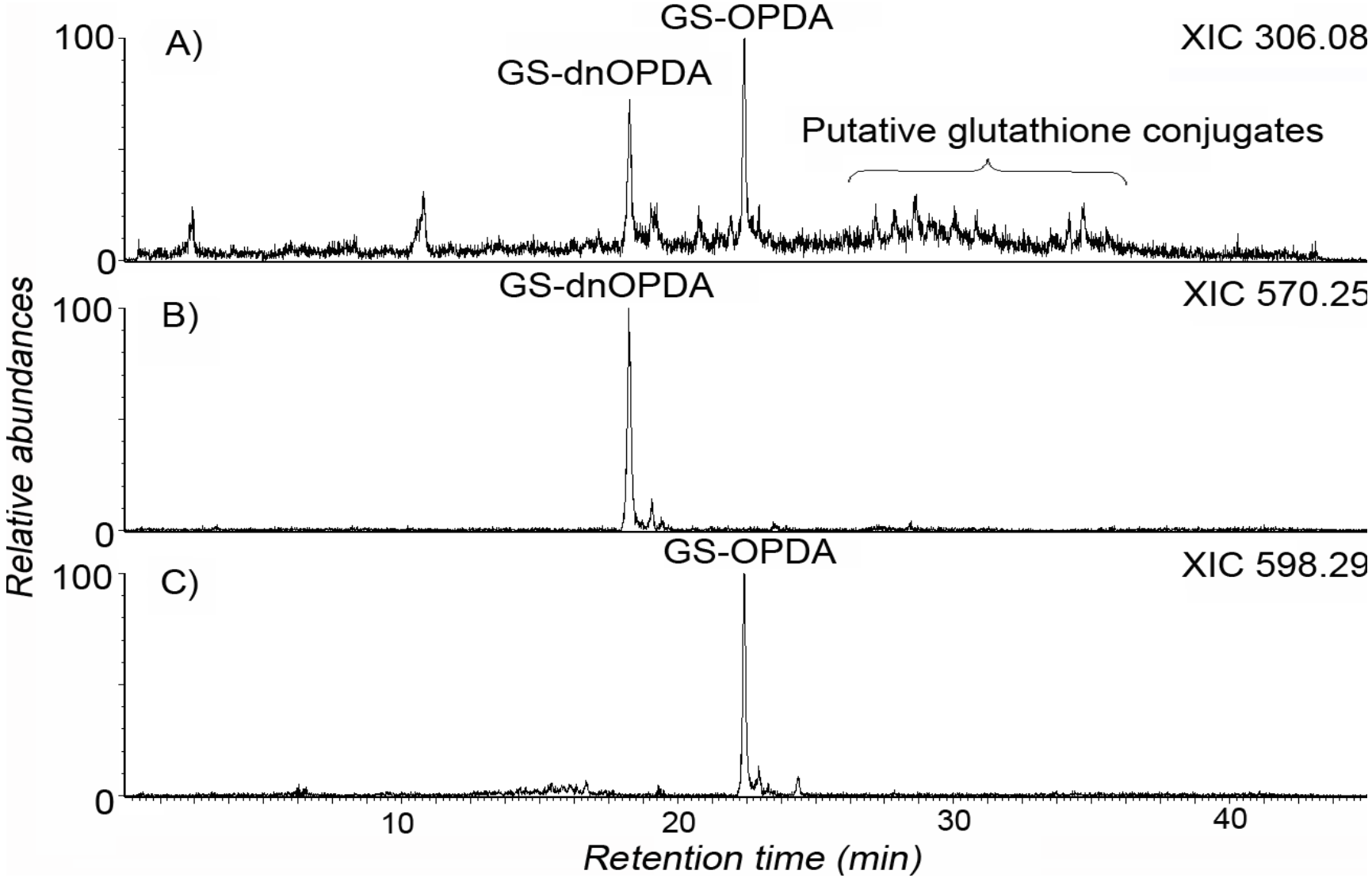

Figure 3.1. GS-(dn)OPDA are the predominant endogenous glutathione conjugates in *Arabidopsis* leaves. XICs of *m/z* A) 306.08, B) 570.3 and C) 598.3 from TOF MS in 45 min gradient of wildtype *Arabidopsis* leaf extract. Leaf samples were collected 1 hour after wounding.

Shown in Figure 3.1A is the extracted ion chromatogram (XIC) of *m/z* 306.08 in the fourth MS function, where Aperture 1 voltage was set to 35 V to generate more energetic collision in the QTof collision cell. The two most abundant peaks were those from GS-dnOPDA and GS-OPDA. In Figure 3.1B and 3.1C are the XICs of *m/z* 570.3 and 598.3, the $[M-H]^-$ masses of dnOPDA and OPDA, respectively in the first MS function with Aperture 1 voltage set at 5 V for minimal fragmentation. The deprotonated molecule ($[M-H]^-$) peaks of *m/z* 570.3 and 598.3 showed matching retention times with their fragment ion *m/z* 306.08 in the fourth function in Figure 3.1A. Nevertheless, there are other smaller peaks indicating putative glutathione conjugates, whose identities have not been reported before.

To identify these *m/z* 306.08 ion-producing compounds, a 110-min gradient was used on a longer (100 mm) C-18 column in separating these peaks hoping to better resolve them from other metabolites. The resulting XICs are shown in Figure 3.2.

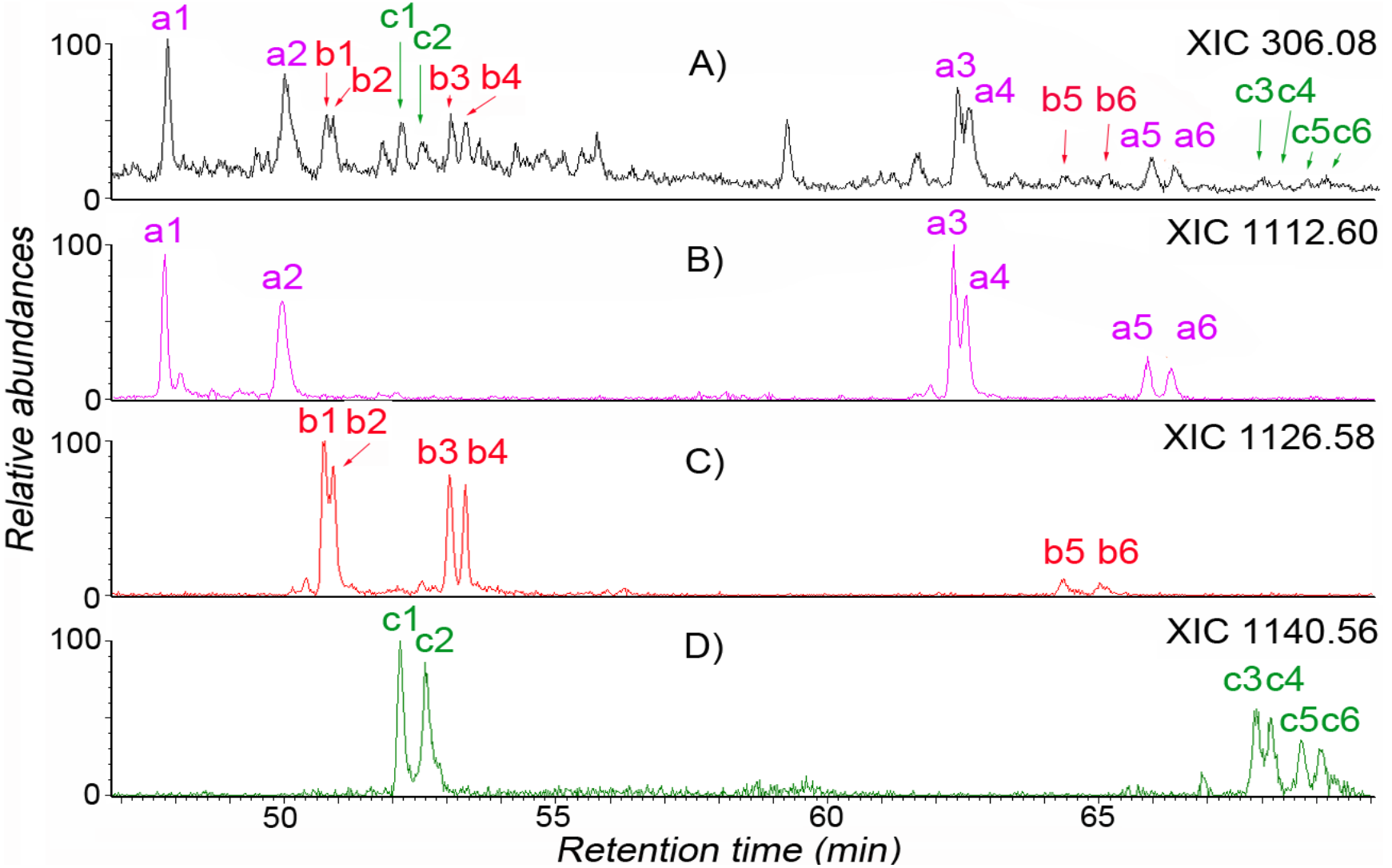

Figure 3.2. Detection of glutathione conjugates as the fragment ion $[GSH-H]^-$ (*m/z* 306.08) using a 110-min LC gradient revealed 3 series of low abundance glutathione conjugates. XICs of *m/z* A) 306.08, B) 1112.6, C) 1126.6 and D) 1140.6 from TOF MS of wildtype *Arabidopsis* leaf extract. Leaf samples were collected 1 hour after wounding.

In Figure 3.2A is shown the XIC of *m/z* 306.08 in the fourth function, with Aperture 1 voltage set as 35 V in the 110 min gradient from 48 to 70 min, which corresponds to 26-35 min in the 45 min gradient. Examination of MS spectra at other MS functions at the same retention time revealed that 3 *m/z* values, namely *m/z* 1112.6, 1126.6 and 1140.6 in the first mass function are responsible for most of the peaks in Figure 3.2A). In Figure 3.2B, C, and D the XICs of these three masses are presented using a 0.3 *m/z* units window, where all peaks aligned with the peaks in Figure 3.2A, suggesting multiple isomers in these compounds. For convenience, in the rest of this paper these peaks are annotated into 3 series for 3 masses and numbered according to their retention times.

3.C.2 MS/MS analysis of putative glutathione conjugates and proposed structure

Using the same 110-min gradient, MS/MS analyses were performed in both positive- and negative-ion modes on a Q-Tof instrument to obtain more structural information of these compounds. For the peaks *m/z* 570.36 at 32.13 min and *m/z* 598.38 at 37.94 min in ESI- of 45 min gradient, the MS/MS spectra obtained while ramping collision energy from 10-45 V in both positive and negative modes are consistent with our hypothesis that they are the glutathione conjugates of dnOPDA and OPDA, as shown in Figure 3.3.

In negative mode, glutathione conjugates of both OPDA and dnOPDA formed product ions at *m/z* 306.08 (deprotonated glutathione) as the predominant product ion. Fragments at *m/z* 272.10, the residue ion resulting from further loss of H_2S and *m/z* 254.09, the dehydrated version of *m/z* 272.10, were also observed. In positive mode, by contrast, more extensive fragmentation was observed. Interestingly, the classical $[M+H-129]^+$ ion produced from loss of the glutamate residue (*m/z* 443.21 and 471.24), was present but at low abundance. The signal from $[M+H-147]^+$ ion (*m/z* 425.20 and 453.23), by contrast, after further loss of another molecule of water or

loss of a glutamic acid through a intra-molecular reaction in the first place, were more abundant. The product ions with highest yields were $[GSH+H-129]^+$ (*m/z* 179.03), $[GSH+H]^+$ (*m/z* 308.09), and $[(dn)OPDA+H]^+$ (*m/z* 265.17 and 293.20) . Other minor fragments include $[GS-(dn)OPDA-gly+H]^+$ (*m/z* 497.23 and 525.26) and $[(dn)OPDA-S-CH_2-CH=NH_2]^+$ (*m/z* 340.19 and 368.22), which is similar to $[M-232]^+$ reported from a bile drug metabolite glutathione conjugate study(Waldon, et al., 2010). Fragments corresponding to $[(dn)OPDA+H-H_2O]^+$ (*m/z* 247.16 and 275.19), $[GSH-gly+H]^+$ (*m/z* 233.06) and $[gly+H]^+$ (*m/z* 76.03) were also detected. These mass spectra show solid evidence for the structure determination of GS-(dn)OPDA and also that both the traditional $[M+H-129]^+$ and $[M-H-272]^-$ may not be sufficient for searching for glutathione conjugates of plant oxylipins.

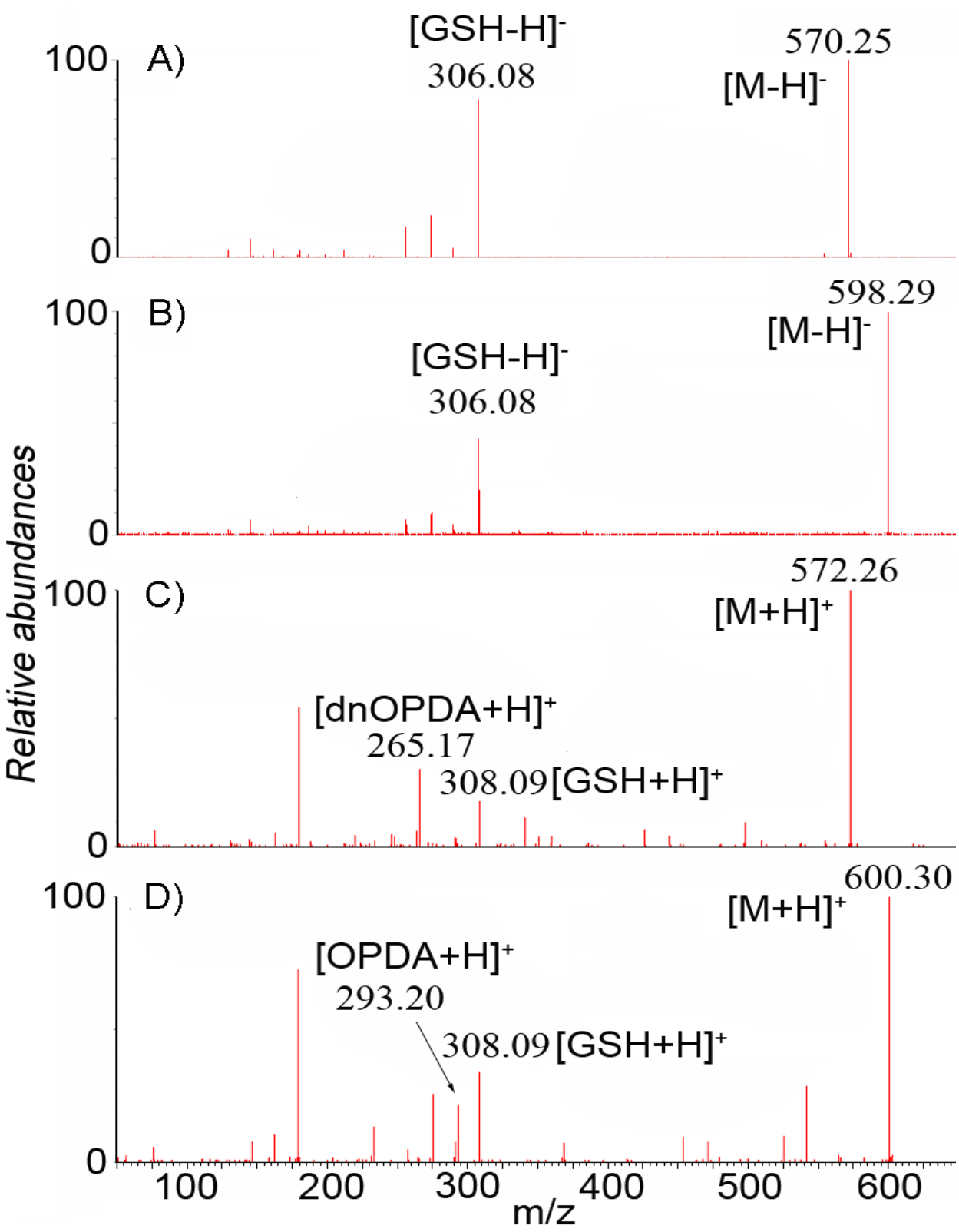

Figure 3.3. MS/MS results of GS-(dn)OPDA from wildtype *Arabidopsis* leaf extract. Leaf samples were collected 1 hour after wounding. A) and B) are in negative mode while C) and D) are in positive mode for GS-dnOPDA and GS-OPDA, respectively.

To generate adequate yields of a broad range of product ion yields for the peak of *m/z* 1112.6 (and 1114.6 in ESI+), collision energy was ramped from 10 V to 100 V for positive-ion mode and 5 V to 70 V for negative-ion mode MS/MS to get satisfactory fragmentation. MS/MS product ion spectra for *m/z* 1126.6 and 1140.6 were limited by the low metabolite abundances. MS/MS spectra were almost identical for the multiple chromatographic peaks for *m/z* 1112.6. Shown in Figure 3.4 are the MS/MS spectra from the first peak at 48.2 min using the 110 min gradient. From these spectra, it is proposed that these compounds are glutathione conjugates of monogalactosyl diacylglycerides (GS-MGDG) esterified to electrophilic oxylipins, as described below. This peak has been annotated as GS-MGDGa1.

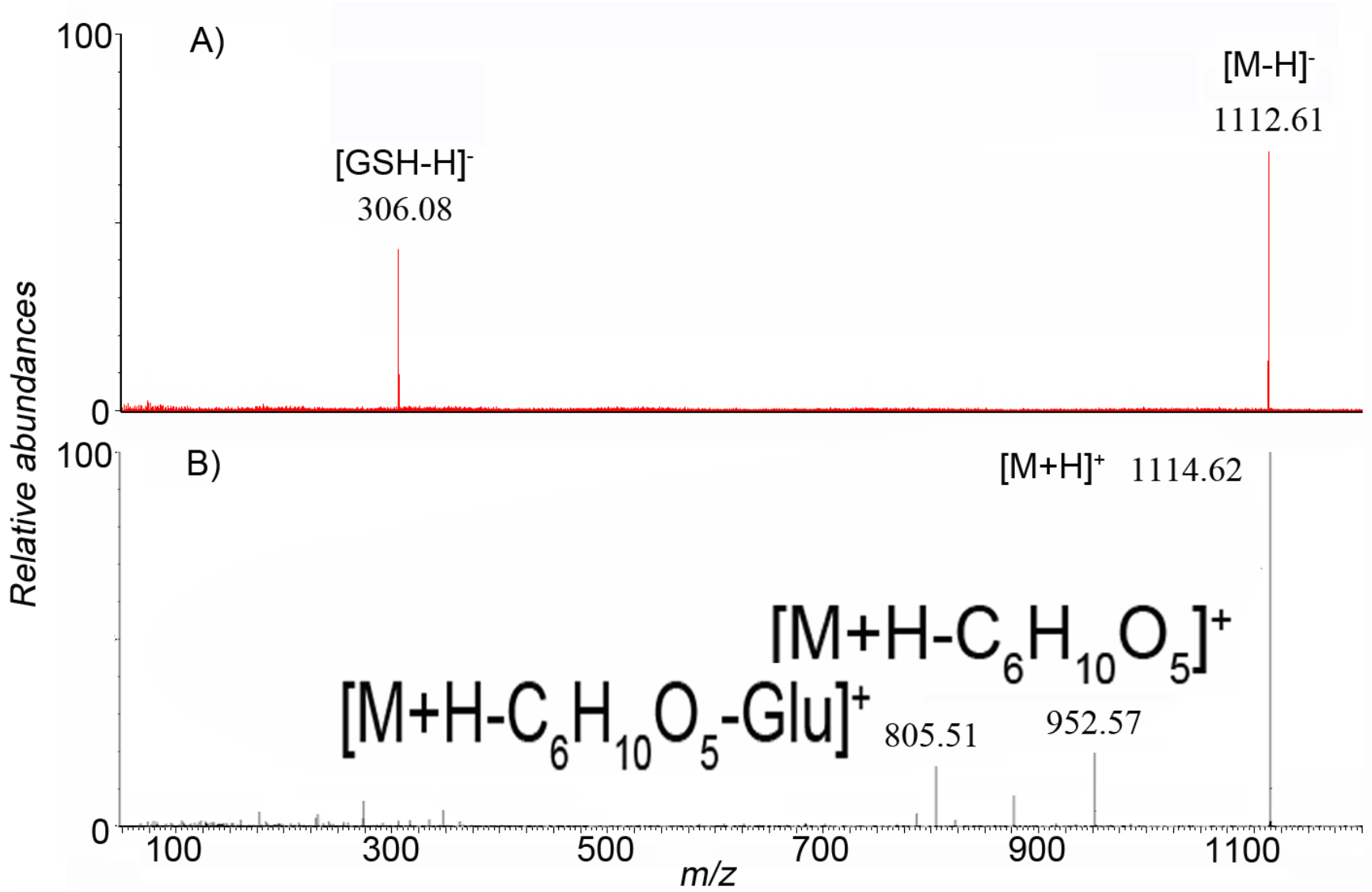

Figure 3.4. Evidence for GS-MGDG structure features: MS/MS spectra from Q-TOF instrument of GS-MGDGa1 extracted from *Arabidopsis* leaf tissues in (A) negative and (B) positive mode, respectively. Leaf samples were collected 1 hour after wounding. C): proposed structures for GS-MGDGs.

Figure 3.4 (cont'd)

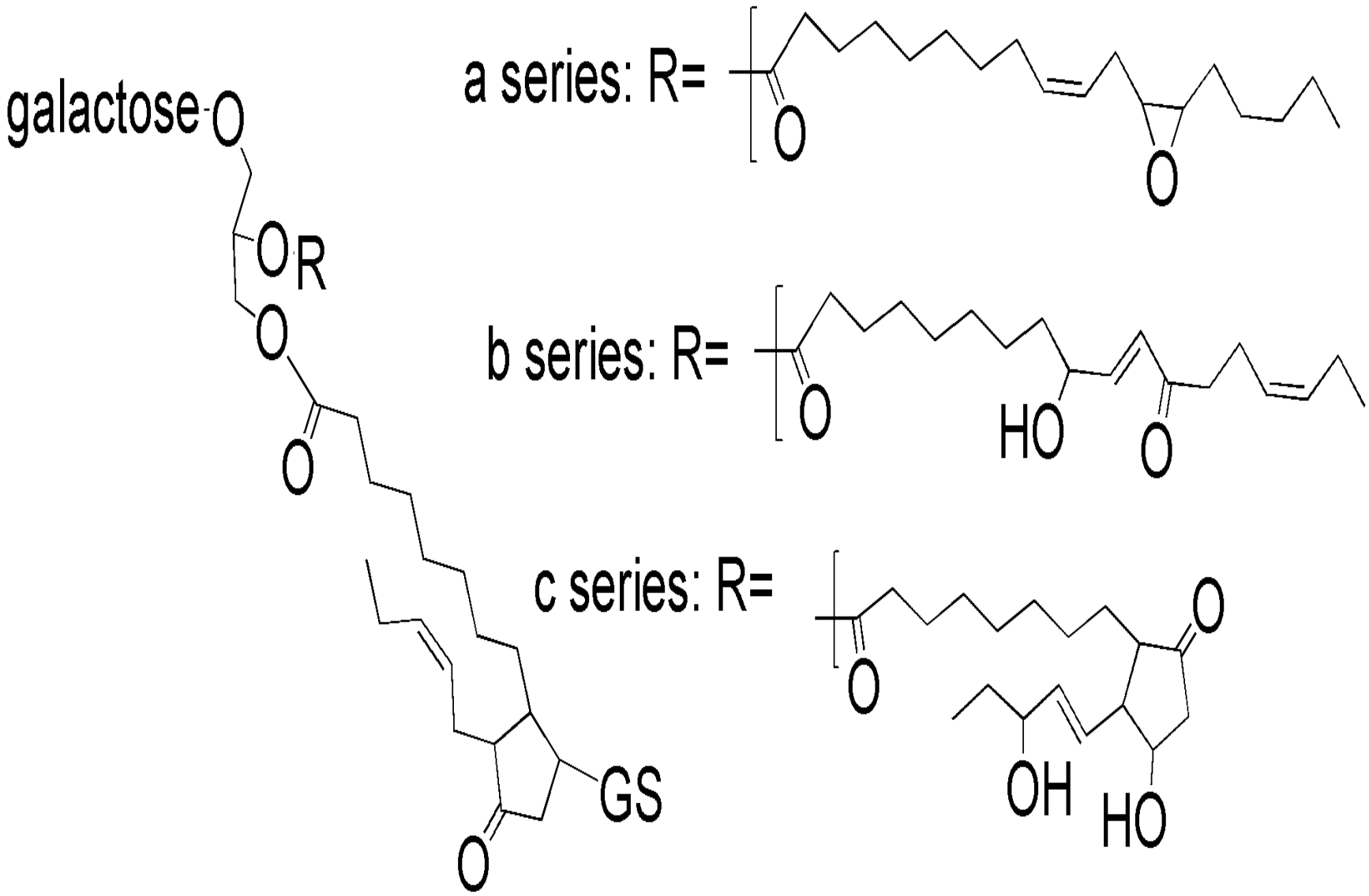

For GS-MGDGa1, in negative mode MS/MS, *m/z* 306.09 was the only fragment produced. In positive mode, the products after loss of anhydrogalactose (*m/z* 952.57) and a further loss of glutamic acid (*m/z* 805.51) were the dominant fragment ions. Other fragments can be interpreted as further losses of glycine after dehydrated sugar 952.57 (*m/z* 877.54), $[OPDA\text{-}H_2O+H]^+$ (*m/z* 275.19), $[GSH+H]^+$ (*m/z* 308.08), $[HO\text{-}CH_2\text{-}CH{=}CH\text{-}O\text{-}OPDA+H]^+$ (*m/z* 349.23) and [GSH-dehydrated glu+H]$^+$ (*m/z* 179.04). Surprisingly, the traditional $[M+H\text{-}129]^+$ is missing, suggesting this screening method won't work at all against these oxylipin glutathione conjugates. For GS-MGDGb1, similar spectra were obtained but at lower ion counts due to low abundances, as shown in Figure A1.

Based on the accurate mass measurement of the intact molecule and fragments, the fragments that provided evidence of a sugar group (most probably galactose because galactolipids are the most abundant membrane lipids in *Arabidopsis* (Holzl and Dormann, 2007) and a glutathione moiety, and the fragments that are consistent with OPDA attached to a glyceride core structure, and the knowledge that OPDA-containing galactolipids are known to be accumulated in *Arabidopsis* leaf after wounding (Stelmach, 2001), we propose that these compounds are glutathione conjugates of OPDA-containing monogalactosyl diacylglycerides (GS-MGDG), in which OPDA are specifically esterified on the *sn*-1 position and the galactose is attached on the *sn*-3 position of the glyceride, exactly the same as the OPDA-containing galactolipids characterized with NMR (Andersson, *et al.*, 2006, Buseman, 2006, Hisamatsu, *et al.*, 2003, Hisamatsu, *et al.*, 2005, Nakajyo, *et al.*, 2006, Stelmach, 2001). For the acyl group on the *sn*-2 position, no structural information is available from fragmentation. Because the abundance is so low that even reliable MS/MS is challenging, NMR structure determination would be not

feasible without growing substantially more plants. Two GS-MGDG conjugates have molecular masses consistent with epoxy-octadecaenoic acid and oxo-hydroxy-octadecadienoic acid (oxoHOTrE), previously reported oxylipins (Blee, 1998, Davoine, et al., 2005, Feussner and Wasternack, 2002, Montillet *et al.*, 2004). These assignments, of course, do not preclude the possibilities of these compounds being other isomeric forms. Detailed putative structures are shown in Figure 3.4.3).

3.C.3 Proposed method to search for GS-MGDGs

Since the loss of dehydrated galactose is one of the major fragments made in MS/MS of GS-MGDGs, we now propose that this neutral loss yielding $[M+H-162.05]^+$ can be used in conjunction with precursor scans for *m/z* 306.08 in negative-ion mode to find GS-MGDGs. Example XICs can be used to illustrate the method in Figure 3.5, showing the matching peaks from most of the a and b series of GS-MGDGs. The abundances of c series and some peaks in b series are too low for the fragment to be visible.

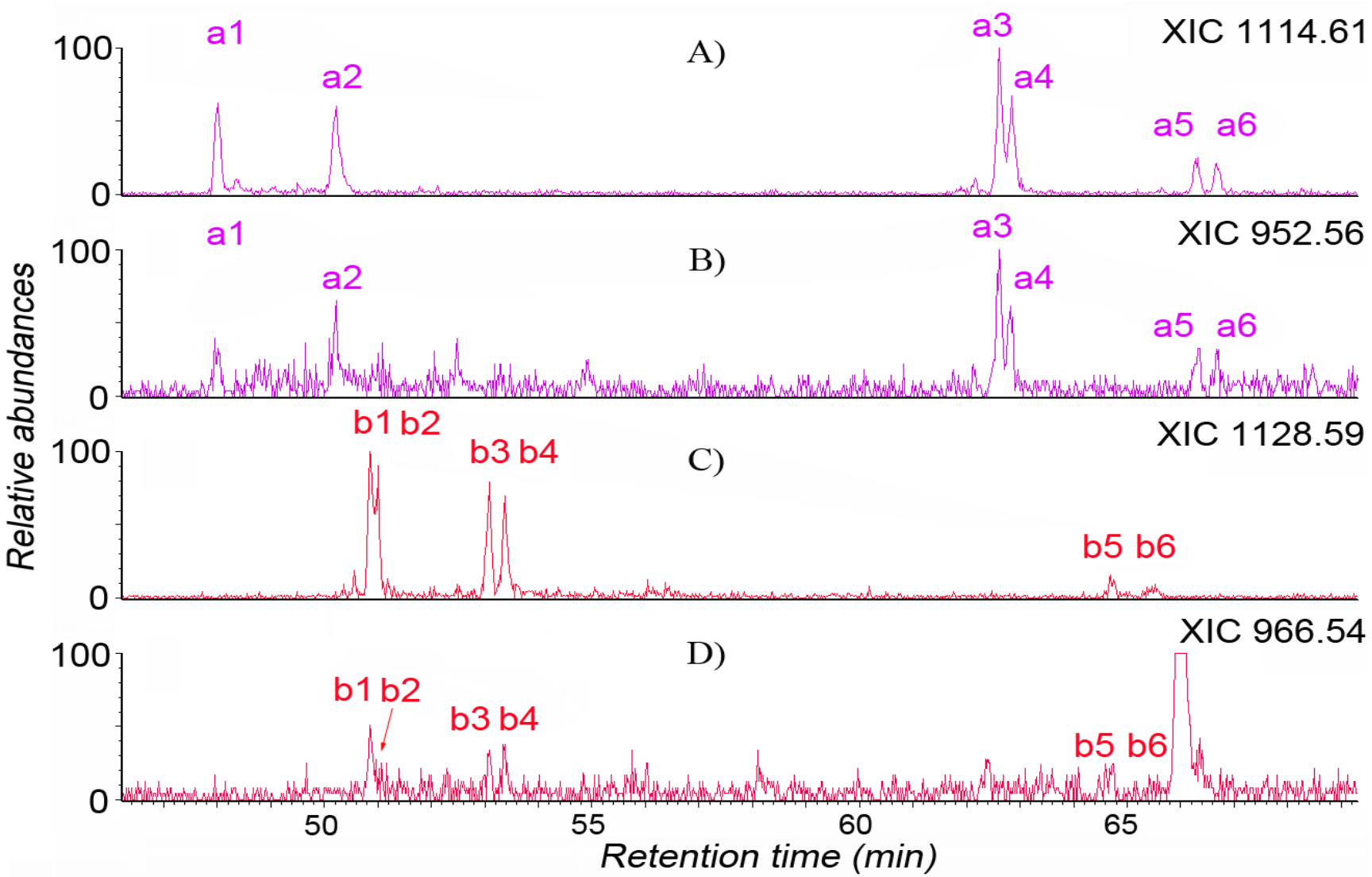

Figure 3.5. $[M+H-162.05]^{+}$ is reveals GS-MGDGs. XICs of *m/z* A) 1114.6, B) 952.5, C) 1126.6 and D) 966.5 from TOF MS in 45 min gradient of wildtype *Arabidopsis* leaf extract. Leaf samples were collected 1 hour after wounding.

3.C.4 Quantification of glutathione conjugates to probe roles in signaling

Investigation of the natural abundance of these endogenous glutathione conjugates is essential in understanding their biological roles in response to stress. Wild type and a few homozygous *At*GSTU gene knockout mutants were used in this wounding experiment. The selection of mutants was based on seed availability, literature reports of GST expression levels (Dixon, *et al.*, 2010), and sequence similarity (because these candidates represent the diversity within the tau family, which can be seen from the published phylogenetic tree (Dixon, *et al.*, 2010). After sampling tissues four hours after wounding, glutathione conjugates were profiled using the 45-min gradient, and the accumulation of these compounds after wounding is illustrated in Figure 3.6. In Figure 3.6A and 3.6B, GS-OPDA and GS-dnOPDA levels increased significantly after mechanical wounding in wild type *Arabidopsis thaliana* plants (solid lines), which is consistent with reported detection of these two compounds in tobacco after stimuli (Davoine, 2006, Davoine, *et al.*, 2005). Figure 3.6C and D, document the accumulation of GS-MGDGa1 and GS-MGDGa2 as well, but the increase in levels was slower than for glutathione conjugates of OPDA and dnOPDA, since most of the increase in abundance did not occur until 4 hours after wounding. In Figure 3.6A and B, metabolite levels from the leaf extract of *atgstu5* (dashed lines) are also presented, and the lack of accumulation of GS-OPDA suggests that the missing enzyme may be responsible for catalyzing the *in vivo* glutathione conjugation of OPDA. This lack of increase in level did not occur for the galactolipid conjugates GS-MGDGa1 and GS-MGDGa2 (dashed lines in Figure 3.6C and D), suggesting that alternative GSTs are responsible for catalyzing the conjugation for these compounds, perhaps because they are primarily located in the chloroplast membrane, while OPDA and dnOPDA are more capable of migrating to other subcellular locations. The results shown in Figure 3.6E was from a separate wounding experiment

comparing wildtype and 5 mutant genotype plants, which again showed that the accumulation of GS-OPDA was lowered in *atgstu5,* but roughly the same in all other tested plants. T-test showed that the difference between *atgstu5* and wild type plants was significant with the chance for this to result from a random process, with $P < 0.001$.

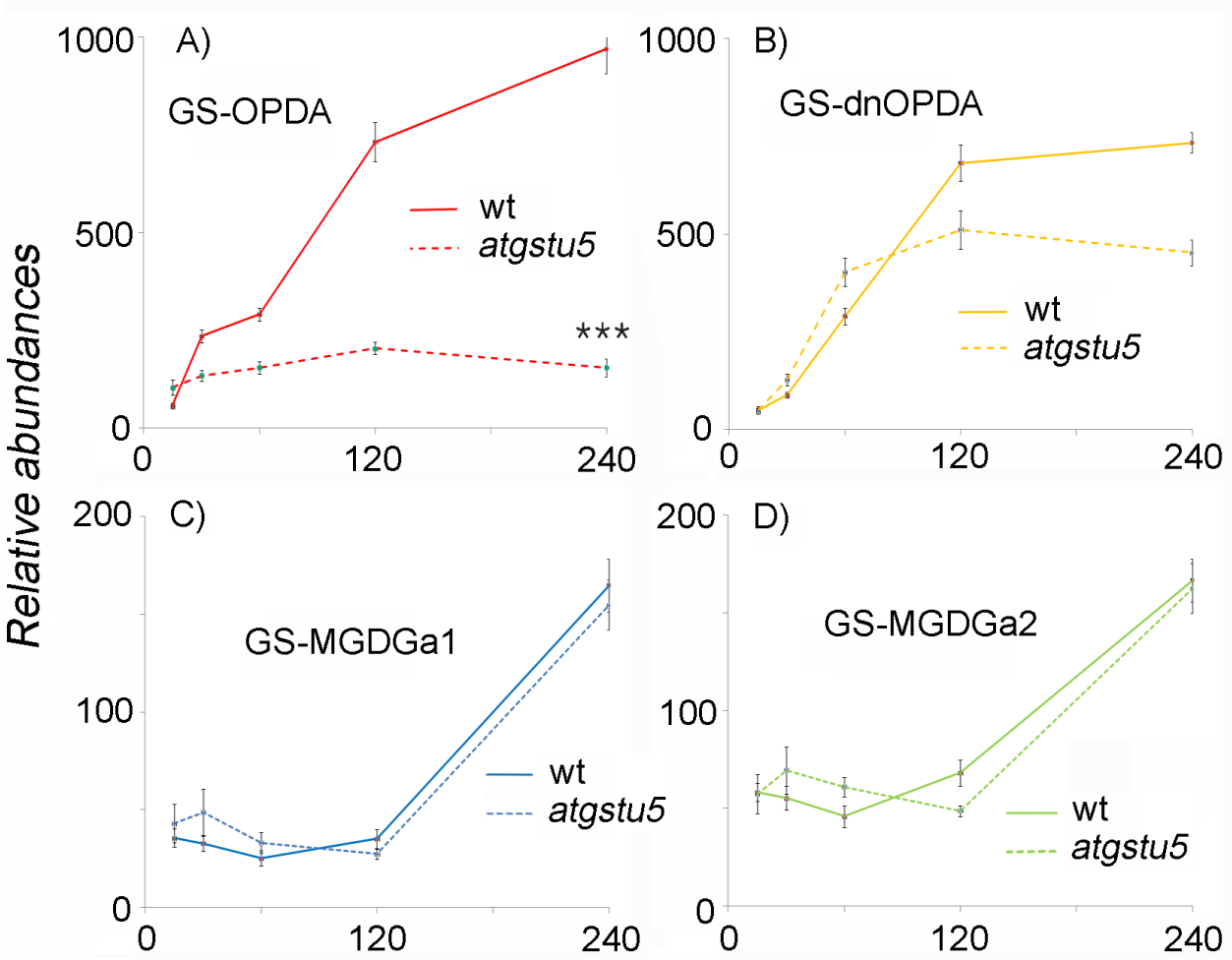

Figure 3.6. Wounding-induced accumulation of endogenous oxylipin glutathione conjugate in *Arabidopsis thaliana* leaf extract. A), B), C), D): GS-OPDA, GS-dnOPDA, GS-MGDGa1 and GS-MGDGa2 in wild type *Arabidopsis* and *atgstu5* mutant. E) Comparison of GS-OPDA in 6 genotypes with various *At*GSTUs knocked out. All relative abundances represent peak areas normalized to total MS signal. Stars indicate significance according to *t*-test with $P < 0.001$. Error bars show standard deviation from 8 biological replicates.

Figure 3.6 (cont'd)

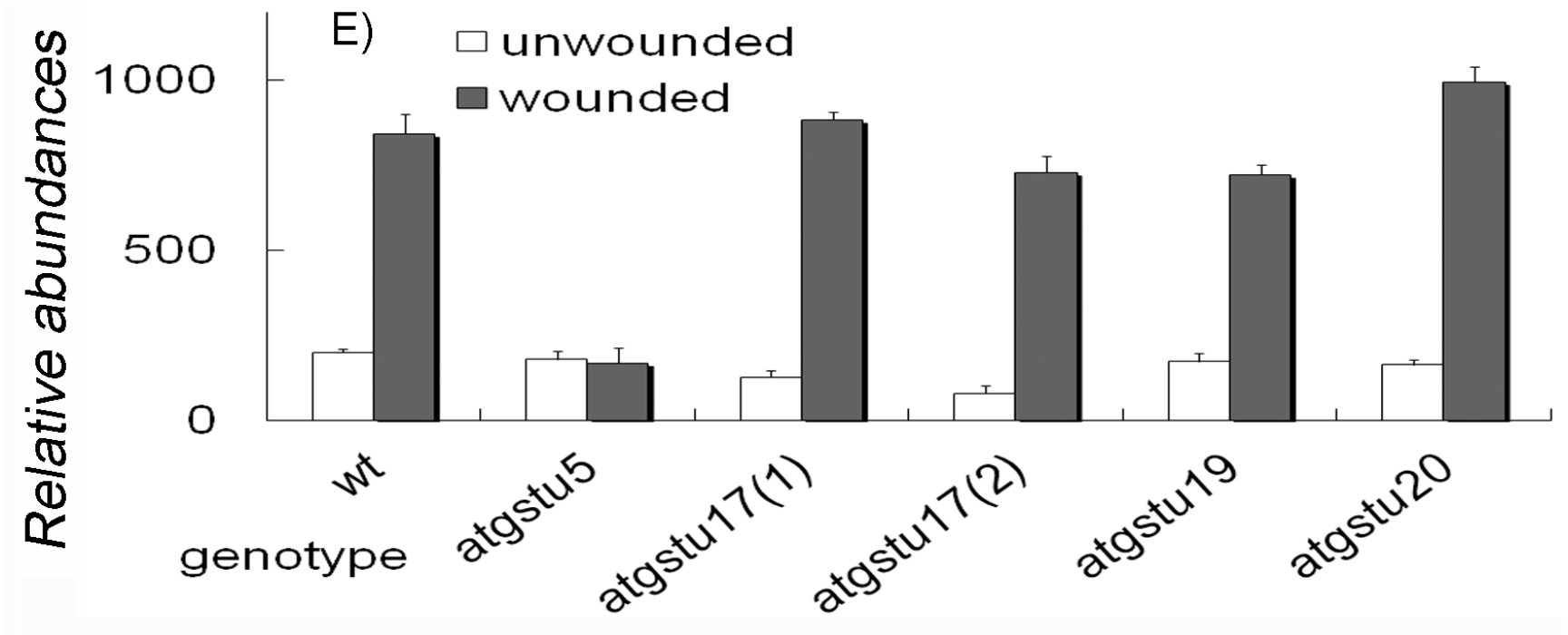

*At*GSTUs, or tau class of GSTs in *Arabidopsis*, are known for their cytosolic abundance and probable transferase activity based on DNA sequences, though their detailed catalytic activities are not well understood (Wolf, *et al.*, 1996). *In vitro* examination of GST expression in *Escherichia coli* and expression of individual *At*GSTs in *Arabidopsis* and tobacco has shown that glutathione conjugation of OPDA can be catalyzed by *At*GSTF8 and *At*GSTU19 (Dixon and Edwards, 2009) (Mueller, et al., 2008). In Figure 3.6E, however, the accumulation of GS-OPDA *At*GSTU19 deficient plant was not altered significantly relative to wild type. This, taken with the fact that the GS-OPDA levels in *At*GSTU5 knockout mutant plant did not approach zero, indicate that these enzymes may overlap in their substrate specificity and capacity to conjugate OPDA *in vivo* under physiological conditions.

In earlier reports, *At*GSTU5 was expressed in adult *Arabidopsis* leaf and exhibited conjugation activity with substrate 1-chloro-2,4-dinitrobenzene (CDNB) and benzyl isothiocyanate (BITC) (Dixon, *et al.*, 2009, Zimmermann, *et al.*, 2004). Its expression can be induced by methyl jasmonate (MeJA) (Wagner, *et al.*, 2002). Its cytosolic localization was further supported by the observation that many other *At*GSTUs were expressed in cytosol (Wagner, *et al.*, 2002). This work will be the first specific evidence for the *in vivo* substrate selection and catalytic activity of this particular enzyme.

OPDA-containing galactolipids are made in the chloroplast membranes after stress (Nilsson, *et al.*, 2012) while the biosynthesis of phytohormone JA from OPDA is believed to occur in peroxisomes (Kazan and Manners, 2008). OPDA transport has been proposed to be either passive or active with ATP-binding cassette transporter COMATOSA (CMS). The glutathione conjugation of OPDA-containing galactolipids found in this work may participate in regulation of jasmonate signaling by regulating the amount of galactolipids hydrolyzed to release OPDA

into cytosol. However, the absence of OPDA-containing MGDGs corresponding to GS-MGDGs identified in this thesis, and the absence of GS-MGDGs correspond to arabidopsides, abundant OPDA-containing MGDGs, indicate that much future work need to be done to fully understand the glutathione conjugation specificity of electrophilic oxylipins and its biological roles.

The roles of glutathione conjugation in jasmonate signaling can also be further explained if we take into account the time frame of accumulating these compounds *in vivo*. The rapid wounding-induced accumulation of active phytohormone JA-Ile peaks in just 15-20 minutes (Koo, *et al.*, 2009b). The precursor of JA biosynthesis, OPDA, reaches its highest concentration in about 1 hour (Koo, *et al.*, 2009b). GS-OPDA and GS-dnOPDA accumulation reach a plateau 2 hours after wounding as shown in Figure 3.6A and 3.6B. GS-MGDGs do not accumulate until roughly 4 hours post wounding as shown in Figure 3.6C and 3.6D. These observations together suggest that glutathione conjugation, as a wound-induced defense signal quenching reaction, is delayed until the signaling molecules have finished their responsibilities to start removing them from the tissue environment to protect the cell from their potential toxicity. This delay may be the consequences of the time needed to transcribe and translate new *At*GSTU5 proteins after mechanical wounding. No significant difference were found, however, between the *atgstu5* mutant and wild type *Arabidopsis* plants, for the accumulation concentration profiles of OPDA and dnOPDA in the first 4 hours after mechanical wounding. This is consistent with the fact that the relative abundances of GS-(dn)OPDA were found to be much lower (10^2 difference in extraction ion chromatogram peak areas) than OPDA and dnOPDA and suggesting the glutathione conjugation is not the limiting factor of electrophilic oxylipin concentrations in this time period.

3.D Conclusions

This work introduces a LC-MS protocol for searching for endogenous glutathione conjugates in plants utilizing XIC of *m/z* 306.08 in multiplexed CID and confirmation of structures using MS/MS in positive mode. A new family of glutathione conjugates, those of OPDA-containing galactolipids, was discovered with likely structures proposed. *At*GSTU5 knockout mutant failed to accumulate GS-OPDA upon wounding and GS-MGDGs were accumulated in wild type plants at 4 hours post wounding. These observations supported our hypothesis that glutathione conjugation modulates wound-induced signaling and down-regulate the activities from signaling molecules.

Chapter 4. Unusual negative charge-directed fragmentation: collision-induced dissociation of cyclopentenone oxylipins in negative ion mode

4.A. Introduction

4.A.1. Occurrence and functions of electrophilic oxylipins

Oxidized fatty acids, known as oxylipins, serve as potent regulators of a wide array of physiological functions ranging from enhancement (or suppression) of inflammation, cell proliferation, apoptosis, and tissue repair in animals. In animals, most of these known signaling molecules are eicosanoids such as prostaglandins derived from the 20-carbon polyunsaturated fatty acid (PUFA) arachidonic acid. Prostaglandins are well-characterized mediators of inflammation including pain and fever and a wide assortment of biological functions in virtually all human cells (Narumiya, *et al.*, 1999, Tsuboi, *et al.*, 2002). In plants, however, the most important oxylipins are oxidized metabolites of the 18-carbon PUFA linolenic acid. In both animals and plants, oxylipins regulate a wide assortment of immune functions. The isoleucine conjugate of the oxylipin jasmonic acid (JA, Figure 1) functions as a master switch that regulates expression of hundreds of downstream genes in plant defense responses to various biotic and abiotic forms of stress (Balbi and Devoto, 2008, Browse and Howe, 2008, Devoto *et al.*, 2005, Glazebrook, 2005, Howe and Jander, 2008, Mandaokar *et al.*, 2006, Reymond *et al.*, 2000, Schenk *et al.*, 2000, Staswick and Tiryaki, 2004, Wasternack, 2007). Jasmonates also play important roles as regulators of plant development.(Balbi and Devoto, 2008, Yan, *et al.*, 2007, Zhang and Turner, 2008) More recently, it has been learned that the octadecanoid oxylipin 12-oxophytodienoic acid (OPDA), a biosynthetic precursor of JA, and dinorOPDA (dnOPDA), another cyclopentenone octadecanoid with 16 carbons, exhibit independent functions as plant defense gene regulators (Stelmach *et al.*, 1998, Stintzi, *et al.*, 2001, Taki, *et al.*, 2005, Weber *et*

al., 1997). These substances also exist as complex esters of galactolipids in *Arabidopsis*. Since they accumulate in leaves after mechanical wounding, they have been proposed to serve as stored signaling oxylipins that enable a more rapid biochemical response to a sudden stress (Andersson, *et al.*, 2006, Bottcher and Weiler, 2007, Buseman, 2006, Glauser *et al.*, 2008, Hisamatsu, *et al.*, 2003, Hisamatsu, *et al.*, 2005, Kourtchenko, *et al.*, 2007, Stelmach, 2001). The biological functions of cyclopentenone oxylipins have been attributed in substantial measure to their reactivity as electrophiles, which confer potential to alter protein functions through covalent modification of protein nucleophiles (Stelmach, *et al.*, 1998, Stintzi, *et al.*, 2001, Taki, *et al.*, 2005, Weber, *et al.*, 1997). Some oxylipin electrophiles, including 15-deoxy-$\Delta^{12,14}$-prostaglandin J_2 (15dPGJ_2; Figure 4.1) may form by spontaneous dehydration of enzymatically-synthesized eicosanoids (PGD_2 in this case).

Discoveries of novel oxylipin metabolites continue, with recent reports describing a new glucoside of the jasmonate precursor OPC:4, acetylenic oxylipins, and a series of anti-inflammatory cyclopentenone neuroprostanes derived from docosahexaenoic acid (DHA; C22:6ω3)(Glauser *et al.*, 2010, Stelmach, *et al.*, 1998, Stintzi, *et al.*, 2001, Taki, *et al.*, 2005, Weber, *et al.*, 1997) .These findings highlight the continuing importance of characterizing and quantifying electrophilic oxylipins and their metabolites.

4.A.2. Characterization of oxylipins using tandem mass spectrometry

Structure elucidation and quantification of oxylipins has relied on mass spectrometric analysis in negative mode because this approach provides better ionization efficiencies and lower limits of detection than are achieved in positive-ion mode. (Chung, *et al.*, 2008, Koo, *et al.*, 2009b) However, structure assignments of oxylipins, particularly discrimination of isomers, depend on

fragments generated by breaking of carbon-carbon bonds, since fragment ion masses can be used to establish positions of oxidative substitution. However, low energy ion-molecule collisions of fatty acid anions often fail to generate abundant product ions from C-C cleavage aside from neutral loss of CO_2, and the chemistry of lipid anion fragmentation is not understood as well as fragment ion chemistry in positive ion mode. The scarcity of diagnostic C-C fragment pathways in negative ion mode makes it challenging to distinguish analytes from their numerous structural isomers. Negative mode CID mass spectra of oxylipins generated at high (KV) collision voltages display fragments derived from charge-remote elimination of neutral molecules, including elimination of alkenes from saturated fatty acids.(Jensen and Gross, 1986, Jensen *et al.*, 1985) Lower collision energies yielded neutral alkenes and aldehydes from hydroxy polyunsaturated fatty acids, which have been proposed to take place through α-hydroxy-β-ene and γ-ene arrangements. (Hankin *et al.*, 1997, Oliw *et al.*, 1998, Savagnac *et al.*, 1989, Wheelan *et al.*, 1993, Wheelan *et al.*, 1996, Zirrolli *et al.*, 1990) Similar eliminations of neutral aldehydes from deprotonated epoxy fatty acids (MacMillan and Murphy, 1995) and hydroperoxides of fatty acids, (Oliw, *et al.*, 1998) and alkenes from saturated and mono-unsaturated fatty acids have been observed, (Cordero and Wesdemiotis, 1994) but factors that lead to specific product ions have yet to be fully explained.

Several investigations have explored behavior of oxylipin negative ions upon collisional activation. Product ions corresponding to neutral losses of aldehydes from hydroxylated fatty acids and isoprostanes are consistent with charge-directed cleavage of carbon-carbon bonds. (Moe *et al.*, 2004, Oliw, *et al.*, 1998, Wheelan, *et al.*, 1993, Wheelan, *et al.*, 1996, Zirrolli, *et al.*, 1990) Other examples of C—C bond cleavage include elimination of CO_2 from the carboxylate group of hydroxylated fatty acids,(Moe, *et al.*, 2004) losses of CH_2O_2 or $C_2H_4O_2$ from β-

hydroxy fatty acids, (Kerwin and Torvik, 1996) and formation of acetate, acrylate and similar short unsaturated carboxylic acid anions from PUFA. (Kerwin *et al.*, 1996, MacMillan and Murphy, 1995) Multi-step charge-directed fragmentation mechanisms have been proposed, which are usually initiated by intramolecular nucleophilic displacement, sigmatropic rearrangements, or additions to π-bonds.(Dickinson and Murphy, 2002, MacMillan and Murphy, 1995) Fragmentation of hydroxylated fatty acids negative ions (Moe, *et al.*, 2004, Wheelan, *et al.*, 1996) via radical or homolytic mechanisms has also been proposed and investigated using deuterium labeling.

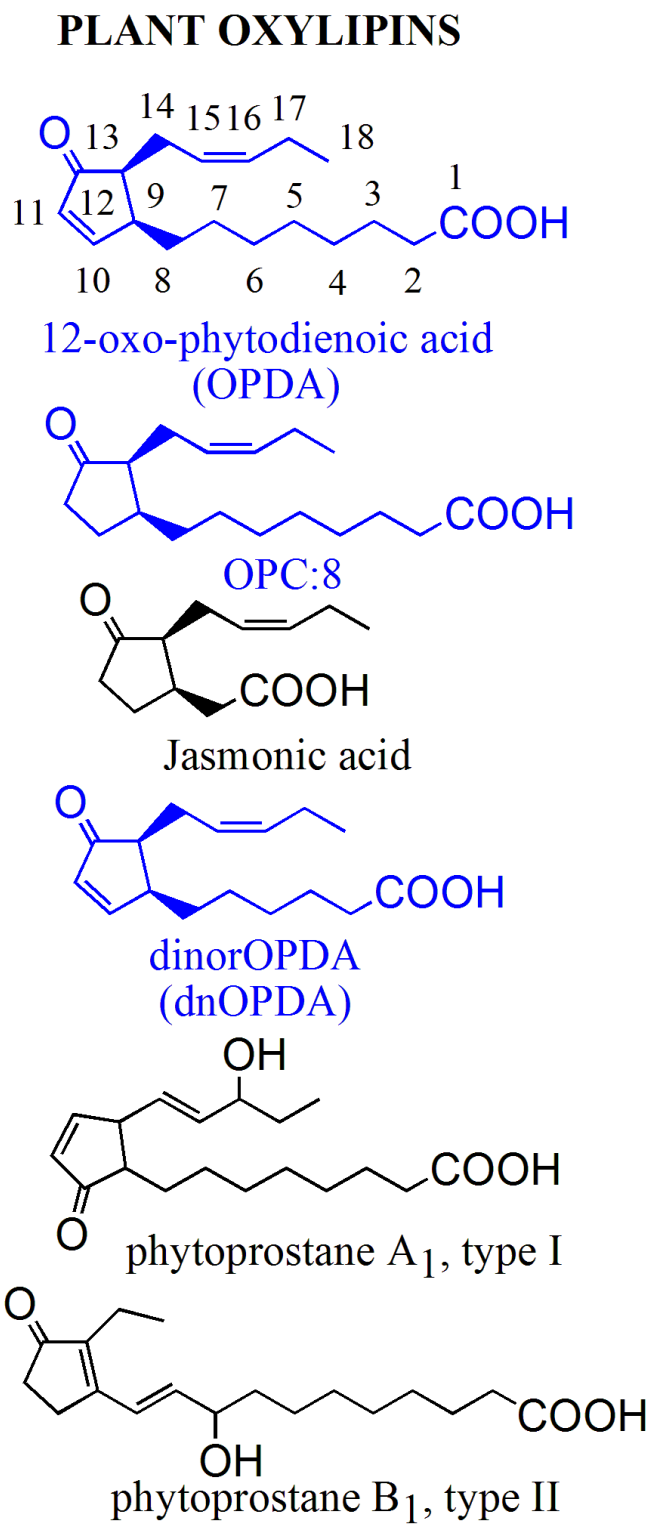

Figure 4.1 Structures of cyclopentanone and cyclopentenone oxylipins including those investigated in this study (highlighted in blue in online version).

Figure 4.1 (cont'd)

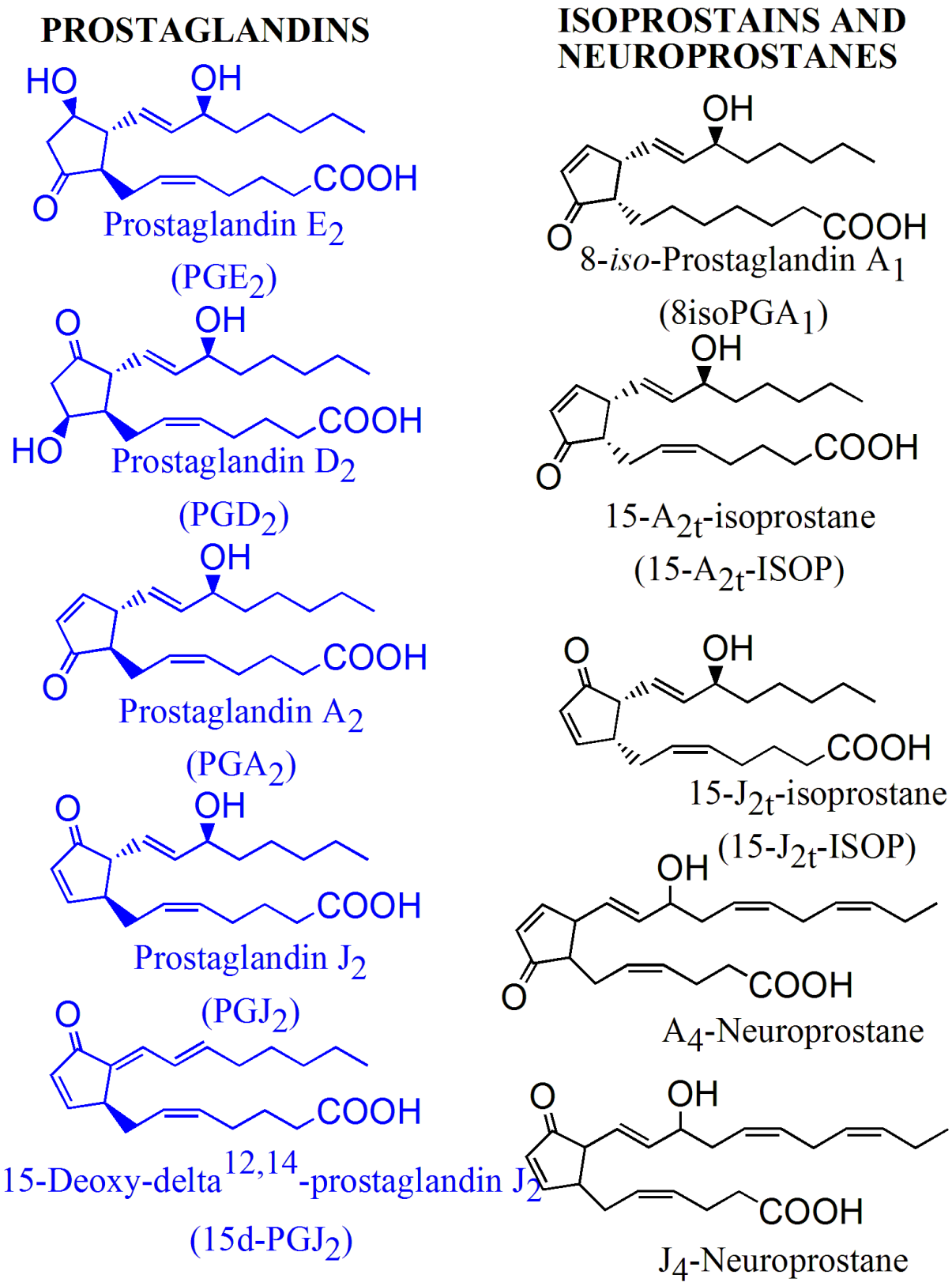

Earlier work from our laboratories demonstrated that two homologous plant oxylipins, OPDA and dnOPDA, yielded a common and dominant fragment ion at *m/z* 165 upon CID of $[M-H]^-$ precursor ions (Koo, *et al.*, 2009b). The negative-ion mode CID mass spectrum of $[^2H_5]$OPDA with all deuteriums in positions 17 and 18 yielded a corresponding fragment at *m/z* 170, providing evidence that the portion most remote from the carboxylic acid group was retained in the fragment ion. Despite the high relative abundance of this fragment, understanding of the chemistry responsible for its formation remained elusive because this fragment is 2 Da heavier than any product anticipated from simple eliminations or nucleophilic displacements. Similar fragments 2 Da heavier than expected from carbon-carbon bond cleavage have been reported for PUFAs, (Dickinson and Murphy, 2002) monohydroxy fatty acids, (Kerwin and Torvik, 1996, Kerwin, *et al.*, 1996) and hydroperoxy and long chain conjugated keto-fatty acids, (MacMillan and Murphy, 1995) where product ions 2 Da heavier mass than expected were observed and interpreted as involving hydrogen migration. In the current study, fragmentation of an assortment of plant and animal cyclopentenone oxylipins has been performed to improve our understanding of the factors that generate structurally useful product ions.

4.B. Materials and methods

4.B.1. Materials

OPDA was purchased from Cayman Chemical (Ann Arbor, MI, USA). ^{18}O-labeled water (97% ^{18}O) was purchased from Isotec, Inc. (Miamisburg, Ohio). Cyclopentenone prostaglandin HPLC mixture (containing PGE_2, PGD_2, PGA_2, PGJ_2, PGB_2 and 15-deoxy-$\Delta^{12,14}$-PGJ_2) was purchased from Cayman Chemical (Ann Arbor, MI). The plant oxylipin dnOPDA and OPC:8 were extracted from 30-day old rosette leaves of *Arabidopsis thaliana* (ecotype Col-0) 12 hours

after mechanical wounding with a hemostat, and the extract was used directly for LC-MS/MS without further sample treatment. Liquid chromatographic separations were performed on an Ascentis Express C18 column (50 x 2.1 mm; 2.7 μm particles) column (Sigma-Aldrich, St. Louis, MO).

4.B.2. Preparation of ^{18}O-labeled oxylipins

^{18}O-labeled forms of OPDA were prepared by exchange with $H_2{}^{18}O$ following an earlier method.(Mueller *et al.*, 2006) To exchange all oxygen atoms using acid catalysis, 29.2 μL of 1 mg/mL OPDA solution in ethanol (100 nmol) was dried under vacuum using a SpeedVac, and 60 μL of ^{18}O water followed by 18 μL of 12 M HCl were added to the dried residue. The mixture was incubated at 70 °C for 2 hours. Back-exchange of the ketone oxygen was conducted by drying the reaction mixture under vacuum, followed by addition of 30 μL of methanol and 20 μL of 1 M aqueous KOH, followed by incubation at 40 °C for 1 hour.

4.B.3 Wounding of *Arabidopsis* leaves and extraction of oxylipins including dnOPDA

Fully expanded 30-day old rosette leaves of Arabidopsis wild type plants were wounded with a hemostat, harvested 12 hours later, and immediately frozen in a -80° freezer. Frozen leaves were ground to powder under liquid nitrogen using a mortar and pestle, transferred to polypropylene centrifuge tubes. For each sample, 0.3 g of leaf tissue was extracted with 1.5 mL of 80% methanol containing 0.01% butylated hydroxytoluene (BHT, or 2,6-bis(1,1-dimethylethyl)-4-methylphenol)) at 4 °C for 16 hours. Extracts were centrifuged at 10,000 *g* for 10 min at 0° C, and supernatants were withdrawn and stored at -20 °C.

4.B.4 Mass spectrometric analysis of oxylipins

All MS/MS experiments were performed on an AB/Sciex (Framingham, MA) QTRAP 3200 mass spectrometer. Synthetic OPDA was analyzed using flow-injection analysis after dissolving into a solution of 40% of 0.15% aqueous formic acid and 60% of methanol. Injections of 10 µL were made, and delivered to the ion source at a flow rate of 0.2 mL/min in negative electrospray mode to generate deprotonated molecular ions. Generation of CID spectra of deprotonated dnOPDA and OPC:8 involved separating these constituents of *Arabidopsis* leaf extract from other metabolites using a gradient of 0.15% aqueous formic acid (solvent A) and methanol (solvent B) ramping from 5% to 95% of B in 45 minutes at 0.2 mL/min, generating deprotonated molecular ions using electrospray ionization in negative-ion mode. Metabolites dnOPDA and OPC:8 were annotated based on matching of molecular masses and chromatographic retention times with synthetic standards analyzed previously.(Koo *et al.*, 2009a, Koo *et al.*, 2006) Various cyclopentenone prostaglandins were analyzed by injecting an aliquot of the cyclopentenone prostaglandin HPLC mixture onto the HPLC column, and performing gradient elution using 0.15% aqueous formic acid (solvent A) and acetonitrile (solvent B), ramping from 37.5% to 42.5% of B over 45 minutes using a flow rate of 0.2 mL/min. Ion source settings for Gas 1 (nebulizing gas) and Gas 2 (desolvation gas) (both are parameters specific to this ion source) were kept at 50 and 10 (arbitrary units), respectively. Temperature was 450 $^{\circ}$C. Collision cell entrance potential was -10 V. Declustering potential (DP) was set to -20 V and collision cell potential (CE) was set to -25 V for CID of deprotonated OPDA and dnOPDA. DP was set to -80 V for in-source fragmentation to produce $[M\text{-}H_2O]^-$ and $[M\text{-}CO_2]^-$ from dnOPDA and OPDA for CID using CE of -25 V. DP was set to -80V and CE was set to -40V for the *m/z* 165 fragment from dnOPDA and OPDA. For pseudo-MS^3 experiments of prostaglandins, $[M\text{-}H\text{-}2H_2O]^-$ for PGD_2 and PGE_2

generated by in source fragmentation at DP of -65 V, $[M-H_2O]^-$ for PGA_2 and PGJ_2 at DP of -45 V, and $[M-H]^-$ for $15dPGJ_2$ at DP of -35V were chosen as precursor ions. All these ions were further isolated by Q1 and collisionally dissociated in the collision cell using enhanced product ion mode (an ion trap scan of products formed in the collision cell) at collision cell potential of -25 V.

Accurate mass measurements of deprotonated molecular ions and product ions in negative mode ESI and CID were performed using a Waters LCT Premier mass spectrometer, an orthogonal time-of-flight instrument purchased from Waters (Milford, MA), using the same HPLC separations as described above. Product ions were generated by quasi-simultaneous switching of the Aperture 1 potential (a voltage applied across the exit of the first transit lens and the entrance to the next ion transit region to facilitate non-selective fragmentation) across multiple values (multiplexed nonselective CID).(Gu *et al.*, 2010a) The formation of all product ions from specific precursor ions was confirmed independently by performing enhanced product ion scans on the QTRAP mass spectrometer.

4.C. Results and Discussion

4.C.1. Collision induced dissociation mass spectra of OPDA and OPC:8

The observation of a fragment ion at *m/z* 165 common to OPDA and dnOPDA, which differ only in the number of $–CH_2–$ groups between the carboxylate and the cyclopentenone (Figure 4.2b and 4.2c), provided evidence that important dissociation reactions occur remote from the site of the carboxylate. Furthermore, CID of the deprotonated cyclopentanone oxylipin OPC:8, which differs only by lacking the carbon-carbon double bond conjugated to the ketone, failed to yield analogous fragments in the same *m/z* region of the mass spectrum, and primarily yielded

fragments arising from neutral losses of H_2O and CO_2 using identical collision conditions (Figure 4.2a). Inspection of the OPDA structure revealed that cleavage of the C—C bond between carbons 7 and 8 would yield a fragment of *m/z* 163, 2 *m/z* units lighter than the observed fragment. The 2 *m/z* units difference in nominal mass suggested two possibilities: a difference of two hydrogen atoms, or the replacement of a CH_2 with an oxygen atom. Fortunately, nonselective multiplexed CID(Gu *et al.*, 2010b) on an LC-TOF instrument generated the *m/z* 165 fragment from OPDA and allowed accurate measurement of its mass as *m/z* 165.1300 (calculated *m/z* 165.1285 for $C_{11}H_{17}O^-$), consistent with the fragment arising from the cyclopentenone ring plus the 5-carbon side chain, but requiring migration of two hydrogens from the remaining portion of OPDA.

The lack of double bonds between the cyclopentenone ring and the carboxylate in OPDA makes it less attractive to invoke sigmatropic hydrogen shifts, proposed as important mechanistic steps in fragmentation of eicosanoid epoxides, (MacMillan and Murphy, 1995) to explain migrations of hydrogens toward the cyclopentenone. The selectivity in cleaving the C7—C8 bond also drove our focus toward mechanistic steps that would localize the negative charge on the adjacent carbon (C9), as this would facilitate elimination by cleaving C7—C8. Given the absence of this cleavage in the cyclopentanone analog OPC:8, we considered the possibility of an intramolecular Michael addition of the carboxylate anion to the electrophilic enone moiety as a prelude to subsequent rearrangements.

4.C.2. CID mass spectra of ^{18}O-labeled OPDA

To aid further exploration of these reactions and with fragment ion annotations, labeling of the OPDA carboxylate oxygens with ^{18}O was performed in solution,(Mueller, *et al.*, 2006) and

product ion MS/MS spectra of deprotonated dnOPDA and OPDA isotopologs were generated. Spectra of unlabeled and singly- and doubly- ^{18}O-labeled isotopologs of the latter are presented in Figure 2. In all cases, *m/z* 165 was observed the major fragment apart from fragments resulting from losses of H_2O or CO_2, which are common in the CID spectra of carboxylic acids in ESI negative mode. In Figure 4.2d, the product ion spectrum for singly ^{18}O-exchanged OPDA isotopolog (products of *m/z* 293), documents that products form as a mixture of $[M\text{-}H\text{-}H_2{}^{18}O]^-$ (*m/z* 273) and $[M\text{-}H\text{-}H_2O]^-$ (*m/z* 275) at nearly the same abundances, and $[M\text{-}H\text{-}C^{16}O^{18}O]^-$ verifies labeling of the carboxylate. Corresponding product ions of the doubly-labeled isotopolog (Figure 2e) are assigned as neutral losses of $H_2{}^{18}O$ and $C^{18}O_2$, showing that both oxygen atoms at the carboxylate group are exchanged to ^{18}O. However, these CID spectra yielded no evidence of heavy isotopologs of the *m/z* 165 fragment ion, which proved that carboxylate oxygens are not part of the fragment.

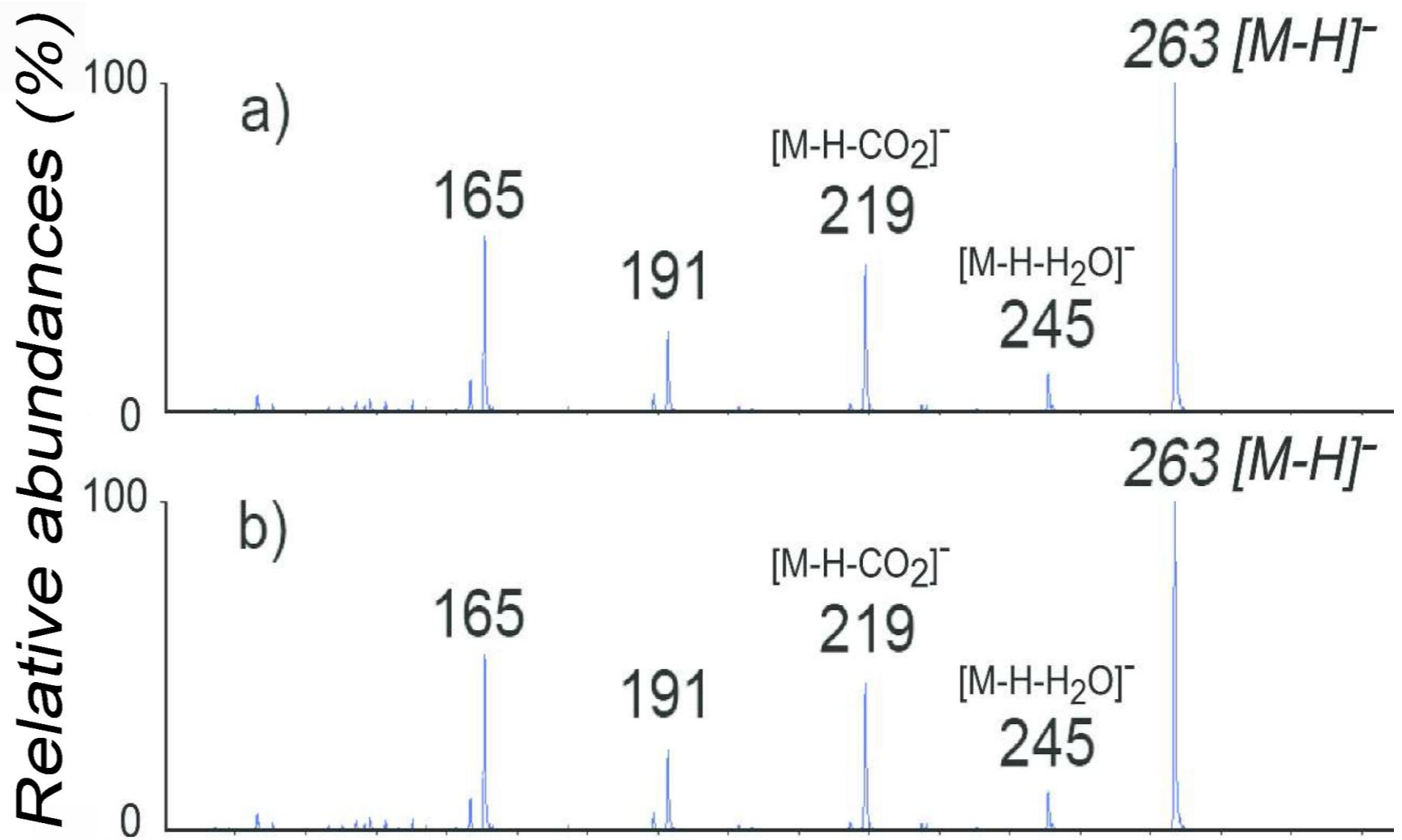

Figure 4.2. Negative ion mode enhanced product ion mass spectra for $[M-H]^-$ of a) OPC:8, b) dnOPDA, c) unlabeled OPDA, d) singly ^{18}O-labeled OPDA and e) doubly ^{18}O-labeled OPDA using a collision cell potential of -25 V.

Figure 4.2 (cont'd)

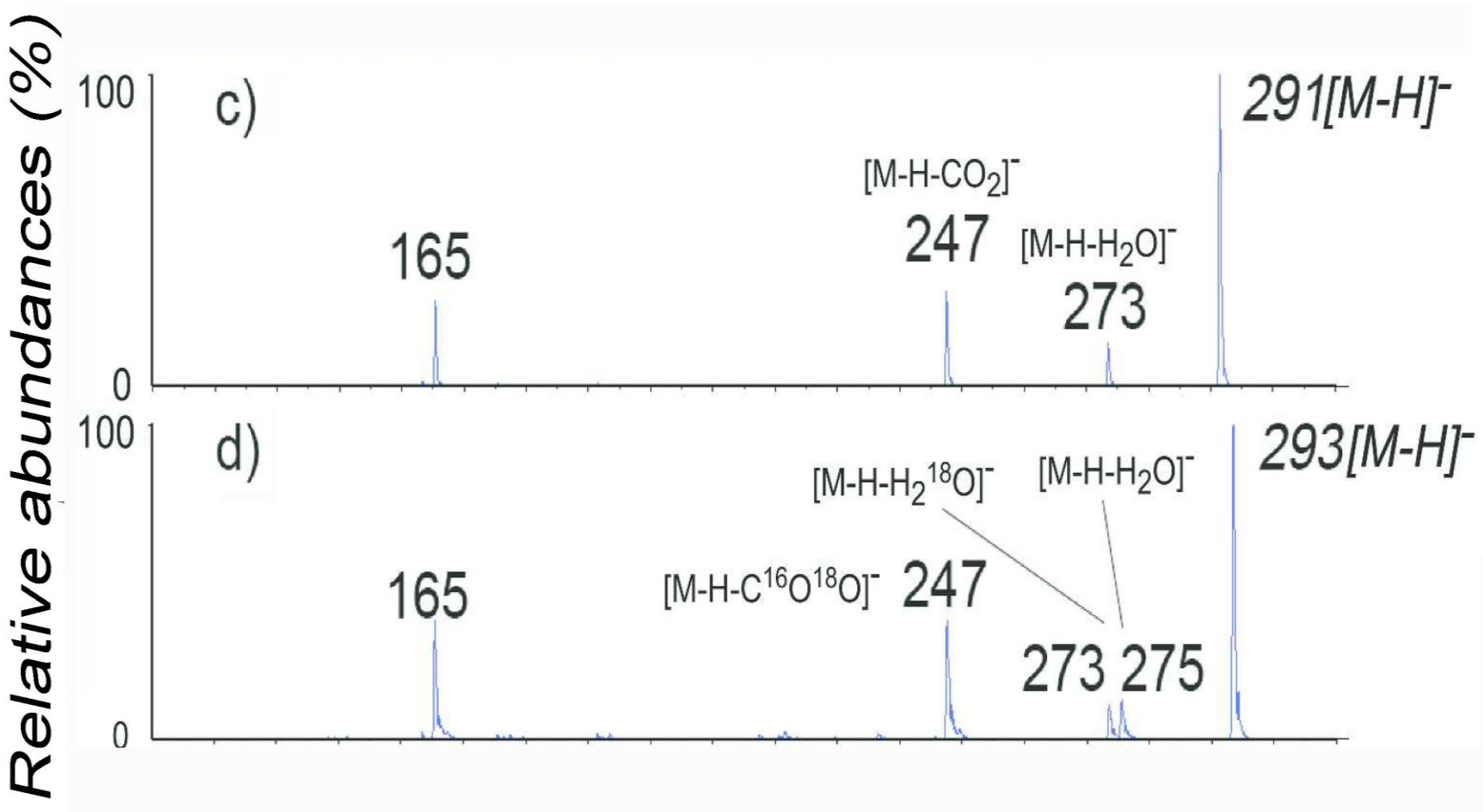

Figure 4.2 (cont'd)

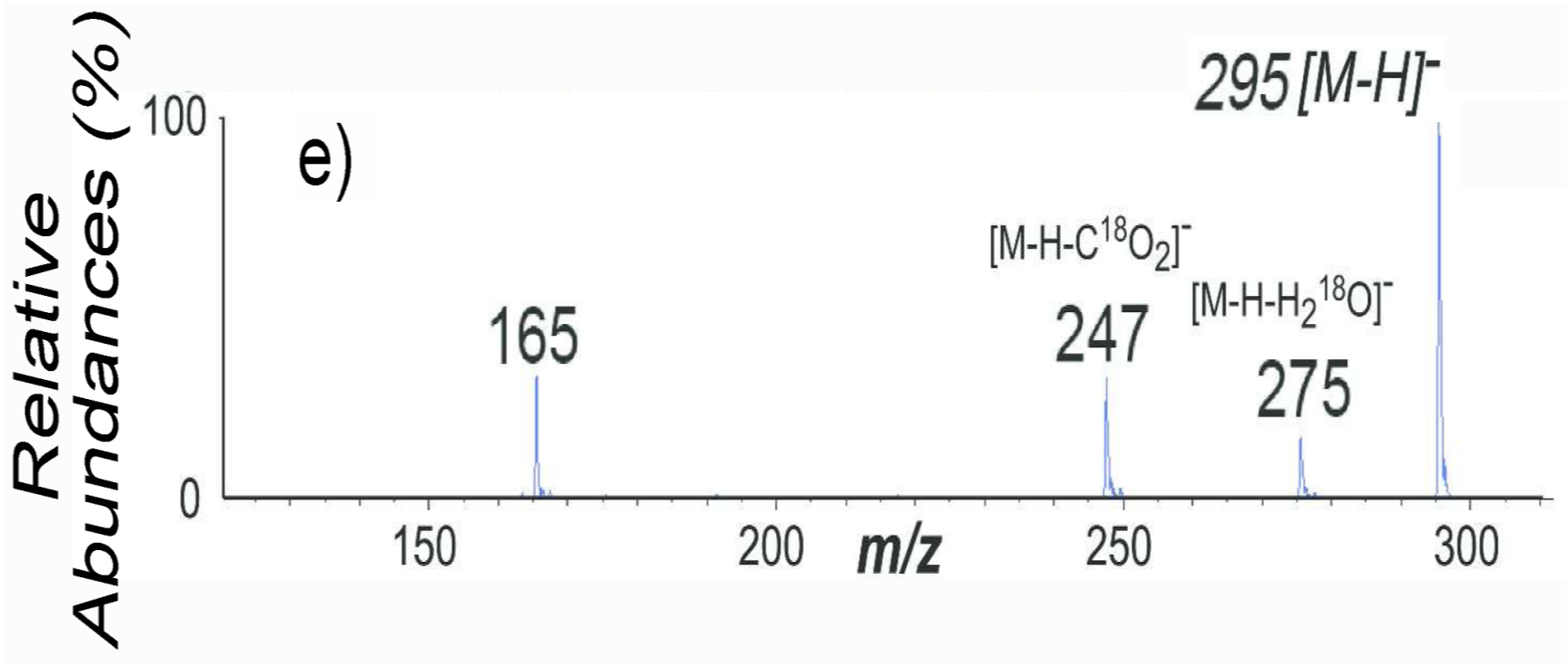

To learn more about the *m/z* 165 fragment including alternative routes for its generation, pseudo-MS^3 analyses were performed by generating enhanced product ion spectra for $[M\text{-}H\text{-}H_2O]^-$ and $[M\text{-}H\text{-}CO_2]^-$ of both OPDA and dnOPDA that were generated in the ion source by application of a high source declustering potential (80 V). Fragments of *m/z* 165 were also generated from these precursors, albeit at higher collision energies and at lower yields relative to other fragments (Figure A2).

4.C.3. Pseudo MS^3 analyses

Pseudo MS^3 analyses were performed by generating product ion MS/MS spectra for the *m/z* 165 product ions generated in-source from OPDA to generate information about this ion. Collision cell potential of >40 V was necessary to produce sufficient fragment ion yields, and the products were predominantly *m/z* 134 ($C_{10}H_{14}^{-\bullet}$), which is 31 *m/z* units ($CH_3O^{\bullet}$) lighter than the precursor, as shown in Figure A3. The chemistry responsible for this unusual formation of an odd-electron second generation product ion from even-electron precursors is not yet understood, but this product may offer potential for distinguishing isomeric oxylipins through isomer-selective product ions.

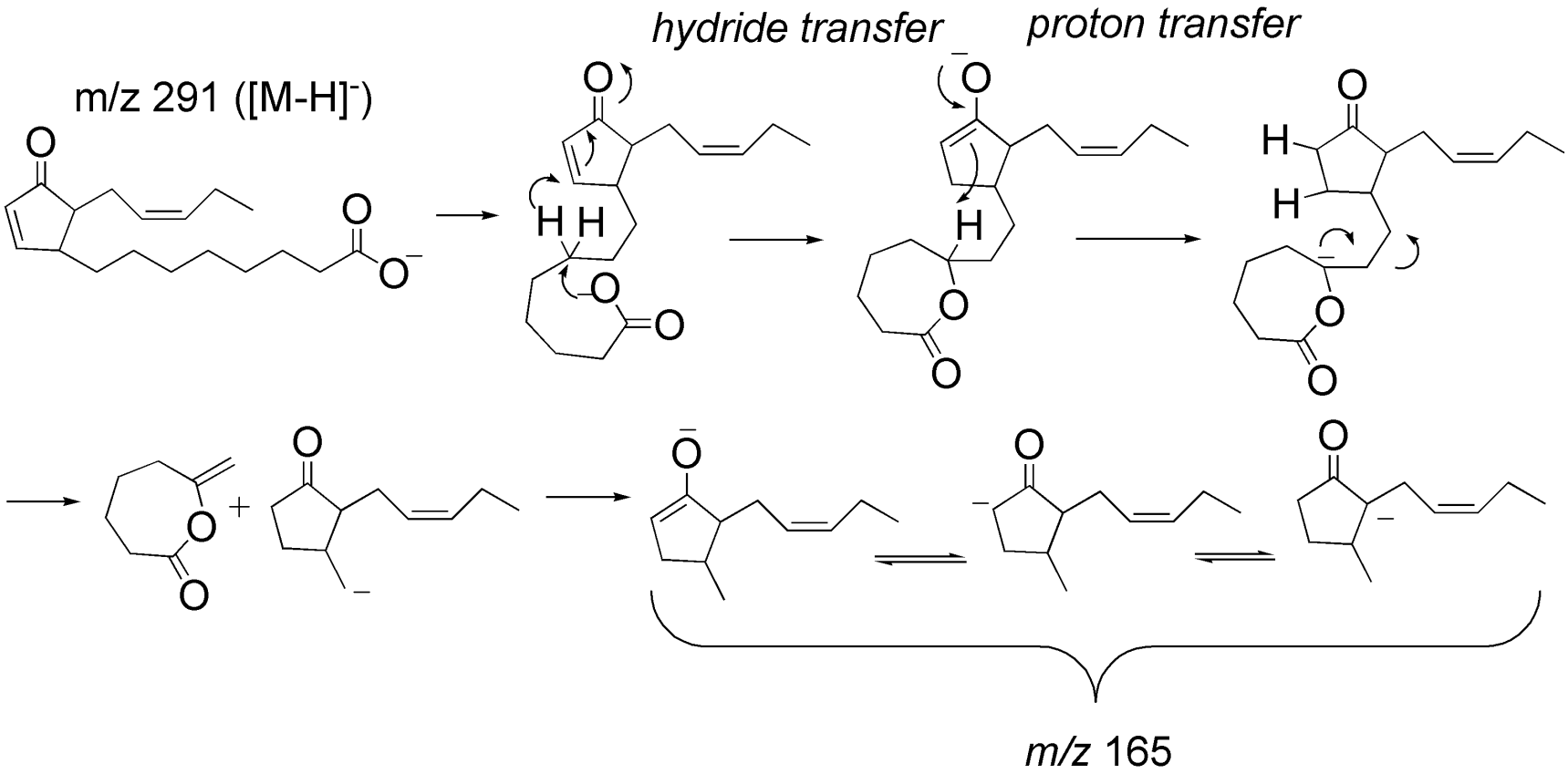

Figure 4.3. Proposed intramolecular hydride and proton transfer reactions of $[M-H]^-$ of OPDA consistent with observation of a dominant fragment ion at *m/z* 165 formed upon collision-induced dissociation.

The cyclopentanone analog OPC:8 yields a fragment corresponding to neutral loss of CO_2, but did not yield fragments analogous to the *m/z* 165 fragment of OPDA. The striking differences in fragmentation behavior of OPDA and OPC:8 suggest that the cyclopentenone ring, an electrophilic α,β-unsaturated ketone, plays an essential role in formation of the *m/z* 165 fragment, and we propose that the electrophilic enone ring is capable of serving as a hydride acceptor. Documentation of hydride migrations following collisional activation of negative ions has been rare, but examples include CID spectra of PUFAs including arachidonic acid,(Kerwin, *et al.*, 1996) fatty acid peroxides and conjugated keto fatty acids,(MacMillan and Murphy, 1995) both generating fragments 2 *m/z* units heavier than expected, and a hydride transfer from CH_3S^- to the electron deficient neutral molecule CF_3COCF_3.(Staneke *et al.*, 1996) The unusual fragmentation behavior of deprotonated OPDA and dnOPDA at relatively low collision energy is consistent with sequential intramolecular hydride transfer to the electrophilic enone followed by proton transfer and subsequent displacement of the C7—C8 bond by the negative charge site (Figure 4.3). Subsequent proton transfers may result in multiple tautomeric forms of this fragment. This proposed mechanism matches with the observation of fragment *m/z* 170 from previous MS/MS result of $^2H_5$-OPDA in our laboratory, because the deuterium atoms, remote from the carboxylate chain, are retained in the fragment.

4.C.4. Comparisons of cyclopentenone prostaglandin MS/MS spectra

Prostaglandins present examples to explore whether similar hydride transfer/proton transfer mechanisms are at play in other cyclopentenone oxylipins. PGA_2, PGJ_2, and $15dPGJ_2$ have cyclopentenone groups in common, but differ in having double bonds between the

cyclopentenone ring and the carboxylate group. In addition, PGD_2 and E_2 may undergo two steps of dehydration upon collisional activation to yield cyclopentenone ion intermediates. Pseudo-MS^3 experiments were performed using in-source collisional activation to produce the dehydrated ions $[M\text{-}H\text{-}2H_2O]^-$ for PGD_2 and PGE_2, and $[M\text{-}H_2O]^-$ for PGA_2 and PGJ_2. Enhanced product ion spectra were generated for these and $[M\text{-}H]^-$ of $15dPGJ_2$ and are shown in Figure 4.4. In the CID MS/MS spectra of the prostaglandins, aside from common fragments that come from neutral losses of H_2O and CO_2, *m/z* 203 and 217 are the only major product ions, and can be explained by cleavages between C6—C7 and C5—C6 respectively (Figure 5). Such fragmentation chemistry would be facilitated by double bond migration away from carbons 5-7 to avoid the need to cleave at a sp^2 carbon, followed by charge migration toward the carbon next to the cleavage site. In view of this, we propose, as shown in Figure 5, a scheme involving intramolecular proton transfer and tautomerization before elimination to yield product ions of *m/z* 203, and a similar route involving intramolecular proton transfer and tautomerization for the formation of *m/z* 217 product ions.

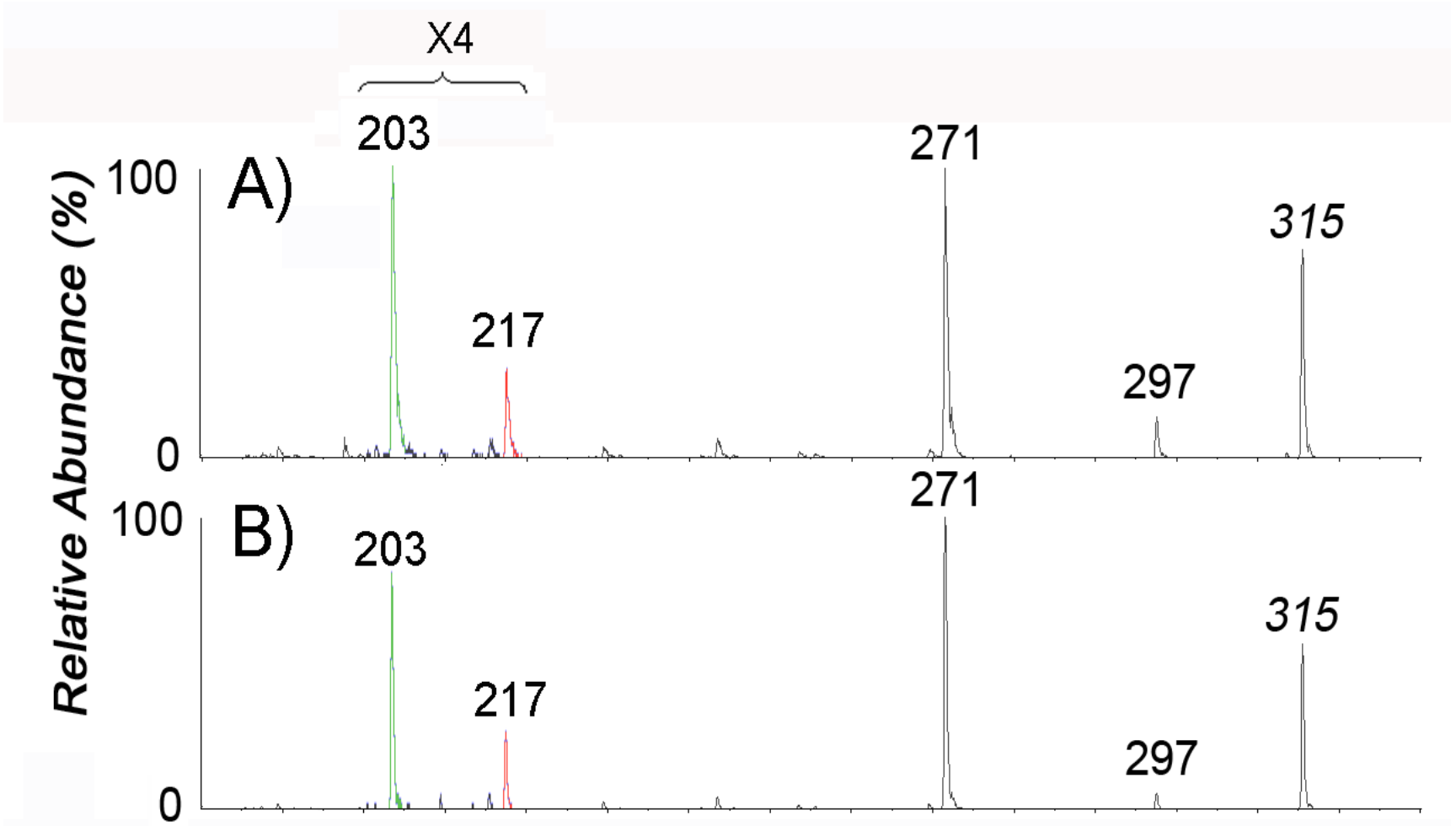

Figure 4.4. Enhanced product ion mass spectra derived from of $[M-H]^-$ of (A) 15-deoxy-$\Delta^{12,14}$-PGJ_2 and in-source fragments at *m/z* 315 (pseudo-MS^3) of (B) $[PGD_2\text{-}H\text{-}2H_2O]^-$, (C) $[PGJ_2\text{-}H\text{-}H_2O]^-$, (D) $[PGE_2\text{-}H\text{-}2H_2O]^-$, and (E) $[PGA_2\text{-}H\text{-}H_2O]^-$ at collision cell potential of -25 V.

Figure 4.4 (cont'd)

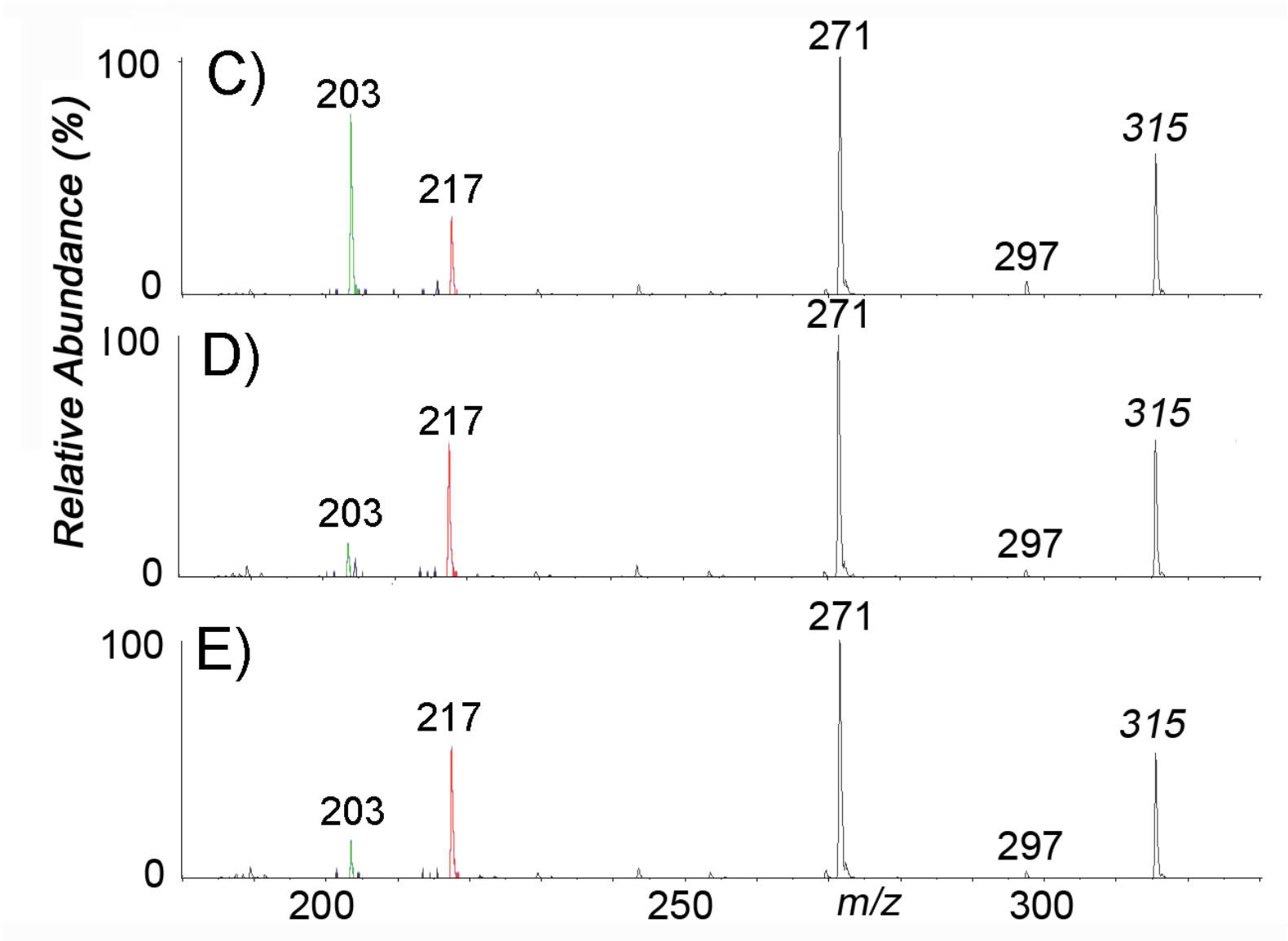

The *m/z* values of these prostaglandin fragments suggest that no hydride transfers are necessary to explain the observed product ions in the prostaglandins investigated here. In addition, no analog of the *m/z* 165 fragment observed in OPDA CID spectra was observed. We anticipated that hydride transfer will be facilitated in oxylipins such as OPDA that lack double bonds between the cyclopentenone and the carboxylate, as this facilitates sequential hydride and proton transfer from a single carbon as depicted in Figure 3. Such chemistry would be assisted by formation of another bond at this carbon such as the covalent displacement of hydride by a negatively-charged group (*e.g.* carboxylate anion).

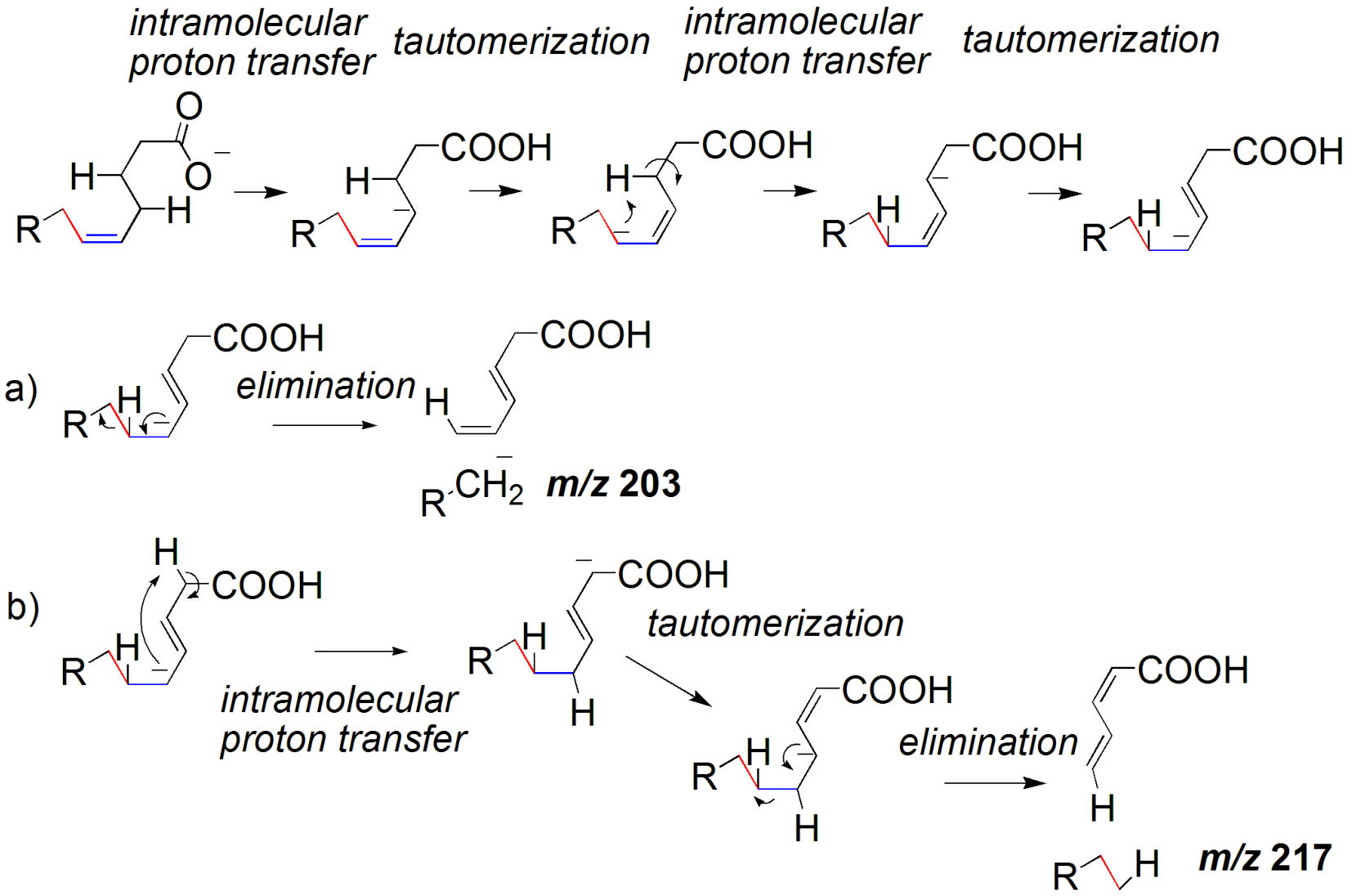

Figure 4.5. Proposed scheme for generating product ions of *m/z* 203 via cleavage of C6-C7 carbon-carbon bond and *m/z* 217 via cleavage of C5-C6 carbon-carbon bond from collision-induced dissociation of negative ions generated from selected prostaglandins

Figure 4.5. (cont'd)

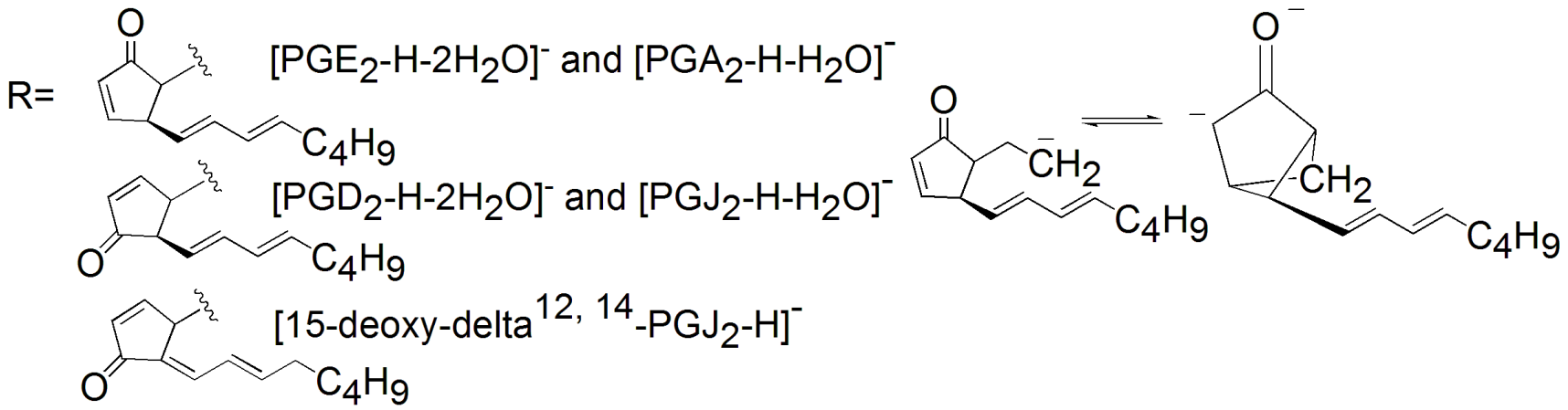

It is notable that the CID behavior of the five prostaglandins can be classified into two groups based on their MS/MS spectra, one group including 15-deoxy-$\Delta^{12,14}$-PGJ_2, $[PGD_2\text{-H-}2H_2O]^-$ and $[PGJ_2\text{-H-}H_2O]^-$ (Figure 4.4A, 4.4B, and 4.4C) which yield more *m/z* 203 than 217, and the other group of $[PGE_2\text{-H-}2H_2O]^-$ and $[PGA_2\text{-H-}H_2O]^-$, (Figure 4.4D and 4.4E), which just do the opposite. These two groups of prostaglandins differ in the orientation of the cyclopentenone ring relative to the chain bearing the carboxylate.

4.D. Conclusion

Fragmentation of deprotonated cyclopentenone anions is distinct from many oxylipin anions, and appears to be driven by the reactivity of the electrophilic α, β-unsaturated carbonyl core. For cyclopentenone carboxylic acids with saturated side chains, the formation of fragments from carbon-carbon bond cleavage remote from the initial negative charge site is consistent with hydride migrations from saturated groups to the electrophilic cyclopentenone moiety followed by proton transfer and carbon-carbon bond cleavage. For unsaturated oxylipin chains, the direction of charge directed intra-molecular nucleophilic addition, as the first and determining step of fragmentation, is affected by the orientation of the cyclopentenone group relative to the carboxylate.

New discoveries of bioactive oxylipins continue, but structures are often not evident from MS or MS/MS data alone. Better understanding of formation of product ions in ESI negative mode can help guide isolation of targeted metabolites. Recognition of the importance of electrophilic groups, perhaps including epoxides and nitro groups, in guiding formation of product ions should

accelerate discoveries of oxylipins signaling molecules in animals, plants and other organisms, and help distinguish them from isomeric substances.

Chapter 5 Perspectives regarding plant oxylipin metabolism

5.A Current challenges and unanswered questions

In the last decade, databases of complete genomic sequences have begun facilitating global "omics" research, revealing new gene functions and regulatory pathways. The accelerated pace and reduced costs of genome sequencing shift experimental bottlenecks away from genetic information and toward limitations in defining phenotypes. Metabolite identification and profiling, and associated needs to perform biochemical assays, now present greater limitations on such functional genomic investigations. However, the past decade has also witnessed advances in mass spectrometry limits of detection, mass resolution, mass accuracy, and analytical throughput that have made it more feasible to obtain extensive phenotypic information. These advances have enabled analysis of both low abundance metabolites and proteins. Many gene functions and regulation pathways are described in detail by global research groups. JA signaling is one good example of this.

However, we are still far from overcoming all of the technical barriers in functional genomics, but large-scale investigations using heterologous expression are planned that will pursue the most pressing questions about metabolic gene functions. Such investigations will require improved throughput and automated data analysis to define gene functions both in both *in vivo* and *in vitro* expression systems. One may well expect that overexpression or silencing of candidate genes will lead to formation of metabolites never observed before, and these research efforts will need rapid analytical methods capable of revealing their presence and supporting their annotation.

Mass spectrometry only measures mass-to-charge ratios of ions, and is often not enough for unambiguous structural elucidation. While nuclear magnetic resonance (NMR) requires amounts

of pure metabolites in thousand-fold greater quantities than mass spectrometry, it is superior in distinguishing isomers? Many natural products, including oxylipins, exist in multiple isomeric forms that yield identical MS/MS spectra. The research community can be expected to demand further improvements in analytical technologies and in mass spectrum databases to support growing research needs.

5.B Future work in this area

The research described in this dissertation demonstrated the discovery of a new family of glutathione conjugates of OPDA-containing galactolipids. Their detailed structures have still yet to be determined by NMR and techniques that would assign absolute stereochemical configurations. Their accumulation after wounding suggests they may play important roles in plant responses to wounding and stress. More detailed quantification of these compounds in the context of genotype/phenotype matching will help reveal the roles of glutathione conjugation in regulation of OPDA release after wounding, and may raise awareness of the roles of GSTs in plant signaling.

The knockout mutant *atgstu5* has been shown to be slow in accumulating GS-OPDA in response to stress. Further complementation of the mutant with this will help test the hypothesis that *At*GSTU5 catalyzes *in vivo* glutathione conjugation of OPDA. Testing this mutant against various pathogen/stresses will help determine whether plant responses to stress can be modulated through control of GST expression.

APPENDIX

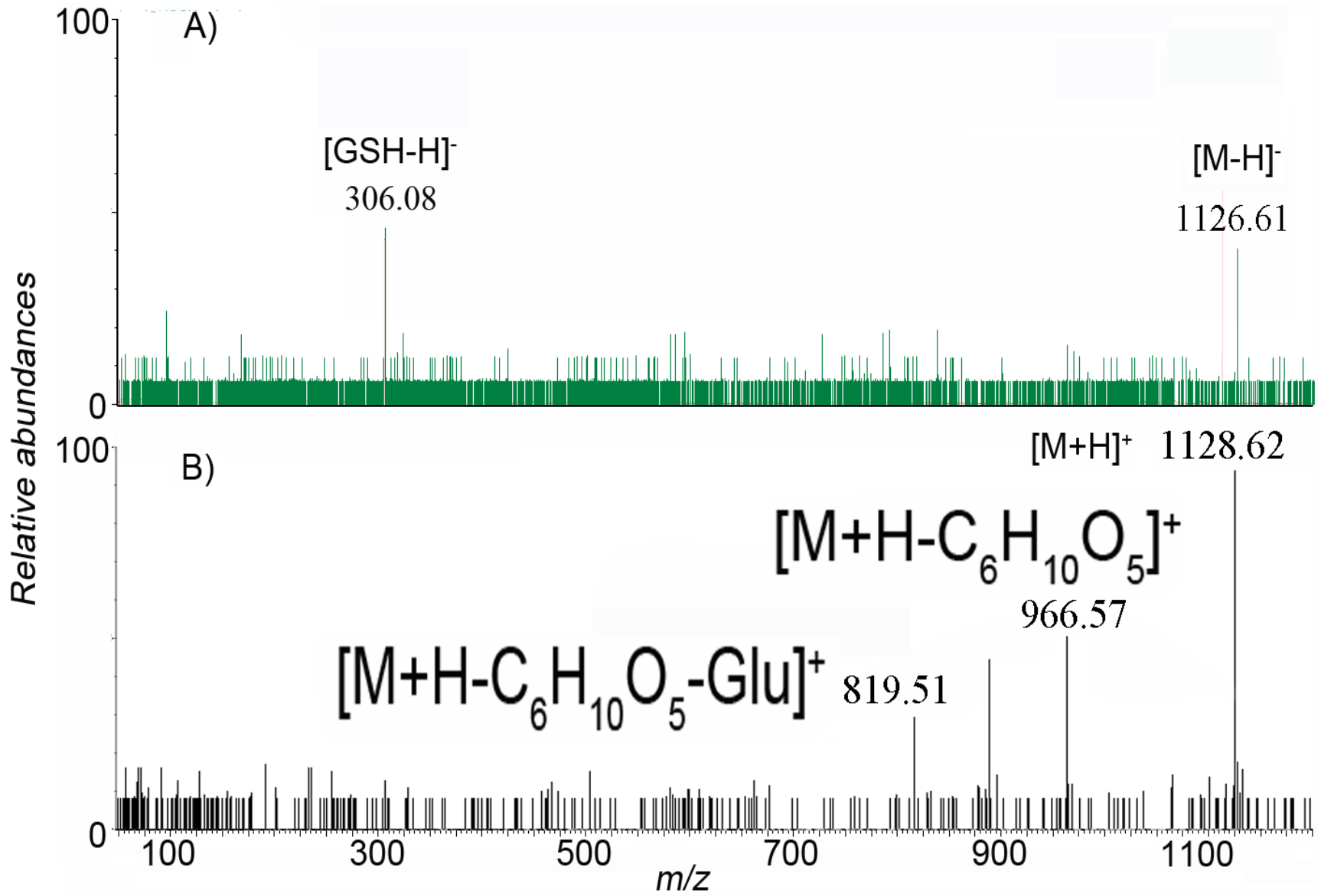

Figure A1. Evidence for GS-MGDG structure features. A) and B): MS/MS spectra from Q-TOF instrument of GS-MGDGb1 in negative positive and positive mode, respectively.

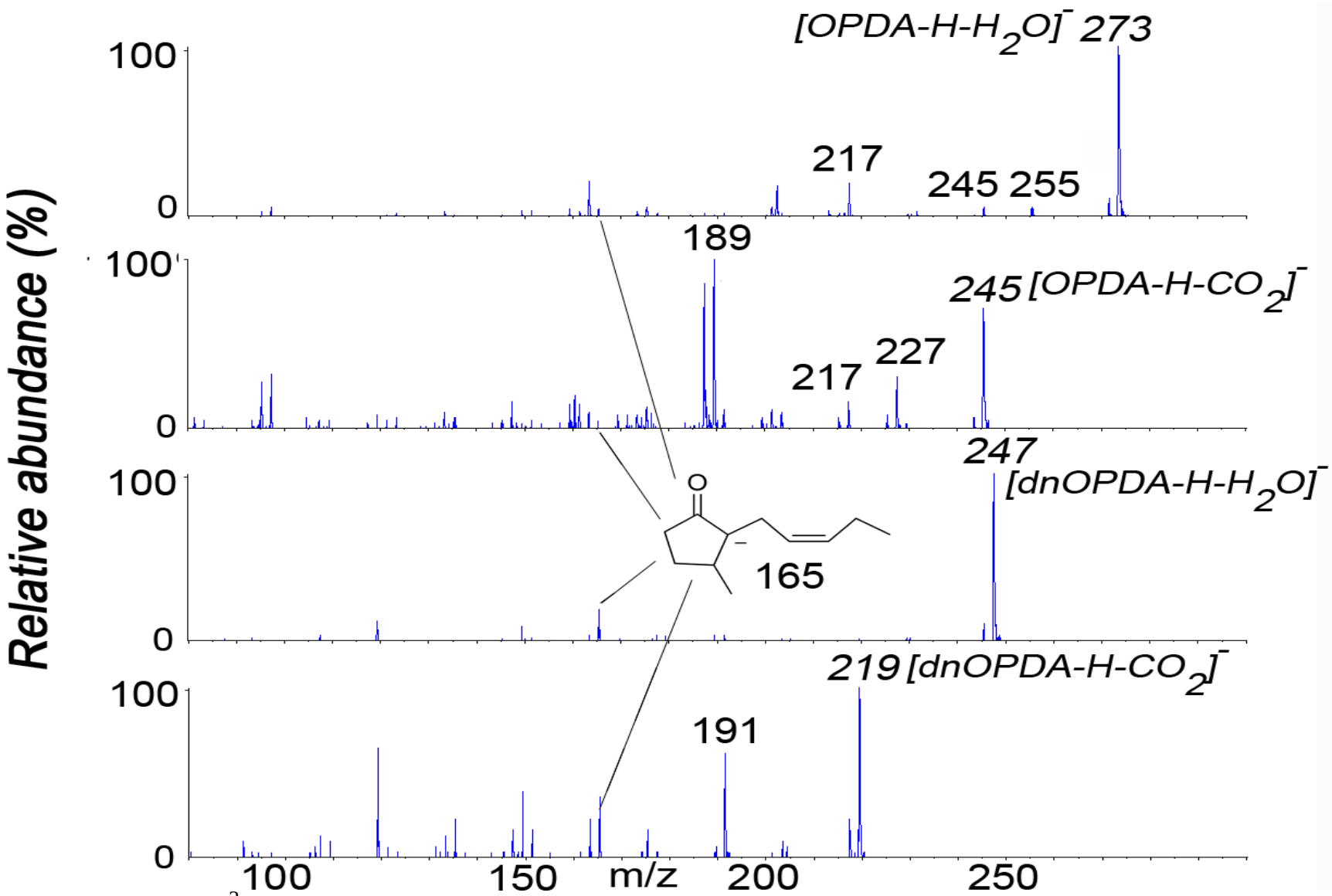

Figure A2. Pseudo-MS^3 of the fragments of OPDA and dnOPDA resulted from loss of water and carbon dioxide.

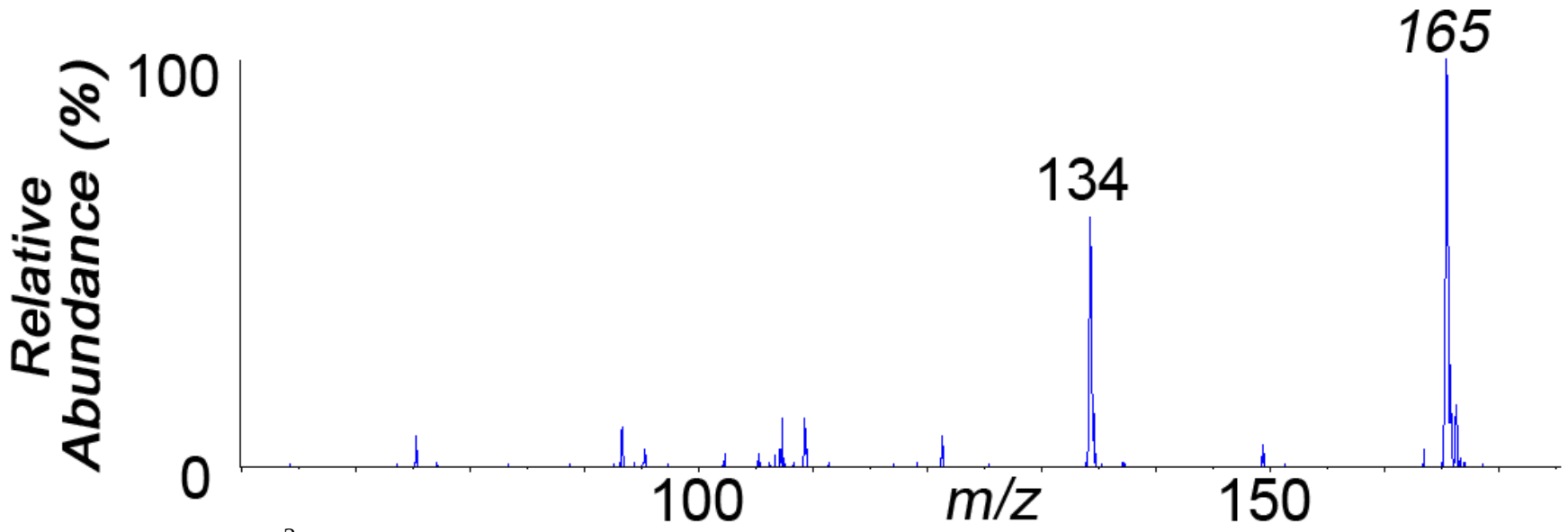

Figure A3. Pseudo-MS^3 spectrum of the fragment at *m/z* 165.09 from OPDA.

REFERENCES

REFERENCES

Alonso, J.M. and Ecker, J.R. (2006) Moving forward in reverse: genetic technologies to enable genome-wide phenomic screens in Arabidopsis. *Nat Rev Genet*, **7**, 524-536.

Andersson, M.X., et al. (2006) Oxylipin Profiling of the Hypersensitive Response in Arabidopsis thaliana: Formation of a Novel Oxo-Phytodienoic Acid-Containing Galactolipid, Arabidopside E. *J Biol Chem*, **281**, 31528-31537.

Andreou, A., et al. (2009) Biosynthesis of oxylipins in non-mammals. *Prog Lipid Res*, **48**, 148-170.

Balbi, V. and Devoto, A. (2008) Jasmonate signalling network in Arabidopsis thaliana: crucial regulatory nodes and new physiological scenarios. *New Phytologist*, **177**, 301-318.

Bantscheff, M., et al. (2007) Quantitative mass spectrometry in proteomics: a critical review. *Anal Bioanal Chem*, **389**, 1017-1031.

Bargmann, B.O. and Munnik, T. (2006) The role of phospholipase D in plant stress responses. *Curr Opin Plant Biol*, **9**, 515-522.

Bartling, D., et al. (1993) A Glutathione-S-Transferase with Glutathione-Peroxidase Activity from Arabidopsis-Thaliana - Molecular-Cloning and Functional-Characterization. *Eur J Biochem*, **216**, 579-586.

Bechtold, N., et al. (1993) In-Planta Agrobacterium-Mediated Gene-Transfer by Infiltration of Adult Arabidopsis-Thaliana Plants. *Comptes Rendus Acad. Sci. Ser. III-Sci. Vie-Life Sci.*, **316**, 1194-1199.

Bell, E., et al. (1995) A Chloroplast Lipoxygenase Is Required for Wound-Induced Jasmonic Acid Accumulation in Arabidopsis. *Proc Natl Acad Sci USA*, **92**, 8675-8679.

Biemann, K. (1992) Mass-Spectrometry of Peptides and Proteins. *Annu Rev Biochem*, **61**, 977-1010.

Blechert, S., et al. (1999) Structure-activity analyses reveal the existence of two separate groups of active octadecanoids in elicitation of the tendril-coiling response of Bryonia dioica Jacq. *Planta*, **207**, 470-479.

Blee, E. (1998) Phytooxylipins and plant defense reactions. *Prog Lipid Res*, **37**, 33-72.

Bleuel, C., et al. (2011) Degradation of Glutathione S-Conjugates in Physcomitrella patens is Initiated by Cleavage of Glycine. *Plant Cell Physiol*, **52**, 1153-1161.

Bonaventure, G., et al. (2007) A gain-of-function allele of TPC1 activates oxylipin biogenesis after leaf wounding in Arabidopsis. *Plant J*, **49**, 889-898.

Bonaventure, G., et al. (2011) Revealing complexity and specificity in the activation of lipase-mediated oxylipin biosynthesis: a specific role of the Nicotiana attenuata GLA1 lipase in the activation of jasmonic acid biosynthesis in leaves and roots. *Plant Cell Environ.*, **34**, 1507-1520.

Bottcher, C. and Weiler, E.W. (2007) cyclo-Oxylipin-galactolipids in plants: occurrence and dynamics. *Planta*, **226**, 629-637.

Böttcher, C. and Weiler, E.W. (2007) cyclo-Oxylipin-galactolipids in plants: occurrence and dynamics. *Planta*, **226**, 629-637.

Browse, J. and Howe, G.A. (2008) New weapons and a rapid response against insect attack. *Plant Physiol.*, **146**, 832-838.

Buseman, C.M. (2006) Wounding Stimulates the Accumulation of Glycerolipids Containing Oxophytodienoic Acid and Dinor-Oxophytodienoic Acid in Arabidopsis Leaves. *Plant Physiol*, **142**, 28-39.

Caccuri, A.M., et al. (1997) Catalytic mechanism and role of hydroxyl residues in the active site of theta class glutathione S-transferases - Investigation of Ser-9 and Tyr-113 in a glutathione S-transferase from the Australian sheep blowfly, Lucilia cuprina. *J Biol Chem*, **272**, 29681-29686.

Caldelari, D., et al. (2011) Arabidopsis lox3 lox4 double mutants are male sterile and defective in global proliferative arrest. *Plant Mol Biol*, **75**, 25-33.

Castro-Perez, J., et al. (2005) A high-throughput liquid chromatography/tandem mass spectrometry method for screening glutathione conjugates using exact mass neutral loss acquisition. *Rapid Commun Mass Spectrom*, **19**, 798-804.

Chehab, E.W., et al. (2011) Intronic T-DNA Insertion Renders Arabidopsis opr3 a Conditional Jasmonic Acid-Producing Mutant. *Plant Physiol*, **156**, 770-778.

Chen, H., et al. (2007) Stability of plant defense proteins in the gut of insect herbivores. *Plant Physiol*, **143**, 1954-1967.

Chen, M.S. (2008) Inducible direct plant defense against insect herbivores: A review. *Insect Sci.*, **15**, 101-114.

Chini, A., et al. (2009) The ZIM domain mediates homo- and heteromeric interactions between Arabidopsis JAZ proteins. *Plant J*, **59**, 77-87.

Chini, A., et al. (2007) The JAZ family of repressors is the missing link in jasmonate signalling. *Nature*, **448**, 666-U664.

Chiwocha, S.D.S., et al. (2003) A method for profiling classes of plant hormones and their metabolites using liquid chromatography-electrospray ionization tandem mass spectrometry: an analysis of hormone regulation of thermodormancy of lettuce (Lactuca sativa L.) seeds. *Plant J*, **35**, 405-417.

Chung, H.S., et al. (2010) Alternative splicing expands the repertoire of dominant JAZ repressors of jasmonate signaling. *Plant J*, **63**, 613-622.

Chung, H.S. and Howe, G.A. (2009) A Critical Role for the TIFY Motif in Repression of Jasmonate Signaling by a Stabilized Splice Variant of the JASMONATE ZIM-Domain Protein JAZ10 in Arabidopsis. *Plant Cell*, **21**, 131-145.

Chung, H.S., et al. (2008) Regulation and Function of Arabidopsis JASMONATE ZIM-Domain Genes in Response to Wounding and Herbivory. *Plant Physiol.*, **146**, 952-964.

Cordero, M.M. and Wesdemiotis, C. (1994) Characterization of the Neutral Products Formed Upon the Charge-Remote Fragmentation of Fatty-Acid Ions. *Anal Chem*, **66**, 861-866.

Cummins, I., et al. (1999) A role for glutathione transferases functioning as glutathione peroxidases in resistance to multiple herbicides in black-grass. *Plant J*, **18**, 285-292.

Cummins, I., et al. (2011) Multiple roles for plant glutathione transferases in xenobiotic detoxification. *Drug Metab Rev*, **43**, 266-280.

Davoine, C. (2006) Adducts of Oxylipin Electrophiles to Glutathione Reflect a 13 Specificity of the Downstream Lipoxygenase Pathway in the Tobacco Hypersensitive Response. *Plant Physiol*, **140**, 1484-1493.

Davoine, C., et al. (2005) Conjugation of keto fatty acids to glutathione in plant tissues. Characterization and quantification by HPLC-tandem mass spectrometry. *Anal Chem*, **77**, 7366-7372.

Devoto, A., et al. (2005) Expression profiling reveals COI1 to be a key regulator of genes involved in wound- and methyl jasmonate-induced secondary metabolism, defence, and hormone interactions. *Plant Mol. Biol.*, **58**, 497-513.

Dickinson, J.S. and Murphy, R.C. (2002) Mass spectrometric analysis of leukotriene A(4) and other chemically reactive metabolites of arachidonic acid. *J Am Soc Mass Spectrom*, **13**, 1227-1234.

Dieckhaus, C.M., et al. (2005) Negative ion tandem mass spectrometry for the detection of glutathione conjugates. *Chem Res Toxicol*, **18**, 630-638.

Dirr, H., et al. (1994) Refined Crystal-Structure of Porcine Class-Pi Glutathione-S-Transferase (Pgst P1-1) at 2-Center-Dot-1 a-Angstrom Resolution. *J. Mol. Biol.*, **243**, 72-92.

Divol, F., et al. (2007) Involvement of the xyloglucan endotransglycosylase/hydrolases encoded by celery XTH1 and Arabidopsis XTH33 in the phloem response to aphids. *Plant Cell Environ.*, **30**, 187-201.

Dixon, D. (2000) Characterisation of a Zeta Class Glutathione Transferase from Arabidopsis thaliana with a Putative Role in Tyrosine Catabolism. *Arch Biochem Biophys*, **384**, 407-412.

Dixon, D.P., et al. (1998a) Purification, regulation and cloning of a glutathione transferase (GST) from maize resembling the auxin-inducible type-III GSTs. *Plant Mol Biol*, **36**, 75-87.

Dixon, D.P., et al. (1998b) Glutathione-mediated detoxification systems in plants. *Curr Opin Plant Biol*, **1**, 258-266.

Dixon, D.P., et al. (2002) Functional divergence in the glutathione transferase superfamily in plants - Identification of two classes with putative functions in redox homeostasis in Arabidopsis thaliana. *J Biol Chem*, **277**, 30859-30869.

Dixon, D.P. and Edwards, R. (2006) Enzymes of tyrosine catabolism in Arabidopsis thaliana. *Plant Science*, **171**, 360-366.

Dixon, D.P. and Edwards, R. (2009) Selective Binding of Glutathione Conjugates of Fatty Acid Derivatives by Plant Glutathione Transferases. *J Biol Chem*, **284**, 21249-21256.

Dixon, D.P., et al. (2009) Enzyme activities and subcellular localization of members of the Arabidopsis glutathione transferase superfamily. *J Exp Bot*, **60**, 1207-1218.

Dixon, D.P., et al. (2010) Roles for glutathione transferases in plant secondary metabolism. *Phytochemistry*, **71**, 338-350.

Du, L.Q., et al. (2009) Ca2+/calmodulin regulates salicylic-acid-mediated plant immunity. *Nature*, **457**, 1154-U1116.

Edwards, R., et al. (2005) Differential induction of glutathione transferases and glucosyltransferases in wheat, maize and Arabidopsis thaliana by herbicide safeners. *Z Naturforsch C*, **60**, 307-316.

Edwards, R. and Dixon, D.P. (2005) Plant glutathione transferases. In *Glutathione Transferases and Gamma-Glutamyl Transpeptidases*. San Diego: Elsevier Academic Press Inc, pp. 169-186.

Edwards, R., et al. (2000) Plant glutathione S-transferases: enzymes with multiple functions in sickness and in health. *Trends Plant Sci*, **5**, 193-198.

Evans, D.C., et al. (2004) Drug-protein adducts: An industry perspective on minimizing the potential for drug bioactivation in drug discovery and development. *Chem Res Toxicol*, **17**, 3-16.

Farmaki, T., et al. (2007) Differential distribution of the lipoxygenase pathway enzymes within potato chloroplasts. *J Exp Bot*, **58**, 555-568.

Farmer, E.E. and Davoine, C. (2007) Reactive electrophile species. *Curr Opin Plant Biol*, **10**, 380-386.

Farmer, E.E. and Ryan, C.A. (1990) Interplant Communication - Airborne Methyl Jasmonate Induces Synthesis of Proteinase-Inhibitors in Plant-Leaves. *Proc Natl Acad Sci USA*, **87**, 7713-7716.

Feldmann, K.A. and Marks, M.D. (1987) Agrobacterium-Mediated Transformation of Germinating-Seeds of Arabidopsis-Thaliana - a Non-Tissue Culture Approach. *Mol. Gen. Genet.*, **208**, 1-9.

Fernandez-Canon, J.M. and Penalva, M.A. (1998) Characterization of a fungal maleylacetoacetate isomerase gene and identification of its human homologue. *J Biol Chem*, **273**, 329-337.

Feussner, I. and Wasternack, C. (2002) The lipoxygenase pathway. *Ann Rev Plant Biol*, **53**, 275-297.

Fonseca, S., et al. (2009) (+)-7-iso-Jasmonoyl-L-isoleucine is the endogenous bioactive jasmonate. *Nat. Chem. Biol.*, **5**, 344-350.

Fridman, E. and Pichersky, E. (2005) Metabolomics, genomics, proteomics, and the identification of enzymes and their substrates and products. *Curr Opin Plant Biol*, **8**, 242-248.

Frova, C. (2003) The plant glutathione transferase gene family: genomic structure, functions, expression and evolution. *Physiol. Plant.*, **119**, 469-479.

Frova, C. (2006) Glutathione transferases in the genomics era: New insights and perspectives. *Biomolecular Engineering*, **23**, 149-169.

Funk, C.D. (2001) Prostaglandins and leukotrienes: Advances in eicosanoid biology. *Science*, **294**, 1871-1875.

Gao, X. (2009) Liquid chromatography/mass spectrometry basedmetabolite profiling in reverse genetic investigations ofwounding and pathogen stress responses in *Arabidopsis thaliana*. *A dissertation. Michigna State University. ISBN: 9781109415247*.

Gilchrist, A., et al. (2006) Quantitative proteomics analysis of the secretory pathway. *Cell*, **127**, 1265-1281.

Glauser, G., et al. (2010) Mass spectrometry-based metabolomics oriented by correlation analysis for wound-induced molecule discovery: identification of a novel jasmonate glucoside. *Phytochem Anal*, **21**, 95-101.

Glauser, G., et al. (2009) Velocity Estimates for Signal Propagation Leading to Systemic Jasmonic Acid Accumulation in Wounded Arabidopsis. *J Biol Chem*, **284**, 34506-34513.

Glauser, G., et al. (2008) High-resolution profiling of oxylipin-containing galactolipids in Arabidopsis extracts by ultra-performance liquid chromatography/time-of-flight mass spectrometry. *Rapid Commun Mass Spectrom*, **22**, 3154-3160.

Glazebrook, J. (2005) Contrasting Mechanisms of Defense Against Biotrophic and Necrotrophic Pathogens. *Annual Review of Phytopathology*, **43**, 205-227.

Gobel, C. and Feussner, I. (2009) Methods for the analysis of oxylipins in plants. *Phytochemistry*, **70**, 1485-1503.

Goetz, S., et al. (2012) Role of cis-12-Oxo-Phytodienoic Acid in Tomato Embryo Development. *Plant Physiol*, **158**, 1715-1727.

Gonneau, J., et al. (1998) A Nicotiana plumbaginifolia protein labeled with an azido cytokinin agonist is a glutathione S-transferase. *Physiol. Plant.*, **103**, 114-124.

Goodman, R.N., Novacky, A.J. (1994) The Hypersensitive Reaction in Plants to Pathogens. *APS Press, St Paul. 256* .

Gu, L., et al. (2010a) Broad connections in the Arabidopsis seed metabolic network revealed by metabolite profiling of an amino acid catabolism mutant. *Plant J.*, **61**, 579-590.

Gu, L., et al. (2010b) Broad connections in the Arabidopsis seed metabolic network revealed by metabolite profiling of an amino acid catabolism mutant. *Plant J*, **61**, 579-590.

Han, X.M., et al. (2008) Mass spectrometry for proteomics. *Curr Opin Chem Biol* **12**, 483-490.

Hankin, J.A., et al. (1997) Identification of novel metabolites of prostaglandin E-2 formed by isolated rat hepatocytes. *Arch Biochem Biophys*, **340**, 317-330.

Harris, S.G., et al. (2002) Prostaglandins as modulators of immunity. *Trends Immunol.*, **23**, 144-150.

Hayes, J.D., et al. (2005) Glutathione transferases. In *Annu Rev Pharmacol*. Palo Alto: Annual Reviews, pp. 51-88.

Heil, M. and Silva Bueno, J.C. (2007) Within-plant signaling by volatiles leads to induction and priming of an indirect plant defense in nature. *Proc Natl Acad Sci USA*, **104**, 5467-5472.

Heil, M. and Ton, J. (2008) Long-distance signalling in plant defence. *Trends Plant Sci*, **13**, 264-272.

Herschman, H.R., et al. (1999) Function and regulation of prostaglandin synthase 2. In *Eicosanoids and Other Bioactive Lipids in Cancer, Imflammation and Radiation Injury, 4*. New York: Kluwer Academic / Plenum Publ, pp. 3-8.

Hisamatsu, Y., et al. (2003) Arabidopsides A and B, two new oxylipins from Arabidopsis thaliana. *Tetrahedron Lett.*, **44**, 5553-5556.

Hisamatsu, Y., et al. (2005) Oxylipins arabidopsides C and D from Arabidopsis thaliana. *J Nat Prod*, **68**, 600-603.

Holzl, G. and Dormann, P. (2007) Structure and function of glycoglycerolipids in plants and bacteria. *Prog Lipid Res*, **46**, 225-243.

Howe, G.A. and Jander, G. (2008) Plant immunity to insect herbivores. *Annu Rev Plant Biol*, **59**, 41-66.

Howe, G.A. and Schilmiller, A.L. (2002) Oxylipin metabolism in response to stress. *Curr Opin Plant Biol*, **5**, 230-236.

Humphreys, J.M., et al. (1999) New routes for lignin biosynthesis defined by biochemical characterization of recombinant ferulate 5-hydroxylase, a multifunctional cytochrome P450-dependent monooxygenase. *Proc Natl Acad Sci USA*, **96**, 10045-10050.

Jensen, N.J. and Gross, M.L. (1986) Fast atom bombardment and tandem mass spectrometry for determing iso- and anteiso-fatty acids. *Lipids*, **21**, 362-365.

Jensen, N.J., et al. (1985) Gas-phase ion decomposition occurring remote to a charge site. *J Am Chem Soc*, **107**, 1863-1868.

Jin, L., et al. (1996) Identification in rat bile of glutathione conjugates of fluoromethyl 2,2-difluoro-1-(trifluoromethyl)vinyl ether, a nephrotoxic degradate of the anesthetic agent sevoflurane. *Chem Res Toxicol*, **9**, 555-561.

Kazan, K. and Manners, J.M. (2008) Jasmonate signaling: Toward an integrated view. *Plant Physiol*, **146**, 1459-1468.

Kerwin, J.L. and Torvik, J.J. (1996) Identification of monohydroxy fatty acids by electrospray mass spectrometry and tandem mass spectrometry. *Anal Biochem*, **237**, 56-64.

Kerwin, J.L., et al. (1996) Identification of fatty acids by electrospray mass spectrometry and tandem mass spectrometry. *J Mass Spectrom*, **31**, 184-192.

Kilili, K.G. (2004) Differential Roles of Tau Class Glutathione S-Transferases in Oxidative Stress. *J Biol Chem*, **279**, 24540-24551.

Koiwa, H., et al. (1997) Regulation of protease inhibitors and plant defense. *Trends Plant Sci*, **2**, 379-384.

Koo, A.J., et al. (2009a) A rapid wound signal activates the systemic synthesis of bioactive jasmonates in Arabidopsis. *Plant J.*, **59**, 974-986.

Koo, A.J.K., et al. (2006) Identification of a Peroxisomal Acyl-activating Enzyme Involved in the Biosynthesis of Jasmonic Acid in Arabidopsis. *J Biol Chem*, **281**, 33511-33520.

Koo, A.J.K., et al. (2009b) A rapid wound signal activates the systemic synthesis of bioactive jasmonates in Arabidopsis. *Plant J.*, **59**, 974-986.

Kourtchenko, O., et al. (2007) Oxo-Phytodienoic Acid-Containing Galactolipids in Arabidopsis: Jasmonate Signaling Dependence. *Plant Physiol*, **145**, 1658-1669.

Krysan, P.J., et al. (1999) T-DNA as an insertional mutagen in Arabidopsis. *Plant Cell*, **11**, 2283-2290.

Kudla, J., et al. (2010) Calcium Signals: The Lead Currency of Plant Information Processing. *Plant Cell*, **22**, 541-563.

Laemmli, U.K. (1970) Cleavage of Structural Proteins during Assembly of Head of Bacteriophage-T4. *Nature*, **227**, 680-&.

Lander, E.S., et al. (2001) Initial sequencing and analysis of the human genome. *Nature*, **409**, 860-921.

Li. J, H.W., Yu. Y (2013) Chromatography Method. *in "Protein engineering - Technology and application". DOI: 10.5772/56265*.

Liu, H.B., et al. (2004) A model for random sampling and estimation of relative protein abundance in shotgun proteomics. *Anal Chem*, **76**, 4193-4201.

Louda, S., Mole, S. (1991) Glucosinolates: chemistry and ecology. . *In Herbivores: their interaction with secondary plant metabolites, G.A. Rosenthal and M.R. Berenbaum, eds (San Diego: Academic Press, Inc.), pp. 123-164.*

Loughlin, A.F., et al. (2001) An ion exchange liquid chromatography/mass spectrometry method for the determination of reduced and oxidized glutathione and glutathione conjugates in hepatocytes. *J Pharm Biomed Anal*, **26**, 131-142.

MacMillan, D.K. and Murphy, R.C. (1995) Analysis of lipid hydroperoxides and long-chain conjugated keto acids by negative ion electrospray mass spectrometry. *J Am Soc Mass Spectrom*, **6**, 1190-1201.

Mahajan, M.K. and Evans, C.A. (2008) Dual negative precursor ion scan approach for rapid detection of glutathione conjugates using liquid chromatography/tandem mass spectrometry. *Rapid Commun Mass Spectrom*, **22**, 1032-1040.

Mandaokar, A., et al. (2006) Transcriptional regulators of stamen development in Arabidopsis identified by transcriptional profiling. *Plant J.*, **46**, 984-1008.

Matsui, K., et al. (2006) Biosynthesis of fatty acid derived aldehydes is induced upon mechanical wounding and its products show fungicidal activities in cucumber. *Phytochemistry*, **67**, 649-657.

Matsushita, N., et al. (1998) Pharmacological studies on the novel antiallergic drug HQL-79: II. Elucidation of mechanisms for antiallergic and antiasthmatic effects. *Jpn J Pharmacol*, **78**, 11-22.

McGonigle, B., et al. (2000) A genomics approach to the comprehensive analysis of the glutathione S-transferase gene family in soybean and maize. *Plant Physiol*, **124**, 1105-1120.

Miller, S.B. (2006) Prostaglandins in health and disease: An overview. *Semin Arthritis Rheu*, **36**, 37-49.

Milligan, A.S., et al. (2001) The expression of a maize glutathione S-transferase gene in transgenic wheat confers herbicide tolerance, both in planta and in vitro. *Mol. Breed.*, **7**, 301-315.

Moe, M.K., et al. (2004) Negative electrospray ionization low-energy tandem mass spectrometry of hydroxylated fatty acids: a mechanistic study. *Rapid Commun Mass Spectrom*, **18**, 1731-1740.

Montillet, J.-L., et al. (2004) The upstream oxylipin profile of Arabidopsis thaliana: a tool to scan for oxidative stresses. *Plant J*, **40**, 439-451.

Mosblech, A., et al. (2009) Oxylipins: Structurally diverse metabolites from fatty acid oxidation. *Plant Physiol Biochem*, **47**, 511-517.

Mozer, T.J., et al. (1983) Purification and Characterization of Corn Glutathione S-Transferase. *Biochemistry*, **22**, 1068-1072.

Mueller, M.J., et al. (2006) Oxylipin analysis methods. *Plant J*, **45**, 472-489.

Mueller, S., et al. (2008) General detoxification and stress responses are mediated by oxidized lipids through TGA transcription factors in Arabidopsis. *Plant Cell*, **20**, 768-785.

Murphy, C.M., et al. (1992) Fragmentation Characteristic of Glutathione Conjugates Activated by High-Energy Collisions. *J Am Soc Mass Spectrom*, **3**, 815-822.

Nakajyo, H., et al. (2006) Arabidopside F, a new oxylipin from Arabidopsis thaliana. *Heterocycles*, **69**, 295-301.

Narumiya, S., et al. (1999) Prostanoid receptors: structures, properties, and functions. *Physiol Rev*, **79**, 1193-1226.

Narvaez-Vasquez, J. and Ryan, C.A. (2004) The cellular localization of prosystemin: a functional role for phloem parenchyma in systemic wound signaling. *Planta*, **218**, 360-369.

Neumann, P., et al. (2012) Crystal Structures of Physcomitrella patens AOC1 and AOC2: Insights into the Enzyme Mechanism and Differences in Substrate Specificity. *Plant Physiol*, **160**, 1251-1266.

Nilsson, A.K., et al. (2012) Oxo-phytodienoic acid (OPDA) is formed on fatty acids esterified to galactolipids after tissue disruption in Arabidopsis thaliana. *Febs Letters*, **586**, 2483-2487.

Noctor, G. and Foyer, C.H. (1998) Ascorbate and glutathione: Keeping active oxygen under control. *Annu Rev Plant Physiol Plant Molec Biol*, **49**, 249-279.

Oberth, C.H. and Jones, A.D. (1997) Fragmentation of protonated thioether conjugates of acrolein using low collision energies. *J Am Soc Mass Spectrom*, **8**, 727-736.

Oerke, E.C. (2006) Crop losses to pests. *Journal of Agricultural Science*, **144**, 31-43.

Ohkama-Ohtsu, N., et al. (2010) 12-Oxo-Phytodienoic Acid-Glutathione Conjugate is Transported into the Vacuole in Arabidopsis. *Plant Cell Physiol*, **52**, 205-209.

Oliw, E.H., et al. (1998) Analysis of novel hydroperoxides and other metabolites of oleic, linoleic, and linolenic acids by liquid chromatography-mass spectrometry with ion trap MS^n. *Lipids*, **33**, 843-852.

Pauwels, L., et al. (2010) NINJA connects the co-repressor TOPLESS to jasmonate signalling. *Nature*, **464**, 788-U169.

Pauwels, L. and Goossens, A. (2011) The JAZ Proteins: A Crucial Interface in the Jasmonate Signaling Cascade. *Plant Cell*, **23**, 3089-3100.

Pichersky, E. and Lewinsohn, E. (2011) Convergent evolution in plant specialized metabolism. In *Ann Rev Plant Biol, Vol 62* (Merchant, S.S., Briggs, W.R. and Ort, D. eds), pp. 549-566.

Qi, X., et al. (2004) A gene cluster for secondary metabolism in oat: Implications for the evolution of metabolic diversity in plants. *Proc Natl Acad Sci USA*, **101**, 8233-8238.

Qiu, Y.J., et al. (2012) Coupling calcium/calmodulin-mediated signaling and herbivore-induced plant response through calmodulin-binding transcription factor AtSR1/CAMTA3. *Plant Mol Biol*, **79**, 89-99.

Rathahao, E., et al. (2004) Liquid chromatography coupled to negative electrospray/ion trap mass spectrometry for the identification of isomeric glutathione conjugates of catechol estrogens. *Int J Mass Spectrom*, **231**, 119-129.

Reymond, P., et al. (2000) Differential gene expression in response to mechanical wounding and insect feeding in Arabidopsis. *Plant Cell*, **12**, 707-719.

Ruscoe, J.E., et al. (2001) Pharmacologic or genetic manipulation of glutathione S-transferase P1-1 (GST pi) influences cell proliferation pathways. *J Pharmacol Exper Therap*, **298**, 339-345.

Saito, K. and Matsuda, F. (2010) Metabolomics for Functional Genomics, Systems Biology, and Biotechnology. In *Annu Rev Plant Biol, Vol 61*. Palo Alto: Annual Reviews, pp. 463-489.

Samuel, K., et al. (2003) Addressing the metabolic activation potential of new leads in drug discovery: a case study using ion trap mass spectrometry and tritium labeling techniques. *Journal of Mass Spectrometry*, **38**, 211-221.

Sandermann, H. (1992) Plant-Metabolism of Xenobiotics. *Trends Biochem Sci* , **17**, 82-84.

Savagnac, A., et al. (1989) Structure determination of mycolic acids by using charge remote fragmentation. *Chem Phys Lipids*, **51**, 31-38.

Schenk, P.M., et al. (2000) Coordinated plant defense responses in Arabidopsis revealed by microarray analysis. *Proc Natl Acad Sci USA*, **97**, 11655-11660.

Schilmiller, A.L. and Howe, G.A. (2005) Systemic signaling in the wound response. *Curr Opin Plant Biol*, **8**, 369-377.

Schilmiller, A.L., et al. (2012) Taming the hydra of specialized metabolism: how systems biology and comparative approaches are revolutionizing plant biochemistry. *Curr Opin Plant Biol*, **15**, 338-344.

Sheard, L.B., et al. (2010) Jasmonate perception by inositol-phosphate-potentiated COI1-JAZ co-receptor. *Nature*, **468**, 400-U301.

Sheehan, D., et al. (2001) Structure, function and evolution of glutathione transferases: implications for classification of non-mammalian members of an ancient enzyme superfamily. *Biochem J*, **360**, 1-16.

Shevchenko, A., et al. (1996) Mass spectrometric sequencing of proteins from silver stained polyacrylamide gels. *Anal Chem*, **68**, 850-858.

Simons, P.C. and Vanderjagt, D.L. (1977) Purification of Glutathione S-Transferases from Human Liver by Glutathione-Affinity Chromatography. *Anal Biochem*, **82**, 334-341.

Skipsey, M., et al. (2005) Manipulation of plant tolerance to herbicides through co-ordinated metabolic engineering of a detoxifying glutathione transferase and thiol cosubstrate. *Plant Biotechnol J*, **3**, 409-420.

Soranzo, N., et al. (2004) Organisation and structural evolution of the rice glutathione S-transferase gene family. *Mol Genet Genomics*, **271**, 511-521.

Staneke, P.O., et al. (1996) Electron transfer as a possible initial step in nucleophilic addition elimination reactions between (radical) anions and carbonyl compounds in the gas phase. *Recl. Trav. Chim. Pays-Bas*, **115**, 179-&.

Staswick, P.E. and Tiryaki, I. (2004) The oxylipin signal jasmonic acid is activated by an enzyme that conjugates it to isoleucine in Arabidopsis. *Plant Cell*, **16**, 2117-2127.

Stelmach, B.A. (2001) A Novel Class of Oxylipins, sn1-O-(12-Oxophytodienoyl)-sn2-O-(hexadecatrienoyl)-monogalactosyl Diglyceride, from Arabidopsis thaliana. *J Biol Chem*, **276**, 12832-12838.

Stelmach, B.A., et al. (1998) Quantitation of the octadecanoid 12-oxo-phytodienoic acid, a signalling compound in plant mechanotransduction. *Phytochemistry*, **47**, 539-546.

Stenzel, I., et al. (2003) Allene oxide cyclase dependence of the wound response and vascular bundle-specific generation of jasmonates in tomato - amplification in wound signalling. *Plant J*, **33**, 577-589.

Stepan, A.F., et al. (2011) Structural Alert/Reactive Metabolite Concept as Applied in Medicinal Chemistry to Mitigate the Risk of Idiosyncratic Drug Toxicity: A Perspective Based on the Critical Examination of Trends in the Top 200 Drugs Marketed in the United States. *Chem Res Toxicol*, **24**, 1345-1410.

Stintzi, A., et al. (2001) Plant defense in the absence of jasmonic acid: The role of cyclopentenones. *Proc Natl Acad Sci USA*, **98**, 12837-12842.

Straus, D.S. and Glass, C.K. (2001) Cyclopentenone prostaglandins: New insights on biological activities and cellular targets. *Med Res Rev*, **21**, 185-210.

Sumner, L.W., et al. (2003) Plant metabolomics: large-scale phytochemistry in the functional genomics era. *Phytochemistry*, **62**, 817-836.

Suzuki, H. and Sugiyama, Y. (1998) Excretion of GSSG and glutathione conjugates mediated by MRP1 and cMOAT/MRP2. *Semin Liver Dis*, **18**, 359-376.

Taki, N., et al. (2005) 12-oxo-phytodienoic acid triggers expression of a distinct set of genes and plays a role in wound-induced gene expression in Arabidopsis. *Plant Physiol*, **139**, 1268-1283.

Tan, K.L., et al. (1996) Mutagenesis of the active site of the human Theta-class glutathione transferase GSTT2-2: Catalysis with different substrates involves different residues. *Biochem J*, **319**, 315-321.

Theodoulou, F.L., et al. (2005) Jasmonoic acid levels are reduced in COMATOSE ATP-binding cassette transporter mutants. Implications for transport of jasmonate precursors into peroxisomes. *Plant Physiol*, **137**, 835-840.

Thines, B., et al. (2007) JAZ repressor proteins are targets of the SCFCO11 complex during jasmonate signalling. *Nature*, **448**, 661-U662.

Thom, R., et al. (2001) The structure of a zeta class glutathione S-transferase from Arabidopsis thaliana: Characterisation of a GST with novel active-site architecture and a putative role in tyrosine catabolism. *J Mol Biol*, **308**, 949-962.

Tommasini, R., et al. (1998) An ABC-transporter of Arabidopsis thaliana has both glutathione-conjugate and chlorophyll catabolite transport activity. *Plant J*, **13**, 773-780.

Tong, X.H., et al. (2012) The rice hydroperoxide lyase OsHPL3 functions in defense responses by modulating the oxylipin pathway. *Plant J*, **71**, 763-775.

Tsuboi, K., et al. (2002) Prostanoid receptor subtypes. *Prostaglandins Other Lipid Mediat.*, **68-9**, 535-556.

Valvekens, D., et al. (1988) Agrobacterium-Tumefaciens-Mediated Transformation of Arabidopsis-Thaliana Root Explants by Using Kanamycin Selection. *Proc Natl Acad Sci USA*, **85**, 5536-5540.

Venter, J.C., et al. (2001) The sequence of the human genome. *Science*, **291**, 1304-+.

Wagner, U., et al. (2002) Probing the diversity of the arabidopsis glutathione S-transferase gene family. *Plant Mol Biol*, **49**, 515-532.

Waldon, D.J., et al. (2010) Identification of Quinone Imine Containing Glutathione Conjugates of Diclofenac in Rat Bile. *Chem Res Toxicol*, **23**, 1947-1953.

Walgren, J.L., et al. (2005) Role of metabolism in drug-induced idiosyncratic hepatotoxicity. *Crit Rev Toxicol*, **35**, 325-361.

Washburn, M.P., et al. (2001) Large-scale analysis of the yeast proteome by multidimensional protein identification technology. *Nat Biotechnol*, **19**, 242-247.

Wasternack, C. (2007) Jasmonates: An Update on Biosynthesis, Signal Transduction and Action in Plant Stress Response, Growth and Development. *Ann Bot*, **100**, 681-697.

Wasternack, C., et al. (2013) Jasmonates in flower and seed development. *Biochimie*, **95**, 79-85.

Wasternack, C. and Hause, B. (2013) Jasmonates: biosynthesis, perception, signal transduction and action in plant stress response, growth and development. An update to the 2007 review in Annals of Botany. *Annals of Botany*, **111**, 1021-1058.

Weber, H., et al. (1997) Dinor-oxo-phytodienoic acid: A new hexadecanoid signal in the jasmonate family. *Proc Natl Acad Sci USA*, **94**, 10473-10478.

Wheelan, P., et al. (1993) Low-energy fast atom bombardment tandem mass spectrometry of monohydroxy substituted unsaturated fatty acids. *Biol Mass Spectrom*, **22**, 465-473.

Wheelan, P., et al. (1996) Electrospray ionization and low energy tandem mass spectrometry of polyhydroxy unsaturated fatty acids. *J Am Soc Mass Spectrom*, **7**, 140-149.

Wilkins, M.R., et al. (1996) From proteins to proteomes: Large scale protein identification by two-dimensional electrophoresis and amino acid analysis. *Bio-Technology*, **14**, 61-65.

Wolf, A.E., et al. (1996) Degradation of glutathione S-conjugates by a carboxypeptidase in the plant vacuole. *Febs Letters*, **384**, 31-34.

Xie, C., et al. (2013) A fragmentation-based method for the differentiation of glutathione conjugates by high-resolution mass spectrometry with electrospray ionization. *Anal Chim Acta*, **788**, 89-98.

Xie, D.X., et al. (1998) COI1: An Arabidopsis gene required for jasmonate-regulated defense and fertility. *Science*, **280**, 1091-1094.

Yan, Y., et al. (2007) A downstream mediator in the growth repression limb of the jasmonate pathway. *Plant Cell* **19**, 2470-2483.

Yates, J.R. (1998) Mass spectrometry and the age of the proteome. *J Mass Spectrom*, **33**, 1-19.

Zhang, Y. and Turner, J.G. (2008) Wound-induced endogenous jasmonates stunt plant growth by inhibiting mitosis. *PLoS ONE*, **3**, e3699.

Zhang, Y.Y., et al. (2013) Protein Analysis by Shotgun/Bottom-up Proteomics. *Chem Rev*, **113**, 2343-2394.

Zhang, Z.P. and Baldwin, I.T. (1997) Transport of [2-C-14]jasmonic acid from leaves to roots mimics wound-induced changes in endogenous jasmonic acid pools in Nicotiana sylvestris. *Planta*, **203**, 436-441.

Zimmermann, P., et al. (2004) GENEVESTIGATOR. Arabidopsis microarray database and analysis toolbox. *Plant Physiol*, **136**, 2621-2632.

Zirrolli, J.A., et al. (1990) Fast-Atom-Bombardment and Collision-Induced Dissociation of Prostaglandins and Thromboxanes - Some Examples of Charge Remote Fragmentation. *J Am Soc Mass Spectrom*, **1**, 325-335.